

This electronic thesis or dissertation has been downloaded from the King's Research Portal at <https://kclpure.kcl.ac.uk/portal/>



Multimodal Optical characterisation of the interface between dental cements and sound or carious dentinal substrates

Sajini, Shara Ismail Ibrahim

Awarding institution:
King's College London

The copyright of this thesis rests with the author and no quotation from it or information derived from it may be published without proper acknowledgement.

END USER LICENCE AGREEMENT



Unless another licence is stated on the immediately following page this work is licensed

under a Creative Commons Attribution-NonCommercial-NoDerivatives 4.0 International

licence. <https://creativecommons.org/licenses/by-nc-nd/4.0/>

You are free to copy, distribute and transmit the work

Under the following conditions:

- Attribution: You must attribute the work in the manner specified by the author (but not in any way that suggests that they endorse you or your use of the work).
- Non Commercial: You may not use this work for commercial purposes.
- No Derivative Works - You may not alter, transform, or build upon this work.

Any of these conditions can be waived if you receive permission from the author. Your fair dealings and other rights are in no way affected by the above.

Take down policy

If you believe that this document breaches copyright please contact librarypure@kcl.ac.uk providing details, and we will remove access to the work immediately and investigate your claim.

**Multimodal Optical characterisation of the interface
between dental cements and sound or carious dentinal
substrates**

Shara Ismail I. Sajini

A thesis submitted for the degree of

Doctor of Philosophy

King's College London

2016

Abstract

Objectives:

Calcium silicate based cements have been mainly used for endodontic applications. Recently, a new formula has been produced as a coronal restoration. The aim of this project was to optically characterise different human dentine substrates. Then to investigate possible mineralisation effects of this new calcium-silicate based cement (Biodentine™) and compare them with those of glass ionomer cements (Fuji IX™) based on the optical properties of the interface.

Methodology:

The interaction of both cements with in-vitro demineralised dentine samples was investigated. A model including sound and demineralised dentine tissues was created and optically evaluated. Then Biodentine and GIC were applied and evaluated using more controlled samples. Various advanced optical imaging techniques were applied; such as multiphoton fluorescence microscopy, fluorescence lifetime imaging and second harmonic generation imaging to assess optical changes before and after aging the samples. In addition, Raman spectroscopy was used to detect changes in the intensity of the mineral peak. These non-invasive optical techniques were then used on carious teeth to characterise different zones of dentine caries based on tissue's auto-fluorescence without labelling. Each zone was then defined by its Knoop microhardness reading. Afterwards, the mineralisation effect of both cements on each dentine zone was assessed after aging the substrate in solutions of (+/- 0.015% tetracycline, PBS and water). In another set of samples, excavated carious teeth were used to mimic the clinical situation, as each half was restored with either GIC or Biodentine. The interface of the two cements was evaluated based on changes in fluorescence intensity and lifetime.

Results:

Significant changes in the fluorescence intensity and lifetime of the interfacial dentine before and after ageing were found under both cements in the demineralised dentine model samples. These optical changes were associated with significant increase in the Raman mineral peak after storage.

Using KHN to indicate tissue type, the single and multiphoton fluorescence intensity, fluorescence lifetime, and SHG signal differentiated significantly between caries-infected, caries-affected and sound dentine. The cement groups showed significant fluorescence changes within infected and affected tissues, indicating possible mineralisation as they were associated with an increase in the mineral peak intensity. Tetracycline mineral-binding induced a reduction in the lifetime with comparable increase in the fluorescence intensity in the Biodentine™ and GIC groups within the affected and sound areas. Similar optical changes were detected as a band of mineralised structure under both cements with deeper infiltration of GIC within inter and peritubular dentine in the excavated caries samples.

Conclusion:

Two-photon microscopy can be efficiently used for non-invasive in-vitro diagnostic dentine caries characterisation. Studying the same lesion-restoration interface over time, changes in the fluorescence lifetime and intensity could indicate that mineralisation may have occurred within the dentine under GIC and calcium silicate cements (Biodentine™).

Table of Contents

Multimodal Optical characterisation of the interface between dental cements and sound or carious dentinal substrates	1
Abstract.....	2
Table of Contents.....	4
List of Figures	8
List of Tables.....	13
List of abbreviations	14
Acknowledgements	16
Introduction	18
Research aims and objectives	20
Thesis structure	21
1. Chapter One: Literature Review.....	23
1.1 Dental biomaterials	23
1.1.1 Calcium silicate cements	24
1.1.2 Glass ionomer cements.....	29
1.2 Substrates used in this project	31
1.2.1 Dentine structure	31
• Organic matrix	31
• Mineral content.....	34
1.2.2 Dentine caries	35
1.2.3 Demineralised dentine.....	46
1.2.4 Dentine remineralisation	48
1.3 Optical Methods used in this project.....	51
1.3.1 Introduction to optics	51
1.3.2 Two-photon fluorescence microscopy.....	53
1.3.3 Raman spectroscopy	58
2. Chapter Two: Evaluation of an In-vitro dentine demineralisation model and assessment of the remineralisation potentials of dental cements	61
2.1 Introduction	62

2.2	Materials and methods	65
2.2.1	Preparation of demineralised dentine samples	65
2.2.2	Assessment of the demineralisation protocol.....	66
2.2.3	Sample preparation for the evaluation of dental cements	69
2.2.4	Statistical analysis	70
2.3	Results	71
2.3.1	Assessment of dentine demineralisation model.....	71
2.3.2	Assessment of dental cements' interaction with sound and demineralised dentine 74	
	Two-photon microscopy imaging	74
2.4	Discussion.....	81
2.4.1	Sample preparation	81
2.4.2	Evaluation of dental cements interaction and remineralisation potentials 84	
3.	Chapter Three: Evaluation of cement-dentine interface after caries excavation: Tetracycline labelling and two-photon fluorescence microscope.....	89
3.1	Introduction	90
3.2	Materials and methods:	92
3.2.1	Sample preparation	92
3.2.2	Imaging and image analysis	94
3.3	Results	96
3.4	Discussion.....	99
4.	Chapter Four: Multimodal optical characterization of dentine caries lesions .	104
4.1	Introduction	105
4.2	Materials and methods	109
4.2.1	Two-photon microscopy AF, SHG and FLIM imaging and AF spectrum detection.....	109
4.2.2	Single-photon spectrometer autofluorescence.....	110
4.2.3	Microhardness measurements	110
4.2.4	Statistical analysis	113

4.3	Results	116
4.3.1	Two-photon fluorescence microscopy.....	116
4.3.2	Single-photon fibre optic spectrometer	119
4.3.3	Results from the statistical classification method.....	119
4.4	Discussion.....	122
5.	Chapter Five: Evaluation of dental cements' interaction with natural carious dentine.....	128
5.1	Introduction	129
5.2	Materials and methods:	132
5.2.1	Sample preparation	132
5.2.2	Imaging	134
5.2.3	Raman spectroscopy.....	135
5.2.4	Statistical analysis	137
5.3	Results	138
5.3.1	Samples stored in PBS without Tetracycline labelling.....	138
A.	Two- photon fluorescence Imaging.....	138
B.	Raman spectroscopy.....	139
5.3.2	Samples stored in PBS and Tetracycline as a mineral labelling fluorophore	143
A.	Two-photon fluorescence imaging	143
5.4	Discussion.....	147
6.	Chapter Six: General summary and suggestions for future work	153
6.1	General summary.....	153
6.2	Suggestions for future work.....	158
7.	Appendices	159
1.	Publication	159
Appendix 1	159
2.	Tables.....	160
Appendix 2	160
Appendix 3	161

Table of contents

Appendix 4	163
Appendix 5	165
Appendix 6	167
Appendix 7	169
Appendix 8	170
References	172

List of Figures

- Figure 1** Organisational flowchart of the experiments accomplished in this study with the analytical methods employed.22
- Figure 1-1** A diagram presenting (a) collagen triple helical structure. (b) Collagen molecule contains non triple helical areas at both ends. (c) Cross-linked staggering of collagen. (d) Collagen fibril showing the repeated periodic banding pattern and demonstrating the D-periodic unit with single overlap and single gap (modified from (Cawston, 1998)).32
- Figure 1-2** A photomicrograph of a carious tooth section displaying the different dentine caries layers. The red line shows the area of caries-infected dentine, it looks dark brown in colour. The green line is the caries-affected dentine, which has a paler brown colour and includes the transparent (TZ) (dotted line) and the subtransparent (STZ) zones (dashed line). The blue line represents normal dentine.36
- Figure 1-3** A Jablonski diagram demonstrating different optical phenomena resulting from changes in the energy level of the electrons within a molecule after interaction with light. **(a)** Rayleigh scattering occurs when the light is scattered with similar wavelength as the incident light. Non-elastic scattering occurs when scattering the incident photon with a reduced energy, known as a Stokes shift **(b)**, or a higher energy described as an anti-Stokes shift **(c)**. **(d)** Following absorption, the gained energy is released with different energy and wavelength in the form of fluorescence. **(e)** Fluorescence through two photons excitation involves two photons, each with half the fluorescence excitation energy to excite the fluorophores and produce fluorescence. Courtesy of (Xu, 2001).52
- Figure 1-4** Raman spectra for sound dentine between 100-3100 cm^{-1} wavenumbers presenting the observed peaks, the assignments for these peaks are summarised in Table 1-259
- Figure 2-1** Sample preparation: **(a)** 10 extracted sound teeth sectioned into two halves with a right angle reference mark. **(b)** Part of the dentine was covered using dental wax leaving 2 mm window for dentine demineralisation. **(c)** Demineralisation is carried out using an acid etching protocol with 37% phosphoric acid for 60 seconds. Then evaluation of the demineralisation protocol is made by assessing

changes in mineral peak, changes in fluorescence intensity and lifetime, measuring the difference in Knoop hardness number and assessing the SHG signal.....66

Figure 2-2 Sample preparation for Raman spectroscopy. (A) A diagram of a sample showing the demineralised dentine window and the selected area for Raman scan. (B) An example of a montage image created to include both sound and demineralised dentine. (C) The representative grey-scale image of Raman phosphate peak intensity at 959 cm⁻¹ of sound (S) and demineralised (D) dentine areas.....68

Figure 2-3 Sample preparation for cement evaluation. (A) Seven demineralised samples were selected as test samples. (B) for each sample, one half was stored with Biodentine and the other half with GIC for future comparison, all samples were stored in PBS containing storage media.³ (C) An additional three samples were used as controls and stored in PBS solution without restoration. (D) After storage, samples were sectioned at the reference mark and the interface was evaluated for changes in mineral peak, fluorescence intensity and lifetime and hardness number. (S) denotes sound dentine and (D) demineralised lesion.....69

Figure 2-4 Multimodal assessment of dentine demineralisation. (A) Autofluorescence intensity. (B) Fluorescence lifetime. (C) Second harmonic generation signal. (D) Raman spectroscopy. (E) Tissue hardness (KHN).....73

Figure 2-5 Representative Two photon images before and after cement application and storage for sound and demineralised dentine. Sound dentine showed decreased fluorescence intensity only with both cements. No change was recognised in the control group.....76

Figure 2-6 Percentage change before and after storage in the (A) Auto-fluorescence intensity, (B) Fluorescence lifetime and (C) KHN regarding each group for both sound (green) and demineralised (blue) dentine. The results show a greater change in the demineralised dentine with both cements regarding all parameters with no change in the control group. Sound dentine shows decreased fluorescence intensity with the cements with no change in the control group. In addition there were no changes in the FLIM or KHN regarding all groups of sound dentine.....78

Figure 2-7 Raman analysis for mineral peak intensity. **(A)** Results of the percentage change in the mineral peak intensity before and after restoration and storage for both sound and demineralised dentine. The highest change is seen in the demineralised dentine stored with Biodentine and GIC. **(B)** Representative Raman spectra for the measured phosphate peak intensity from sound and demineralised dentine before and after restoration with dental cements.....80

Figure 2-8 Representative grey-scale image and the depth profile of phosphate peak intensity of Raman phosphate peak at 959 cm⁻¹ including the lesion of demineralised dentine (L) and sound dentine (S).83

Figure 3-1: Extracted human teeth were prepared, a right angle between the mesial wall and pulpal floor of the cavity (Red arrow) was created using a cylindrical bur. Teeth were divided to six experimental groups. Five teeth to be restored with either GIC (GTP) or Biodentine (BTP) and stored in tetracycline and PBS. Four teeth were left without restoration to act as controls and stored in either PBS alone (CPW,SPW) or with tetracycline storage solution (CTP, STP).94

Figure 3-2 Image analysis. Florescence lifetime (left) and Fluorescence intensity (right) images where analysed by calculating the average intensity and lifetime ratio between two areas in each image. One area just below the interface and the other away from the interface representing unaffected dentine.....95

Figure 3-3 Representative fluorescence intensity (FI) and fluorescence lifetime (FLT) images for the dentine–cement interface of different groups before and after aging. A well-defined band of shorter fluorescence life-time was detected in the (BiodentineTM) filled samples. Reduction of the fluorescence lifetime was also detected in GIC filled samples as a band below the interface with more areas infiltrating the dentine matrix. The restoration-free samples (CTP, STP) that were stored in Tetracycline containing solution, showed minimal and more generalised fluorescence changes. Other controls stored in Tetracycline free solution (CPW SPW) showed non-significant changes in FLT (C = excavated caries, S = sound, T = Tetracycline, P= Phosphate buffered saline).98

Figure 3-4 Normalised fluorescence intensity (FI) and fluorescence lifetime (FLT) presented as percentage differences of samples restored with Biodentine or GIC. Control samples of sound teeth with/ without Tetracycline and excavated carious teeth withand without Tetracycline.99

- Figure 3-5** The actual fluorescence lifetime measurements of Biodentine group (0.62 ns), GIC (0.70 ns) and tetracycline calcium complex (0.56 ns).101
- Figure 4-1** Representative Auto-fluorescence decay curve from caries-infected (red), caries-affected (green) and sound (blue) dentine107
- Figure 4-2** A calibrated photomicrograph of a sample with the reference point created and the test area selected. Geometric representation of the performed techniques, starting with two-photon imaging then single-photon fibre-optic spectrometry and finally Knoop microhardness testing.112
- Figure 4-3** Single-photon spectrometer experimental apparatus. Excitation: Mounted high power blue LED (470 nm), Single excitation bandpass filter 465/30. A dichroic reflector (505 nm LP) positioned at 45° angle in the excitation beam permitting transmission of >505 nm wavelength. A long pass (488 nm) emission filter.....113
- Figure 4-4** A representative example of the calculated probability density function with Variable Kernel Width using Lorentzian Kernel for FLIM data. (A) Density functions for infected, affected and sound dentine. (B) The density function for all carious zones. (C) The probability of all carious zones.115
- Figure 4-5** Representative multiphoton fluorescence images showing a decrease in the fluorescence intensity from infected to sound dentine and an increase in the fluorescence lifetime from (0.9 ns) for infected to (1.6 ns) for sound dentine.116
- Figure 4-6** (A) a photograph of half a sample with an example of the selected caries lesion displaying caries zones (red) is for infected tissue, (green) for affected and (blue) is for sound. Multiphoton imaging results are presented in (B) for lifetime data. Representative histogram showing variations in the lifetime values and the average auto-fluorescence lifetime calculated for each tissue type. (C) Representative histogram of the AF intensity images and the calculated average AF intensity for caries zones. Multiphoton spectroscopy data are presented in (D) representative AF spectra obtained from the lesion. The bar graph represents the average SHG/AF2 ratio and the AF1/AF2 ratio. The averaged spectra from single-photon excitation are presented in (E) with a graph showing the averaged AF signal intensity and the average weighted wavelength for each carious dentine zone ...117

- Figure 4-7** The sensitivity and specificity calculated for individual optical technique regarding each caries zone are presented in (A) and averaged for individual technique in (B) highlighting the superior sensitivity and specificity of the multiphoton intensity imaging technique.120
- Figure 4-8** The sensitivity and specificity of each optical technique when combined with the two-photon intensity imaging (2PI). Regarding each tissue type in (A). The averaged sensitivity and specificity values for the combined technique in (B). The data shows that combining multiphoton intensity and lifetime imaging resulted in the best sensitivity and specificity values121
- Figure 4-9** Plot graph showing the average intensity and lifetime data of caries infected (red), affected (green) and sound (blue) dentine. The graph represents the ability of both parameters to discriminate between infected and affected tissues with less significance regarding affected and sound dentine.122
- Figure 5-1** Diagram showing the experimental groups divided according to the restorative cement and the storage media133
- Figure 5-2** Sample preparation for cement evaluation. (A) Carious tooth before restoration with a chosen area of imaginary line including previously tested data and identified tissues (blue). (B) Application of the cement with exposed reference area. (C) Tooth sectioning at the chosen line to expose the carious tissues from the side. (D) Sample is ready for imaging the interface from the side including different dentinal tissues under the cement.135
- Figure 5-3** Sample preparation for Raman spectroscopy. (A) The selected tested area including all tissue types. (B) Montage image of the sample. (C) The Raman scan after mineral peak analysis starting at the first tested point.137
- Figure 5-4** Representative Two-photon imaging of the interface between carious dentine/ Biodentine -GIC. The figure compares baseline fluorescence intensity and lifetime images for caries infected, affected and sound dentine before cement application with the after storage images for each group (Control (no material), Biodentine and GIC).140

Figure 5-5 The calculated percentage change in both fluorescence intensity and lifetime after image analysis is displayed to show the differences before and after storage of each group regarding different dentinal substrates.	141
Figure 5-6 (A) Raman-mineral peak intensity for caries-infected (red), affected (green) and sound dentine (blue) for each experimental group. (B) Representative Raman spectra of the phosphate peak at 959 cm^{-1} for each tissue type, comparing GIC (orange), Biodentine (purple) and control group (black).	142
Figure 5-7 Representative fluorescence lifetime and intensity images for samples stored in Tetracycline as a mineral labelling fluorophore. Comparison between the fluorescent images of the baseline (before storage) and after storage regarding different dentinal tissues for the control, Biodentine and GIC groups.....	145
Figure 5-8 The percentage change in the fluorescence intensity and lifetime for samples stored in Tetracycline solution. Comparing Biodentine and GIC samples with control group for each dentine tissue type	146

List of Tables

Table 1-1 A summary of various clinical and laboratory methods used to delineate different zones of carious dentine.	41
Table 1-2 The common featured dentine peaks with their tentative assigned bands and correlated histological components (Spencer et al., 2000).....	59
Table 4-1 a summery table representing previous studies that investigated the lifetime of dental tissues with the lifetime results for sound and carious tissues. .	124

List of abbreviations

ACP: amorphous calcium phosphate.

AF: autofluorescence.

CCD: charge-coupled device.

CLSM: confocal laser scanning microscopy.

DHLNL: Dihydroxynorleucine

DMP: dentine matrix protein.

DPP: dentine phosphoprotein

DSP: dentine sialoproteine

DSPP: dentine sialophosphoprotein

EDJ: enamel-dentine junction.

EDTA: ethylenediaminetetraacetic acid

EDX: energy dispersive X-ray spectroscopy.

GIC: glass ionomer cement

FA: fluorapatite.

FISH: fluorescent in-situ hybridisation

HA: hydroxyapatite.

HCA: hydroxycarbonate apatite.

KHN: Knoop hardness number.

MI: minimally intervention.

MID: minimally invasive dentistry.

MMP: matrix metalloproteinase.

MTA: Mineral trioxide aggregate

OCT: optical coherence tomography.

PBS: phosphate buffered solution.

PCR: polymerase chain reaction.

List of abbreviations

QLF: quantitative laser-induced fluorescence.

SIBLINGs: small integrin-binding ligand N-linked glycoproteins

SLRPS: small leucine-rich proteoglycans.

TGF: transforming growth factor.

UV:ultraviolet

Acknowledgements

In the name of Allah most Gracious most Merciful, to whom all praises and thanks for giving me the strength, patience, and determination in completing this academic journey.

I owe my sincere thankfulness and gratitude to:

Professor Timothy Watson, my first supervisor, for his exceptional supervision, guidance and support by all means throughout my PhD study.

Dr. Frederic Festy, my second supervisor, from whom I have derived the strength to challenge myself and perform better at each stage. I am truly indebted for his indefinite support, encouragements and patience.

Professor Abigail Tucker, my postgraduate coordinator for her advice and continuous evaluation of my progress during my studies. Her profound support and consideration have guided me toward the completion of this PhD degree.

Professor Avijit Banerjee, for generously offering his precious time and expertise. I am truly appreciative for the constructive discussions regarding the design and the outcomes of the experiments.

Dr. Richard Cook, for his suggestions for the progression of this work.

Dr. Ee Zuahn Chong, Dr. Neveen Hosny, Mr. Peter Pilecki, and Mr. Richard Mallet for their technical help and assistance in the lab.

Mr. Andiappan Manoharan for his valuable assistance and statistical analysis.

I would also like to extend my deep appreciation and gratitude to my employer, *Faculty of Dentistry - department of restorative and aesthetic dentistry, King AbdulAziz University, Jeddah, Saudi Arabia* and to the *Royal Embassy of Saudi Arabia, Cultural Bureau in London* for their generous financial grant and continuous support.

To all my friends and dear colleagues - thank you for your kindness and inspiration.

I would like to thank my parents' in-law and my sisters for their prayers and the continuous care they provided.

I owe special appreciation and deepest gratitude for my beloved husband, *Reda Sijiny*, who shared with me difficult and pleasant times throughout the years. I would certainly not have achieved this without his tremendous motivation, patience

Acknowledgment

and loving support. My warmest love goes to my beloved son, *Habieb* and daughter, *Zaina* who provided me with strength and determination to accomplish my study and have been truly patient, understanding and loving, and to my son *Ismael* who is a recent addition to my family.

I dedicate this work and achievement to my dear parents *Ismail Sajini* and *Sameera al-Qull* who have been- and will always be a source of strength, inspiration and endless love. I cannot find words to express my gratitude to your support.

Introduction

Dental caries is one of the most common diseases affecting human beings worldwide. It is a challenge for dentists and patients to choose the ideal line of treatment especially when dental caries extends deep within the tooth structure. Nowadays this condition can be treated conservatively and effectively using a minimally invasive approach for managing caries especially if the pulp involvement is considered to be reversible. Advancements in understanding the caries process and the biology of the accompanying dentine-pulp defence and regenerative responses have encouraged the application of minimal caries removal rather than a more aggressive traditional excavation approach. This approach relies on accurate caries diagnosis, then identifying the excavation end point to include only the irreversibly caries-infected dentine. Such a management technique facilitates the healing of the remineralisable caries-affected dentine and prevents pulp injury and thereafter root canal treatment.

In line with these advancements in managing dental caries, the search for the “ideal” material that could support the application of such an approach has been a subject of major interest in the dental and biomaterial research communities. Consequently, a wide range of materials have been introduced as well as withdrawn in the past few years, translating the dynamic relation between development and research. The introduction of bioactive restorative materials is one of the advances that can promote tissue regeneration and eventual healing of carious lesions and have paved the way for this conservative modality to be applied. Among these was the development of calcium silicate based cements in 1993 as mineral tri-oxide aggregate (MTA). Since then, modifications have been carried out to widen their clinical applications. A recent formula (Biodentine™) was developed to be used as a dentine replacement material with potential for carious dentine remineralisation and healing. The assessment of these materials’ interaction with dental tissues and their therapeutic potential is essential to determine their efficacy and thus clinical applications. Several techniques and devices have been used for these assessments.

Microscopes are one of the great human inventions with multiple functions that are not restricted to object magnification. Due to variable modes of interaction between light and matter, microscopes can now provide valuable information about chemical composition, microstructure and the fluorescence behaviour of tissues. Dentine has

a unique structural composition of organic and inorganic substances which provide it with unique optical properties in health and disease. In this context, microscopes have been extremely beneficial in dental research studying the optical behaviour of dental tissues and the interaction between them and dental materials. This understanding has extremely influenced the dental practice and the quality of dental care provided.

This work aimed to study the interaction between calcium silicate cement and the complex structure of carious and sound dentine and to evaluate its potential for tissue remineralisation when compared with an equivalent material with similar clinical applications such as glass ionomer cement. To facilitate this aim, advanced imaging techniques have been applied to evaluate optical and chemical changes within the dentine structure.

Research aims and objectives

The studies carried out and presented in this thesis aimed to evaluate the effect of the recently introduced calcium silicate cement on the optical properties and mineral content of sound and carious dentine tissues. This evaluation was based on the validation of optical non-invasive in-vitro methods using two-photon fluorescence microscopy, fluorescence lifetime imaging and Raman spectroscopy for the characterisation of dentine caries and the evaluation of the remineralisation process within dentinal tissues as an effect of the cements' application.

The objectives of the project are the following:

1. To study and characterise the effect of calcium silicate based coronal restorative materials (Biodentine™) on dentine, and compare it with equivalent materials such as the glass ionomer cement.
2. To assess the effect of in-vitro dentine demineralisation on its optical properties, this will be the first step to establish an understanding of the relation between dentine mineral content and its fluorescence characteristics.
3. To evaluate the changes in dentine optical properties using two-photon fluorescence and fluorescence lifetime imaging as a result of remineralising demineralised dentine. Also evaluating its mineral content using Raman spectroscopy after the application of Biodentine then compare that to the effect of GIC.
4. To evaluate optically the remineralisation potentials of Biodentine and GIC on excavated carious dentine samples in an attempt to mimic the clinical situation where the application of these cements is indicated.
5. To validate the use of multimodal non-invasive optical techniques to characterise dentine caries zones by discriminating caries-infected, caries-affected and sound dentine based on their fluorescence properties.
6. To assess the effect of the interaction between dental cements and different zones of carious dentine and assess the ability of these cements to induce remineralisation in caries zones.

Thesis structure

In this thesis, the first chapter is dedicated to a review of the literature. It includes three main subjects discussing the tested dental materials, the dentinal substrates used and the various techniques applied to conduct this research. The subsequent chapters include the experiments of this project which are divided into four main studies. In chapter 2, the first experiment investigated the effect of Biodentine and GIC on an in-vitro dentine demineralisation model and validated the use of two-photon fluorescence microscopy, fluorescence lifetime imaging and Raman spectroscopy for the evaluation of remineralisation. Excavated carious dentine was used in chapter 3 to mimic the clinical situation, cements were applied and optical evaluation carried out using tetracycline mineral labelling. In chapter 4, multimodal optical techniques were validated to characterise dentine caries zones and baseline data was established prior to cement application. These samples were then used in chapter 5 to evaluate the cements' interaction and remineralisation potentials on different carious dentine zones. A general discussion of these studies was summarised in chapter 6 with suggested future work for potential research areas.

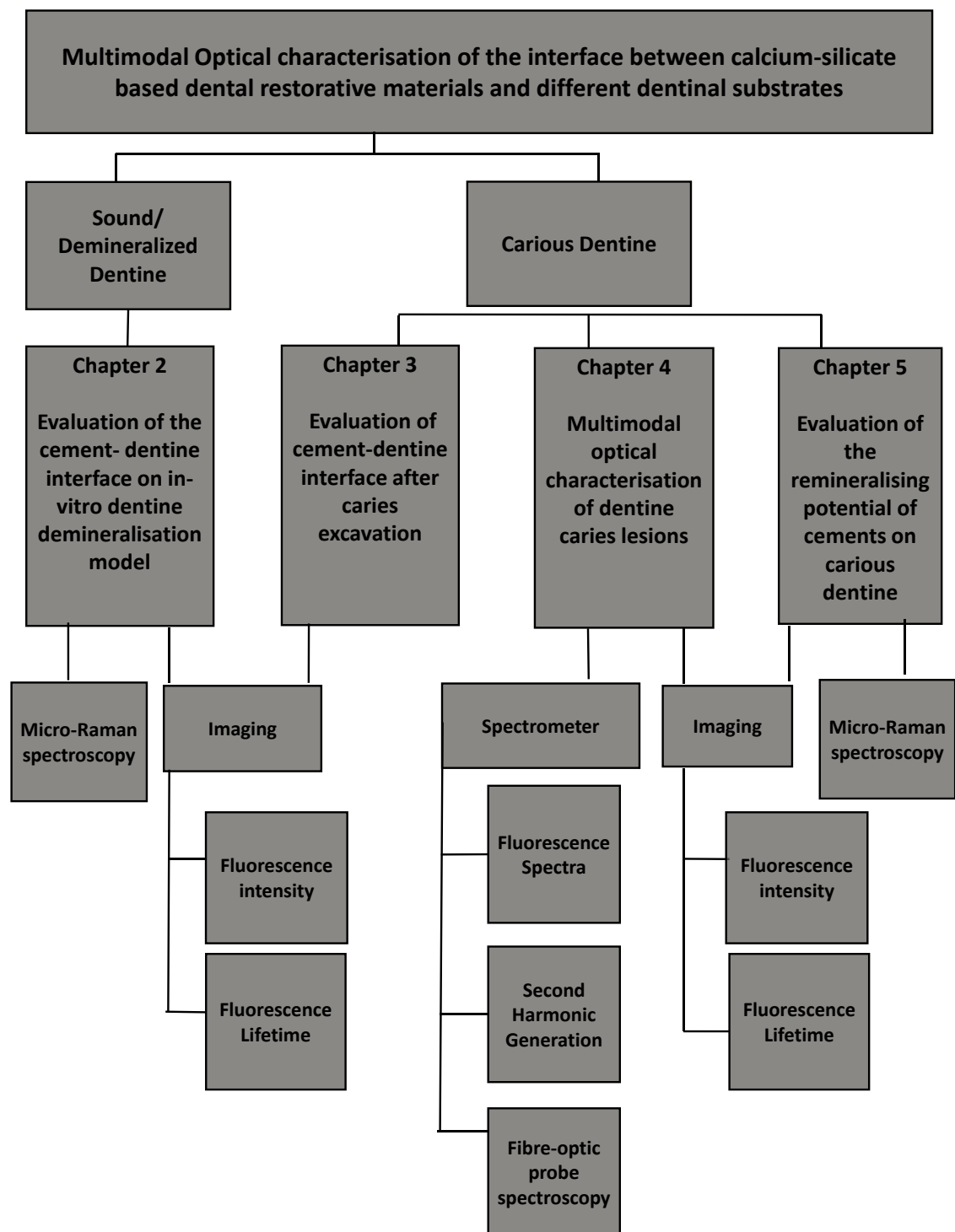


Figure 1 Organisational flowchart of the experiments accomplished in this study with the analytical methods employed.

1. Chapter One: Literature Review

1.1 Dental biomaterials

The evolution of dentistry has been directed towards conservative methodologies under the umbrella of minimal intervention dentistry. Clinically, this approach includes the removal of irreparable infected tissues with maximum preservation of tooth structure. The application of remineralising therapeutic modalities non-operatively may then reverse the demineralisation process caused by dental caries. Advances in dental restorative materials have helped pave the way for conservative treatment modalities to be employed. Initially, an ideal restorative material was required to be biologically inert and biocompatible with acceptable mechanical properties. In the past two decades bioactive materials have emerged to introduce an interaction between restorative materials and tooth tissue. This interaction aims to promote tissue healing and prevent disease progression.

A bioactive material was defined by Hench as “one that elicits a specific biological response at the interface of the material which results in the formation of a bond between the tissues and the material” (Hench et al., 1971). Dental tissues lose most of their mechanical properties as a result of acidic mineral loss caused by the caries process. Bioactive materials are used as an agent for tissue healing which promotes remineralisation and regaining of the tissues’ mechanical properties. They are believed to stimulate biological responses through biochemical and biophysical reactions that result in the formation of an apatite layer, a process known as biomineralisation. The formed apatite-like compounds transform into HA crystals restoring the tissue’s mineral content and thus its mechanical properties. In this project two classes of dental cements (calcium silicate based cement and glass ionomer cement) are investigated for their remineralisation potentials when applied on different dentinal substrates.

1.1.1 Calcium silicate cements

In 1993 Torabinejad introduced the first formula of calcium silicate based cements known as mineral trioxide aggregate (gray MTA) based on the ordinary Portland cement (OPC) (Lee et al., 1993). MTA is a mixture of tri-calcium silicate, di-calcium silicate, tricalcium aluminate, and tetra-calcium aluminoferrite. For better clinical application, calcium sulphate and bismuth oxide was added as a radiopaque (Funteas et al., 2003; Song et al., 2006). The material then became of significant interest as it showed great biocompatibility and potential bioactivity. Its excellent biocompatibility is shown in many biological responses such as minimal toxicity, mild pulpal and periodontal irritation, and dentinal bridge formation (Pitt et al., 1996; Keiser et al., 2000; Nowicka et al., 2013). Subsequently, a newer version of MTA was developed in order to widen its clinical use. White MTA (WMTA) has a similar composition to gray MTA but with reduced aluminate and lacking tetra-calcium aluminoferrite (Song et al., 2006; Camilleri, 2007). Since then, MTA has been used mainly for endodontic applications including root filling, apexification, and pulp capping (Jefferies, 2014).

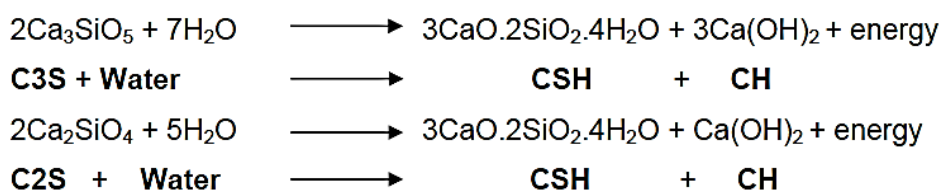
Due to limitations of MTA, mainly associated with clinical handling, extended setting time and reduced mechanical properties, a new calcium silicate based cement called Biodentine™ was recently introduced to the market (Septodont, Saint Maur des Fosse's, France). This material has similar advantages to MTA yet it overcomes most of the clinical problems related to MTA. In addition, the main advantage is that Biodentine™ is commercialised to be used as a novel bulk coronal restoration replacing lost dentine (Koubi et al., 2013). Henceforward Biodentine is the commercial name to be used in this thesis for representation and brevity.

- **Composition and setting reaction:**

Similar to WMTA and Portland cements, Biodentine is composed of mainly tri-calcium and di-calcium silicate that constitute 70% of the total powder weight. In contrast, Biodentine is lacking calcium sulphate, aluminate and aluminoferrite but has the addition of calcium carbonate (acts as a filler) and Zirconium oxide (for radio-opacity). The cement is available in the form of two separate units of capsulated powder and a proportionate liquid containing calcium chloride (a setting reaction accelerator), water, and water reducing agent (Camilleri, 2008; Jefferies, 2014). Other calcium silicate cements such as ProRoot MTA (Dentsply, Tulsa Dental Products, Tulsa, OK) and MTA Angelus (Angelus Soluções Odontológicas,

Londrina, Brazil) are also based on a similar composition. However, the manufacturing process affects the cements behaviour due to the presence of impurities and contamination of their basic components (Camilleri, 2011). On the other hand, Biodentine as well as MTA-bio (Angelus Indústria de Produtos Odontológicos Ltda, Londrina, Brazil) are processed under controlled conditions from raw, highly purified materials in a specialised laboratory rather than from a clinker. This has been advantageous to Biodentine's composition as it helped avoiding powder contamination and the incorporation of aluminum oxide which was found to be associated with some medical conditions such as; Alzheimer's disease (Camilleri, 2011).

As for many calcium silicate based cements although more complex, Biodentine sets through a hydration process (Camilleri, 2007; 2008; 2011). The unhydrated powder phase is converted to the corresponding hydrates in the form of tricalcium silicate hydrate gel and calcium hydroxide this chemical reaction is simplified as follows:



This setting reaction starts with gradual dissolution of both available calcium silicate phases (C3S and C2S) which forms the final hydrated products; calcium silicate hydrates (CSH) and calcium hydroxide (CH). The CSH precipitates and grows on the surface of the remaining un-hydrated calcium silicate particles and thus forming a matrix that holds together all other components and allow for gradual replacement of the un-hydrated granules. Parallel to this, calcium hydroxide diffuses throughout the water filled spaces created between the hydrating components providing the cement with its distinctive high alkalinity (Taylor, 1997; Kjellsen and Justnes, 2004). With continuous maturation and improvement overtime Biodentine exhibits featured physical characteristics. It has been reported that the compressive strength increases gradually until it reaches 300 MP, a similar range with natural dentine after one month (Malkondu et al., 2014).

The initial setting time is reported to be 9-12 minutes, This is faster than the setting time for MTA which is known to be 3-4 hours. Biodentine's faster setting time is attributed to the presence of calcium chloride that is known to accelerate the reaction, the fast dissolution of tri-calcium silicate particles and the absence of calcium sulphate which is known to retard the hydration reaction (Taylor, 1997; Bachoo et al., 2013).

- **Characterisation of the dentine- Biodentine interface:**

Biodentine™ is a biocompatible and bioactive material stimulating tissue repair through the continuous release of ions that act as nucleation sites for hydroxyapatite formation along with inducing inflammatory cell response and hard-tissue formation. Therefore, it became a necessity to investigate its effect on dental and pulpal tissues. Laurent *et al* 2008 were the first to study the interaction of Biodentine with the pulp. In this study, it was concluded that Biodentine is a biocompatible material with no cytotoxic nor genotoxic effect on the pulpal fibroblasts and no modification of the cells' specific function was detected (Laurent et al., 2008). Later, the same authors demonstrated the ability of Biodentine to modulate TGF-1 secretion from pulpal cells and thus induce odontoblast-like cell differentiation and biomineralisation (Laurent et al., 2012).

In another study, the application of Biodentine has been shown to result in reparative dentine synthesis. Biodentine was applied to teeth with a mechanically exposed pulp, the quality of the dentine bridge formed was found to be comparable to that formed by MTA and significantly better than the one under calcium hydroxide (Tran et al., 2012). In another study on deciduous pig teeth, Biodentine resulted in the formation of thick calcification and a completely calcified bridge under the sites of pulpotomy and direct pulp capping respectively. There were no significant differences when compared to the effect of MTA indicating that both were biocompatible as pulp capping materials (Shayegan et al., 2012).

Dentine remineralisation has been gaining increased attention in the last few years. Remineralisation is achieved when dentine undergoes structural and chemical modifications as a result of incorporating several elements that are released from bioactive materials (Han and Okiji, 2011). The biomineralisation ability of Biodentine is related to the large uptake of calcium and silicate ions into the adjacent dentine which has been confirmed by elemental mapping and line-scan analysis. The dentine/Biodentine™ interface displayed a mineral-rich tag like

structure infiltrating into the underlying dentinal tubules in addition to an interfacial mineral infiltration zone (Han and Okiji, 2011; Han and Okiji, 2013; Atmeh et al., 2012). This mineral infiltration (mainly calcium, silicon and carbonate) is found to be accompanied by caustic dentine degradation due to the high alkalinity provided by the cement (Atmeh et al., 2012). Recently, an attempt to determine ultra-microscopically the nature of the formed crystals within the interface was conducted by Kim et al., 2015. It was found that Biodentine displayed an interfacial layer that is thinner than the one produced by MTA with the observation of amorphous calcium phosphate (ACP) within the interface of both materials.

From another perspective, Camilleri reported that the interface is largely affected by the environmental conditions in which Biodentine is stored. It was found that under dry conditions Biodentine shrinks and causes cracks within the bulk material leading to gap formation at the interface which allow the passage of micro-organisms. This is clinically significant, especially when the cement is used as a pulp capping agent (Camilleri et al., 2014).

In-vivo studies, although limited, have been conducted on the interaction of Biodentine with dental tissues. A recent study involving caries-free molars scheduled for extraction reported no significance difference in the responses of teeth between MTA and Biodentine when evaluated as indirect pulp capping agents. In addition, the thickness of the formed dentine bridge was analysed. Although not significant, the dentine bridge thickness was found to be less with Biodentine (Nowicka et al., 2013). This was supported by another study which found comparable results after histologic analysis for dentine bridge formation along with favourable therapeutic effects when Biodentine™ was compared to another two new nanostructured materials based on active silicate cements, and MTA (Popović-Bajić et al., 2013).

A clinical trial by Hashem et al, has evaluated the therapeutic performance of Biodentine when used as an indirect pulp capping agent. The cement was compared to GIC and the patients were evaluated for signs of tissue repair and restoration integrity clinically and radiographically. This study is the only one that has placed Biodentine on what was believed to be caries affected tissues, as chemo-mechanical excavation was used to selectively remove the infected dentine. The outcome indicated that both materials resulted in improved clinical symptoms with no significant difference found. However, radiographically, teeth that received Biodentine showed healing lesions after one year viewed on CBCT while most of

the teeth that did not heal had received GIC. Significant differences between the two materials has been reported in regards to radiographic evaluation (Hashem et al., 2015). The only other clinical trial (Koubi et al., 2013) evaluated the performance and safety of Biodentine as a posterior restoration compared to resin composite. The authors did not mention the characterisation of tissues left in the cavity after caries excavation as the aim of the study was to evaluate the material properties as opposed to tissue healing. The results recommended covering Biodentine with resin composite after a maximum period of 6 months as abrasion increased after this period.

Regarding the interaction of Biodentine with human dentine, the literature provides a comprehensive understanding of Biodentine biological effects when applied to sound or artificially demineralised samples. However, no previous studies investigated this interaction with naturally carious teeth in terms of mineralising potentials. Understanding the nature and dynamics of such interaction would be valuable for the clinical applications of Biodentine as a coronal restoration expected to induce tissue repair.

1.1.2 Glass ionomer cements

Glass ionomer cements (GICs) are also water-based restorative materials. Since their introduction in 1975, they have been the material of choice in various clinical applications (Nicholson, 1998). These cements are conventionally dispensed as a powder and liquid. The powder consists of fluoro-aluminosilicate glass whereas the liquid is formed of an aqueous solution containing polyalkenoic acid. In a later formula the liquid has been introduced as a dried polymer and dispensed with the powder in a capsulated form. In GC Fuji IX_{GP} and some other forms of GICs, calcium has been replaced with strontium to enhance radiopacity. This was found to be a safe replacement with no effect on the cements' setting reaction (Deb and Nicholson, 1999; Billington et al., 2006) or its remineralisation potentials (Ngo et al., 2006).

The setting of the cement involves an acid-base reaction that takes place between the acid polymer and glass particles with its leached ion. At first, dissolution occurs as the acid attacks the glass particle surface leading to ion release (fluoride, aluminum, calcium or strontium). These ions exert the main effect on the cement gelation. As the carboxylic groups within the polyacid become ionised they develop a more linear configuration and a resultant ionic crosslink forms the gel structure of the cement. The final set cement consists of un-reacted glass particles embedded in a polysalt matrix containing cross-links (Walls, 1986; Watson, 1999).

The interaction between freshly mixed GIC and the dentine surface has been characterised to be an interactive ion exchange that results in a chemo-mechanical adhesion between the two substrates. Hydrogen ions released from polyacrylic acid dissolve the glass particles and result in ion release. At the same time, they etch the underlying dentine causing calcium and phosphate ions to move out from hydroxyapatites within the dentine structure (Sennou et al., 1999; Tanumiharja et al., 2001). As a result, an ion rich layer is formed composed of ions leached out from both substrates (Watson, 1999; Yiu et al., 2004). The formation of this ionic layer provides GICs with the ability to chemically adhere to moist dentine resulting in excellent sealing ability and good biocompatibility of the cement (Hilton, 2009).

GIC cements are also believed to prevent caries progression activity by their ability to remineralise the underlying dentine and / or interfere with the remaining cariogenic bacterial growth and metabolism by the release of various ions and by providing an initial low pH. An initial fluoride burst in high concentration was observed during the first 24 h of the setting reaction. This high influx of fluoride decreases the viability of bacteria within the cavity. In addition, fluoride is

incorporated in the formation of fluoroapatite crystals which are more resistant to acid dissolution and, along with calcium and strontium ions, provide the GIC with the capability to remineralise carious tissues (Ngo et al., 2006; Ramasetty et al., 2014). In addition, the presence of silica ions favours the mineralisation effect and enhances the apatite formation (Saito et al., 2003).

Studies conducted in this thesis have used a glass ionomer cement (Fuji IX™) as a control material to which Biodentine was compared. The fact that both cements are water-based type restorative materials with similar clinical application and potentials for remineralising carious dentine justify this selection. However, their interaction and methods of remineralisation with underlying dentine substrate is different and calls for more in depth investigations to enhance understanding the potentials these cements offer.

1.2 Substrates used in this project

1.2.1 Dentine structure

Dentine is a thick mineralised structure that forms the bulk of human teeth. It is a hard, elastic and avascular connective tissue that is assembled by a cell-mediated process. Odontoblasts are highly specialised cells for dentine formation. These cells are responsible for the synthesis of an organic dentine matrix that is then modified by the incorporation of a mineral phase. Dentine's mineralised matrix enables it to withstand stresses from masticatory forces and also provides pulpal protection (Pashley, 1991). The mineral phase composes 70% of the total dentine weight, while organic components and water forms the remaining 30%.

- **Organic matrix**

The organic content of dentine present in the extracellular matrix is composed of mainly collagen type I fibres, with traces of type III and V. In addition, it contains non-collagenous proteins (NCPs) with other growth factors, enzymes (alkaline phosphatase and metalloproteinases), blood serum proteins, and calcium-binding proteins. These major components are distributed into distinctive morphological features that vary with location and undergoes alterations with the influence of age or disease.

Dentinal tubules are a distinct and important feature of human dentine. They represent the tracks that odontoblasts used to move towards the pulp chamber. Their number and morphology varies by location with a high density of tubules present near the pulp. They have an inner diameter about 0.8-2.5µm, occupied with odontoblast cytoplasmic fluid. The tubules' lumens are enclosed by a highly mineralised peritubular dentine with only 10% of its volume consisting of collagen fibrils. The matrix outside the peritubular cylinders (intertubular dentine) contains around 30% mineralised collagen that is wrapped around the tubules perpendicular to their long axis. Thus, dentine is formed of a three-dimensional micro structure that is essential for the tissue's function. Understanding this micro-architecture greatly contributes to the development of the management of different dentine conditions such as caries or cracked teeth syndrome (Elbaum et al., 2007).

• Collagen

Ninety percent of dentine organic matrix weight consists of type I collagen with minimal amounts of type III and V. It is uniformly arranged to form a fibrous three-dimensional interwoven network. Unlike bone collagen, the dentine matrix collagen has numerous crosslinking fibrils. Ultra-structurally, collagen molecules contain one or multiple polypeptide domains arranged in a triple intertwining helical configuration creating a “coiled coil” structure (Figure 1-1). Each of these helical chains has non-triple helical areas located at both ends; NH₂-terminal and COOH-terminal (Butler, 1984). Using electron microscopy collagen molecules showed a staggered arrangement that represents a periodic banding pattern with repeated areas of gaps and overlaps every 690 Å axial length. These repeated units are known as the D-periodic unit in collagen structure (Petruska and Hodge, 1964). This unique interlocking collagen conformation makes up most of the organic matrix of dentine providing uniform spaces and a scaffold for mineral deposition and further crystallisation.

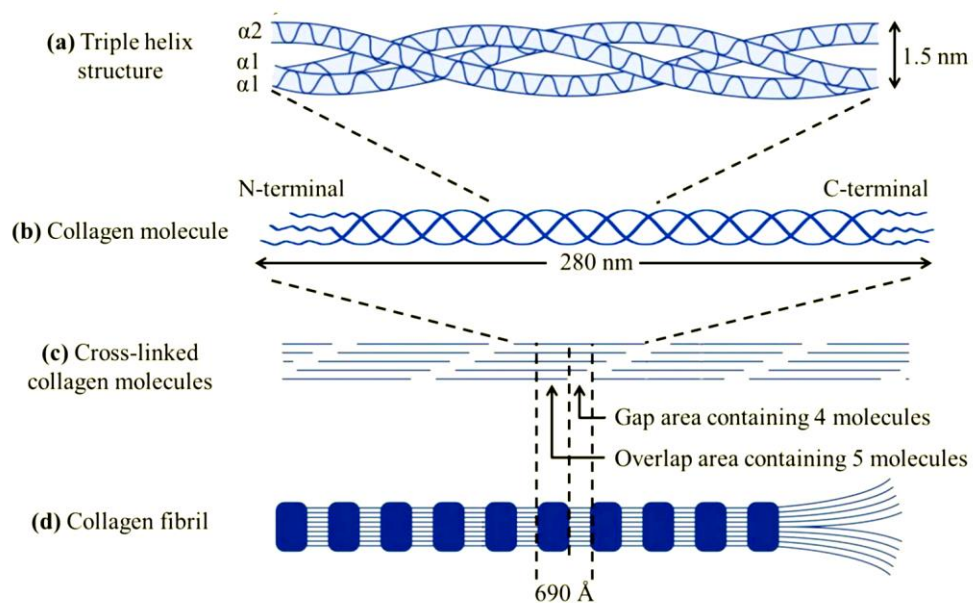


Figure 1-1 A diagram presenting (a) collagen triple helical structure. (b) Collagen molecule contains non triple helical areas at both ends. (c) Cross-linked staggering of collagen. (d) Collagen fibril showing the repeated periodic banding pattern and demonstrating the D-periodic unit with single overlap and single gap (modified from (Cawston, 1998)).

- **Non collagenous proteins (NCPs)**

Generally, non-collagenous proteins (NCPs) constitute the remaining 10% of dentine's organic matrix. They mainly include a family of small integrin binding ligand N-linked glycoproteins (SIBLINGs), proteoglycans (PGs) and γ -carboxyglutamate containing proteins. They are found covering the collagen fibrils with variable extents and are strongly associated with the mineralisation of dentine matrix (Qin et al., 2004). SIBLINGs are acidic non-collagenous proteins that are rich in amino acids. These acidic domains are the main influencers for matrix mineralisation as well as remineralisation. They are found to have a role in nucleating apatite crystallisation, rendering spontaneous mineral deposition thus modulating the growth of apatite crystals to obtain more desirable crystal shapes. In addition, they are flexible molecules that can bind strongly to HA crystals and at the same time provide the rest of the molecular domains available for protein attachment or cell adhesion. Osteopontin (OPN) and matrix extracellular phosphoglycoprotein (MEPE) are found in both mineralised and non-mineralised tissues with their function mainly as inhibitors of mineralisation. On the other hand, more prominent dentine glycoprophosphoproteins are dentine matrix protein 1 (DMP1), and dentine sialophosphoprotein (DSPP) and its subdomains; dentine phosphoproteins or phosphophoryn (DPP) and dentine sialoproteins (DSP) are also expressed during the mineralisation phase of bone and dentine. All of which has its role in regulating the mineralisation phase of the organic matrix. This regulatory role can be explained in two opposite processes. In low concentrations of SIBLINGs, these proteins have high affinity to CaP clusters present in the supersaturated solutions. These amorphous nuclei are then stabilised on the self-assembled proteins and possess a strong affinity towards collagen molecules promoting controlled mineral nucleation on the collagenous template. On the other hand, when these proteins are present in high concentrations, they also bind to the CaP nanoparticles and protect the forming mineral nuclei from further growth and precipitation; this inhibitory role is of great importance in preventing pathologic calcification (George and Veis, 2008).

Other compounds are also present in small percentages within the dentine matrix, including proteoglycans, mainly present in predentine and are essential for collagen fibril formation and aggregation of collagen molecules (Milan et al., 2006). γ -carboxyglutamate containing proteins on the other hand, regulate hydroxyapatite

growth by inhibiting tissue transglutaminase activity in both blood vessels and mineralised tissues (Goldberg et al., 2011).

- **Mineral content**

The mineral phase in dentine is in the form of apatite crystals that are calcium deficient and carbonate rich hydroxyapatite $\text{Ca}_{10}(\text{PO}_4)_6(\text{OH})_2$. The composition of the dentine apatite crystals with low calcium and high carbonate content makes it more soluble to acid and thus more vulnerable to caries attack than stoichiometric apatite (LeGeros and Tung, 1983).

During dentinogenesis, these crystals nucleate within the matrix in the form of spherical structures that grow and fuse with neighbouring spheres to form apatite crystals. The growth and direction of the forming crystals is highly influenced by the organic components, namely type I collagen and non-collagenous proteins within the matrix (Jones and Boyde, 1984). Type I collagen has self-assembling properties which create enclosed spaces where the inorganic minerals can grow. Other biochemical and genetically regulated mechanisms maintain an appropriate saturation of mineral ions in those localised spaces (inter-intra tubular spaces). With high saturation of calcium and phosphate ions, an intermediate precursor polymorph such as; amorphous calcium phosphate (ACP), octacalcium phosphate and dicalcium phosphate dehydrate, are created and then transform to hydroxyapatites. At this stage, Type I collagen only provides the framework with spaces allocated for crystal deposition. Other non-collagenous proteins are involved in controlling the nucleation and growth of apatite crystals by possessing carboxylic acid and phosphate to function as nucleation sites of Ca/P ions and regulate subsequently crystallised apatite form, size and direction (Niu et al., 2014).

1.2.2 Dentine caries

Dental caries is one of the most predominant diseases of the oral cavity. It is a multi-factorial disease, related to lifestyle. It is caused mainly by plaque biofilm which can be modified if its etiologic factors are addressed (Wilson, 2007). The caries process starts when the bacteria within the biofilm produce acids and attack the enamel surface. For demineralisation and caries attack to occur within enamel, many factors are essential, including the time, microbial shift and adherence of the biofilm, pH drop below the critical value (pH 5.5) and oxygen tension (Dawes, 2003).

Dentine is a highly mineralised tissue that is infiltrated by odontoblast extensions from the peripheral pulp. Therefore, dentine is able to respond to those acidic changes even if they were provoked at the enamel surface. The first dentine response is the formation of reactive sclerotic dentine characterised by intratubular mineral deposition located just beneath the demineralised enamel surface (Banerjee and Watson, 2015). At this stage dentine caries is observed as brownish discoloration adjacent to enamel-dentine junction (EDJ), and can be arrested by regular disruption of the biofilm through salivary buffering components, fluoride application, dietary adjustments and physical removal of the biofilm (Selwitz et al., 2007). When further enamel cavitation and demineralisation progresses to a considerable depth within the EDJ, only then will dentine demineralisation be initiated. For dentine caries to spread rapidly along the EDJ, dentine has to be cavitated and colonised by the cariogenic bacteria (Ekstrand et al., 1998). At this stage, the demineralised thus unprotected collagen matrix undergoes direct degradation by means of bacterial by-products and matrix collagenases. The process of dentine degradation and opposing defence reaction by the dentine-pulp complex creates structural changes within dentine that are recognised from the EDJ towards the pulp. These changes are seen as histologically interrelated layers with no clear biological boundaries (Figure 1-2). Carious dentine has been described as two main altered layers, an outer heavily infected with irreversible structural deterioration and an inner layer of caries-affected partially demineralised dentine (Fusayama et al., 1979; Banerjee and Watson, 2015)

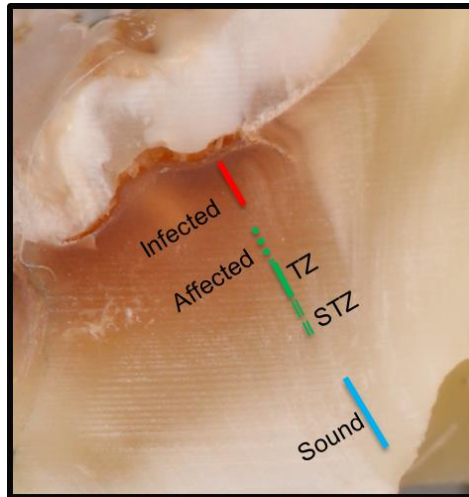


Figure 1-2 A photomicrograph of a carious tooth section displaying the different dentine caries layers. The red line shows the area of caries-infected dentine, it looks dark brown in colour. The green line is the caries-affected dentine, which has a paler brown colour and includes the transparent (TZ) (dotted line) and the subtransparent (STZ) zones (dashed line). The blue line represents normal dentine.

- **Caries infected dentine**

Caries infected dentine is the superficial outer layer of the carious lesion. It is recognised clinically as a soft moist and dark brown layer. It is heavily infected by microorganisms leading to complete demineralisation and degradation of the organic matrix up to a level beyond repair (Fusayama et al., 1966). At an ultrastructural level, the mineral phase of dentine is attacked and totally lost, exposing collagen. Consequently, the unprotected fibres undergo denaturation and degradation resulting in disruption of the fibrillar structure and loss of the characteristic banding pattern and markedly decreased cross-linkage (i.e. DHLNL and HLNL). These structural changes in collagen molecules are permanent and cannot be reversed (Nakornchai et al., 2004). When these tissues were optically examined, significantly higher fluorescent signal was detected and it has been also associated with decreased tissue hardness. The enhanced fluorescence has been attributed to the exposure of chromophore (collagen and organic component) associated with mineral loss in this layer (Banerjee and Boyde, 1998).

- **Caries affected dentine**

The inner layer of dentine caries has recently been gaining more attention due to its potential for remineralisation and repair. Clinically it is described as pale brown, sticky but hard and scratchy (Banerjee et al., 1999). It can be further subdivided into three histological zones: discoloured, transparent and subtransparent (Fusayama et al., 1979; Marshall et al., 1997; Marshall et al., 2001).

In comparison to the infected dentine, the discoloured affected dentine is characterised by less bacterial invasion with partial loss of minerals and reversible damage of the collagen matrix (Kuboki et al., 1977). The mineral phase in this layer is less crystalline, with decreased mineral content compared to normal dentine in which some irregularly scattered crystals have been detected (Ohgushi and Fusayama, 1975). Examining the organic matrix in this layer, it has been found that the general pattern of amino acids within collagen molecules is preserved with no significant differences when compared to sound dentine. However, the intermolecular crosslinks were found to be shifted to their precursor form, which was detected as reduced cross-links but this change is believed to be reversible (Kuboki et al., 1977).

Within the caries process, transparent or sclerotic dentine is formed as a result of the dentine's defence reaction. It involves depositing minerals within the dentinal tubules in an attempt to isolate the carious lesion and indirectly protect the pulp from the penetration of substances. Consequently, the dentinal tubules become occluded with mineral crystals which change the refractive index within the tubules to be similar to the intertubular dentine so it appears histologically translucent when examined using transmitted light. Although the tubules are filled with crystal the overall hardness within this layer is markedly reduced as those crystals are not apatite but "Whitlockite". These crystals are acid-resistant β -octocalciumphosphate which has a lower calcium content than hydroxyapatite and thus are much softer. Moreover, the apatite crystals are significantly decreased in size and number within intertubular and peri-tubular dentine, indicating partial demineralisation. As a result, a decrease in the dentine mechanical properties is detected in this layer since it is largely dependent on the intertubular dentine properties and level of mineralisation. (Banerjee et al., 1999; Marshall et al., 2001).

Under the transparent zone is the subtransparent layer. It is presented as a gradual transition area from the transparent to sound dentine where normal tubular structure appears to be restored and crystals are formed within the intertubular dentine. Thus, the mechanical properties in this layer is enhanced to a degree closer to that of normal dentine (Marshall et al., 2001).

- **Differentiation between caries-infected and caries-affected dentine**

The first guidelines in operative dentistry were established earlier in the past century. It included the term “caries excavation” or alternatively referred to as “cavity preparation”. These terms involved “the mechanical removal of the diseased part of the teeth that were produced by dental caries to prepare the remaining part of the tooth for filling” (Black and Black, 1920). This definition would then mean that cavity preparation is an essential step in caries management to ensure that the remaining tissues are solid sound and provide an adequate retention for the filling material. These cavity preparation guidelines have been modified by the introduction and advances of adhesive restorative materials. Nowadays, caries excavation in view of minimal intervention dentistry is recommended to be confined to the selective removal of infected carious tissues and, if required, bevelling the cavity margins (Banerjee, 2013). Clinical follow ups have revealed that placing bonded restorations over soft carious dentine resulted in long term success of the restoration and arrested caries progression. This is providing that adequate marginal sealing is guaranteed (Mertz-Fairhurst et al., 1998). Consequently, this raised the question: why do we need to remove the caries before placement of the restoration? Apparently, well-sealed margins determine the long-term success of the bonded restoration and since bonding to soft carious dentine is hugely compromised, the answer to that question is that caries excavation is still a mandatory step in caries management in order to achieve better bonding and thus ensure long-term successful restorations (Nakajima et al., 2011). However, there is still no definite clinical identification of the caries excavation limit that will ensure a good quality restoration and at the same time preserve the tooth structure from unnecessary cutting. Tissue hardness testing using a hand instrument is still the gold standard method which translates the biological characteristic of the tissues, although very subjective and dependant on the operator’s clinical skills (Banerjee et al., 1999; Marshall et al., 2001). The removal of infected carious dentine and maximal preservation of remineralisable caries-affected tissue is now a vital

requirement to effectively arrest caries progression and enhancing the survival of the pulp and the restoration. This strongly demanded further input towards more objective and yet conservative delineation between infected and affected dentine to promote selective caries excavation (Banerjee et al., 2000; Kidd, 2004).

Several methods have been implemented in an attempt to discriminate the two main carious layers. Clinical methods include: visual and tactile testing and the use of caries detector dyes. Other methods have been used clinically in laboratory investigations include: techniques based on auto-fluorescence (AF) detection. Bacterial analysis and microhardness measurements (KHN) have been used in laboratory investigations. Table 1-1 summarises these techniques followed by detailed review on the methods used in this PhD project.

Investigation	Technique	General comments	Infected dentine	Affected dentine	Sound dentine	References
Clinical	Visual inspection	Detecting colour changes- subjective	Dark brown	Paler-light brown	Yellowish / white	(Fusayama et al., 1966; Banerjee, 1999)
	Relative tissue hardness	Subjective tactile sensation to detect the consistency and moisture	Wet / soft	sticky/ scratchy	Hard	(Kidd et al., 1993; Banerjee et al., 1999)
	Caries detector dyes	Reflect the status of the organic matrix- subjective with low tissue type specificity	Dark red	Pale-red	Pink	(Fusayama and Terashima, 1972)
Laboratory	Microhardness	Knoop-hardness number- objective but susceptible to operator's skills	KHN > 25	25< KHN<40	KHN<40	(Ogawa et al., 1983; Banerjee et al., 2010a)
	Bacterial analysis	Culturing method: specified known pathogens are cultured	More pathogens detected in infected tissues		No pathogen	(Hoshino, 1985)
		PCR: DNA sequence analysis to detect pathogenic species	Higher species detected in infected tissues		No species detected	(Iwami et al., 2008)
Laboratory	Bacterial analysis	FISH: using fluorescent probe to detect rRNA sequences	Significant decrease is found in species number from infected to sound dentine			(Banerjee et al., 2002)

Clinical and laboratory	AF reduction	Clinical observation using UV light illumination- objective	Drop/ loss of AF signal, not specific for infected/ affected		AF detected	(Sofia Tranæus, 2005)
		QLF: mathematical calculation for changes in AF –objective	Drop/ loss of AF signal, not specific for infected/ affected		AF detected	(Stookey, 2005)
	Blue-green AF	CLSM: Enhances AF signal from carious tissues-objective	Increased AF intensity	Relative decrease AF intensity	No AF signal	(Banerjee et al., 1999; Banerjee et al., 2010b)
		CFOME: CLSM with potential clinical use-objective				(Banerjee et al., 2010a)
	Red-NIR AF	Spectroscopy: Initial spectroscopic AF detection method- objective	Distinct AF signal detected		No AF signal	(Koenig et al., 1993)
		DIAGNO-dent™ Clinical caries AF detection method- objective	Values >30		Values <30	(Hibst et al., 2001; Lussi A et al., 2004)

Table 1-1 A summary of various clinical and laboratory methods used to delineate different zones of carious dentine.

Fluorescence detection

Fluorescence is a distinct property of molecules. When a molecule is excited with a particular wavelength, the energy of the photon is absorbed leading to electronic transition of the object molecule to a higher energy level, then they tend to fall to a more favourable ground state resulting in the emission of the gained energy via radiative (fluorescence) or non-radiative decays (Sofia Tranæus, 2005). The natural fluorescence property of the dental tissues is referred to as autofluorescence (AF) as it occurs without the addition of other luminescent substances. These signals were first reported by Stübel in 1911. Afterwards, it became of great value in investigating dental tissue in health and carious conditions and triggered a vast amount of research to characterise this property and identify its origin. However, to date, these studies have varied in the interpretation of their results especially in regards to the origin of dental autofluorescence.

It has been found that both enamel and dentine exhibit a bluish-white fluorescence signal with a higher intensity related to dentine. This was explained by the role of organic components in the generation of AF signals (König et al., 1999). Moreover, other wavelengths (337 nm and 515 nm) have been used to illuminate dental tissues and accordingly resulted in the detection of multiple emission spectra that were mainly located around 400, 450, 500 and 550 nm wavelengths (Banerjee and Boyde, 1998; Banerjee et al., 2010a; Lin et al., 2011). The majority of these studies have also endorsed the organic components of the dental tissues as the main source of their AF characteristics. Examining the fluorescence of demineralised and hydrolysed dentine suggested that dentine AF is attributed to independent organic molecules of high weight that are not part of the collagen matrix but could be strongly attached to it (Spitzer and Ten, 1976). Consistent with this suggestion, other studies proposed the possible role of collagen cross-linked molecules in the AF of dental tissues, such as dityrosine and pyridinoline. This suggestion was based on the similarity of the excitation and fluorescence characteristics of the crosslinked molecules and those of dentine autofluorescence (Booij and Ten Bosch, 1982; Rivera and Yamauchi, 1993).

On the other hand, other studies have indicated the role of inorganic components as well. Autofluorescence was found to be reduced in carious enamel and was also detected from synthetic hydroxyapatite and deproteinised enamel (Zezell et al., 2007). These findings make it possible to argue the role of inorganic components in

dentine's AF that might be originated from the minerals themselves or from compounds attached to them (Björkman et al., 1991).

Regardless of the multiple theories about the origin of the dental AF, it is well known that it results from the fluorescence characteristic of an intrinsic compound. Thus, the fluorescence must be affected by changes within the dentine structure as in the case of a carious lesion. Fluorescence from carious dental tissues has been of great interest for researchers and clinicians as it proved its significance in clinical application as a non-invasive caries detection and assessment tool. Caries affects the AF behaviour of enamel and dentine, although differently but consistent for both. In enamel the loss of fluorescence is due to internal light scattering in porous enamel structure. Moreover, the fluorescence signal decreases as a result of demineralisation by cariogenic bacteria and their products except for the red region in the fluorescence spectrum where an increase of the fluorescence intensity is detected and believed to be from bacterial by-products (Spitzer and Ten, 1976; König et al., 1999).

Regarding fluorescence detection in dentine caries, the nature of auto-fluorescence is found to be dependent on the excitation wavelength (Ribeiro et al., 2005b). Excitation in the blue region (488 nm) gives green and yellow autofluorescence usually distinguished with a 515–590 nm band pass detection filter (Banerjee and Boyde, 1998). Illumination within the red region (655 nm) produces near-infrared (NIR) fluorescence detected through a long pass filter (transmission > 680 nm). This signal was first found by König et al (1999) who attributed this signal to the production of Protoporphyrin IX by bacterial decomposition and other oral bacterial metabolites.

Cariou lesions alter the dentine structure, as described earlier, to create intermingled zones of caries infected and affected layers. The differences in the dentine structure (mineral and organic phases) between the two layers results in a characteristic fluorescence behaviour for each layer. Therefore, different devices have been used in clinical and laboratory investigations depending on the type of the detected fluorescence signal.

Quantitative laser-induced fluorescence (QLF), uses blue light illumination to detect dental caries depending on the changes in the fluorescence signal detected using a green band pass filter (Stookey, 2005). This device showed satisfactory results when examining enamel caries but has a very low specificity (11%) and high

sensitivity (95.8%) when used to delineate infected and affected carious dentine (Pretty, 2006).

Different devices detecting blue- green AF signal have been utilised in laboratory investigations. The use of confocal laser-scanning microscopy (CLSM) objectively highlighted caries infected dentine where enhanced blue-green caries AF signal was distinguished. This method has been correlated earlier with the change in the mineral content, (Banerjee and Boyde, 1998), tissue hardness number (Banerjee et al., 1999) and bacterial count (Banerjee et al., 2002) . Further development of this technique has been made by introducing a fibre-optic microendoscope (CFOME) which allows accessible detection of the AF signal from different points in the carious lesion and has the potential to be developed for clinical use (Banerjee et al., 2010a).

In addition, spectroscopy has been introduced as a novel, minimal or non-invasive method for caries detection and diagnosis. They are based on the difference in fluorescence between sound and carious tooth structure. This difference was first described by Alfano and Yao, (1981). A study by Koenig et al (1993), was able to detect AF signal within carious lesions based on the detection of the NIR signal using fluorescence spectroscopy (Koenig et al., 1993). In 2005, Subhash *et al.* found significant differences between fluorescence intensities detected at different stages of caries, the sensitivity to these differences was improved by modifying the analysis of the laser-induced fluorescence (LIF) spectra (Subhash et al., 2005). Another in vitro study was conducted to evaluate the ability of a laser operating at 405 nm to detect different stages of enamel caries activity and found significant differences between the fluorescence spectra (Ribeiro et al., 2005a). Zezell et al. observed that the areas under the fluorescence bands at 455 and 500 nm differ significantly between caries enamel lesions and sound tissues (Zezell et al., 2007). These previous spectroscopic studies described the use of this method to detect and differentiate dental caries from sound tissues. However, studies on dentine caries and the application of this method to identify the caries ends point in laboratory research are still minimal.

DiagnoDent is a device used in clinical and laboratory caries investigations. It uses laser excitation within the red region thus AF detected is believed to originate from the bacterial products thus measuring the bacterial content of the carious lesion rather than mineral or structural changes (Shia et al., 2000; Lussi A et al., 2004). A study showed that it has good specificity and sensitivity in detecting both occlusal

and smooth surface lesions (Lussi A et al., 2004). However, these studies lack information about the degree of dentine staining as well as the status of the carious lesion (active, arrested). Other limitations of the device include, the need for the tooth surface to be clean and dried. In addition, the presence of an existing restoration may alter the device readings with no evidence to support its reliability to detect proximal caries or recurrent caries adjacent to any restoration type. Moreover, DiagnoDent readings are found to be affected by the residual dentine staining, calculus and plaque as they may provide false positive results. On the basis of these findings the use of DIAGNOdent in detecting the caries endpoint can be of doubtful benefit (Shi et al., 2001; Pretty, 2006; Neves et al., 2011a).

Microhardness measurement

The significant decrease in the dentine physical properties (i.e. hardness) due to caries attack was found to vary between infected and affected dentine as the bacterial count is reduced in the latter. Accordingly, tissue hardness measurement remains the only visible translation of the structural changes within carious dentine. Clinically, operators depend largely on the relative tissue hardness using probing by hand instrument to determine the endpoint of caries excavation (Banerjee et al., 2010a). When applied to in-vitro studies of carious dentine, it was found that dentine hardness is related to its mineral content (Sakoolnamarka et al., 2005a). Using a Knoop diamond indenter for tissue microhardness measurement has been widely applied in-vitro to delineate different dentine caries layers and to detect changes in the dentine physical properties when different therapeutic materials were applied. (Banerjee et al., 1999; Kirsten et al., 2010). However, this technique is subjective to the operator's skills in addition to its being relatively destructive. Moreover, the hardness value may be affected by the sample position and moisture condition which is technically challenging specially when applied to dentine. In terms of discriminating dentine caries zones, tissues are considered caries-infected dentine if the Knoop hardness number (KHN) was less than 25, while the hardness of caries affected dentine ranges from 25 to 40 and the sound dentine records KHN above 40 (Ogawa et al., 1983; Banerjee et al., 1999; Banerjee et al., 2010a).

1.2.3 Demineralised dentine

In-vitro models of artificial caries have been employed to enable investigations of several aspects of dental research including the application of different preventive and treatment modalities, caries excavation and adhesion. Nowadays caries management is directed towards conservative and preventive approaches. This minimal intervention concept aims to preserve the tooth tissue, so the tendency in cavitated lesions is to solely remove infected carious tissue. Consequently, the caries removal techniques used, the effectiveness of preventive agents and the interaction and efficacy of bioactive restorations placed are essential issues to study. Based on the diversity of the aims of such studies, the methodology used should be carefully chosen. Consequently, various methodologies have been proposed to produce dentine models with caries-like lesions resembling caries-affected dentine in an attempt to overcome standardisation issues when using natural caries samples. These methodologies include either acidic demineralisation or microbiological caries induction.

The use of acidified gel is widely implemented for enamel demineralisation due to its simplicity. In addition the produced lesion shows similar histological and mechanical properties to that of natural caries lesions (Silverstone, 1968). However, subsurface lesions have been found to develop due to impurities in some of the gel-based systems (Pearce, 1983). In addition, models created by acidic gel techniques are criticised of being pure demineralisation models lacking the influence of saliva or biofilm. Other models prepared by pH-cycling are subjected to alternating periods of demineralisation and remineralisation with continuous replacement of the solution. It has been found that pH-cycling produces greater demineralisation compared to acid gelation regarding enamel lesions (Damato et al., 1988). Nevertheless, they still did not implement saliva and biofilm models, which may explain why their lesions were shallower than naturally created lesions.

Dentine demineralisation is more complex than in the enamel lesion as in the natural process it involves degradation of the exposed collagen matrix by means of bacterial acids and proteinases. This breakdown of collagen molecules cannot be reproduced by acidic demineralisation, by either gel or cycling. This may have an advantage of providing dentine models with intact organic matrix similar to that found in caries affected dentine but without the variability of pulpal influence (Kuboki et al., 1977).

Microbiological methods include lesion formation by means of acids produced from bacterial strains or cultures. This method is found to produce models similar to natural dentine caries in terms of colour, hardness and the presence of two distinct layers (Clarkson et al., 1984). However, this method is not without limitations, it is considered more complex and time consuming than acidic demineralisation. Moreover, it is difficult to standardise the protocol or the extent of microbiological effect on the prepared samples. Therefore, the selection of a dentine demineralisation technique depends on what the research is investigating and the characteristics of the dentinal substrate required to implement this research.

1.2.4 Dentine remineralisation

Throughout the individual lifetime, dentine demineralisation and remineralisation co-exist. As discussed earlier, pathological demineralisation of teeth occur as a result of cariogenic bacterial attack. With caries progression, therapeutic intervention is required. In light of minimally invasive caries management, prevention and treatment of dental caries remain a major challenge with nine out of ten adults being affected by dental caries in western countries only (Bagramian et al., 2009). Dental restorations have been frequently reported to fail especially when applied to damaged dentine (Liu et al., 2011c). Thus, biomimetic dentine remineralisation has been extensively targeted within the field of dental biomaterials to limit caries progression and improve the durability of dental restorations.

Different approaches have been proposed for the remineralisation process of dentine. They can be classified into classical and non-classical approaches depending on the mechanism of apatite crystallisation and growth.

- **Classical ion-based remineralisation approach**

Also known as top-down classical remineralisation (Liu et al., 2011b). Different strategies are applied to induce remineralisation such as fluoride releasing restorations and bioactive glass containing adhesives. Remineralisation using these materials is based on epitaxial deposition of calcium and phosphate ions over pre-existing apatite crystals. These crystals act as nucleation sites upon which primary ions from surrounding solutions can precipitate. When the forming ion clusters reach the size of what a so called “critical crystal nucleus” they grow via ion by ion attachment. These crystals are relatively large in size, which prevents their penetration into interfibrillar spaces within the collagen fibres, resulting in only extrafibrillar remineralisation of the collagen matrix (Liu et al., 2011a). Recent studies on this type of classical remineralisation have considered it non-functional or incomplete remineralisation (Tay and Pashley, 2008; Liu et al., 2011a). Moreover, this classical ion-based crystallisation pathway cannot be applied when attempting to remineralise caries infected dentine or completely demineralised dentine that are produced by acid etching, due to the absence of seed crystallites in those areas which are required for apatite formation.

- **Non-classical particle-based remineralisation approach**

This is considered as biomimetic remineralisation, also referred to it as a “bottom-up” approach. This dentine remineralisation pathway does not depend on seed crystallites instead it relies on the stabilisation of liquid like amorphous calcium phosphate (ACP) by means of biomimetic analogues of non-collagenous matrix proteins (NCP). Therefore, it could be considered as a potential approach that re-establishes the dynamic mechanical properties of exposed collagen close to the properties of mineralised tissues. It is therefore believed to be very useful when restoring totally demineralised dentine (Niu et al., 2014).

Recently, evidence of applying this pathway have increased in the literature. It has been proposed as an alternative in-vitro technique to produce a hierarchical structure of intrafibrillar apatite within the collagen matrix (Tay and Pashley, 2008). The first suggested analogue to apply this approach is the use of a polyanionic molecule, such as polyacrylic acid which promotes the formation of nano-precursors (ACP) in the form of flowable liquid-like nano-aggregates (Tay and Pashley, 2008; Liu et al., 2011a; Qi et al., 2012). These small size precursors are able to infiltrate and then precipitate in the water-filled gap zones within collagen fibrils as apatite nanocrystals (Tay and Pashley, 2008). This precipitation and further growing into apatite is guided by a second analogue that substitutes the dentine matrix phosphoproteins (Gu et al., 2011). These are usually phosphorylated molecules that encourage the alignment of the formed crystals and leads to the desired hierarchical dentine remineralisation (Liu et al., 2011a).

Calcium silicate based cements are considered bioactive materials that induce remineralisation through this bottom-up remineralisation approach and have been used as a source of calcium ions. Upon hydration, these cements have the ability to release calcium ions over a long period of time (Tay and Pashley, 2008; Camilleri, 2011). In addition silica ions are also released which are found to be a strong inducer for dentine remineralisation (Saito et al., 2003; Han and Okiji, 2011). Moreover and most effectively, these cements provide a highly alkaline environment. This sequentially favours both matrix phosphorylation (Zhang et al., 2012), and apatite crystallisation to form nano-precursors and complete the remineralisation process (Tay et al., 2007). The advantage of high alkalinity also enhances remineralisation of dentine by its potential proteolytic effect (Inaba et al., 1996). The non-classical remineralisation approach provides continuous

replacement of water spaces within the collagen matrix by apatite crystals, which is controlled by the presence of matrix NCP or their substitutional analogues. However, the use of these analogues is clinically challenging, although some recent attempts to make it available for clinical use has shown promising results (Qi et al., 2012).

In summary, earlier studies on Biodentine cement have confirmed the cement's bioactivity and potential remineralisation effects. These studies investigated the cement's activity on sound and demineralised dentine but no studies has been conducted to confirm the capability of the cement to induce mineralisation in carious dentine which would be valuable regarding the cements' clinical applications in deep carious lesions.

1.3 Optical Methods used in this project

1.3.1 Introduction to optics

The field of optics is defined as; the study of light's propagation either in space or matter, including the interaction between them (Baldwin, 2012). When studying the interaction of light with matter, optics delineate this interaction into two levels. Geometrical physics, that deals with the light interaction when directed to surfaces, such as reflection and refraction. The second is physical optics which deals with the interaction at a molecular level, which will be the subject of the following discussion. A material system depends on the energy transfer between its molecules to control the stability and the interaction of the system including its behaviour when illuminated with light. Light propagates as photons which are considered a form of energy. Thus when a matter interacts with light of a certain wavelength, these photons bombard the surface with a specific energy proportional to their frequency. Energy transfer then takes place between the two via a process involving the interaction of the light's electromagnetic force and the distribution of the electronic cloud within the molecule. Depending on this interaction the energy is either absorbed by the molecules or the photons will be scattered in different directions. Energy absorption will lead to the excitation of the electrons within the molecule up to a higher excited electronic state, whereas the bombarding photons vanish. On the other hand, scattering can be in the form of elastic (Rayleigh scattering) or non-elastic (Raman scattering). When the incident photon energy remains unchanged and the light is scattered with a similar wavelength as the illuminating light it is known as elastic scattering. Soon after, the excited electrons tend to drop to a more favourable ground state by re-emitting the absorbed energy by either non-radiative decay (such as heat) or radiative (fluorescence) (Sofia Tranæus, 2005).

Non-elastic (Raman scattering) involves scattering of photons with a higher or lower energy level. These different optical phenomena and the associated changes in the energy level are described in the Jablonski diagram in Figure 1-3 (Xu, 2001).

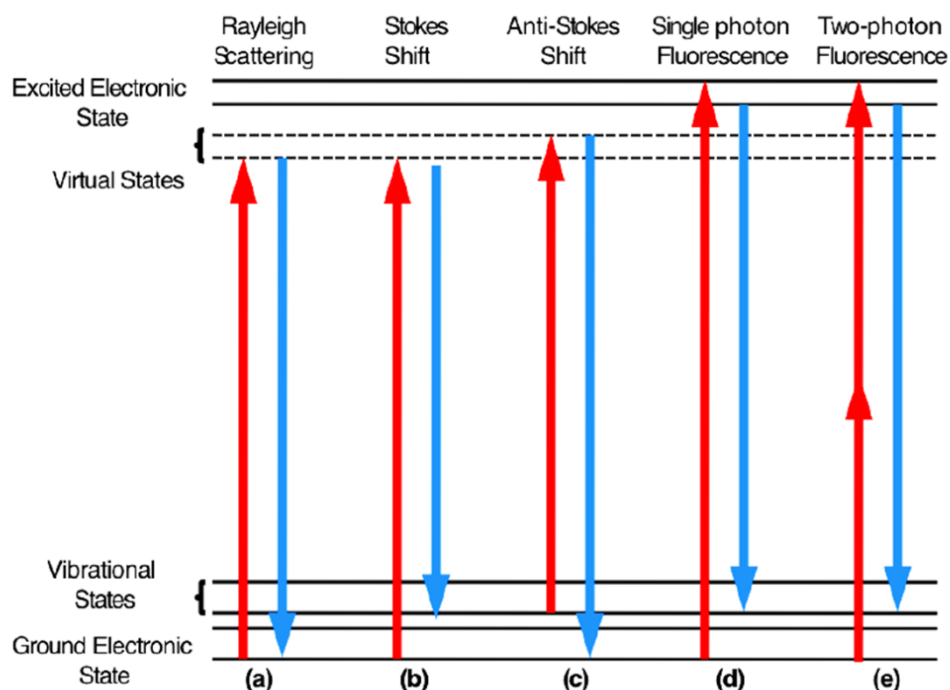


Figure 1-3 A Jablonski diagram demonstrating different optical phenomena resulting from changes in the energy level of the electrons within a molecule after interaction with light. **(a)** Rayleigh scattering occurs when the light is scattered with similar wavelength as the incident light. Non-elastic scattering occurs when scattering the incident photon with a reduced energy, known as a Stokes shift **(b)**, or a higher energy described as an anti-Stokes shift **(c)**. **(d)** Following absorption, the gained energy is released with different energy and wavelength in the form of fluorescence. **(e)** Fluorescence through two photons excitation involves two photons, each with half the fluorescence excitation energy to excite the fluorophores and produce fluorescence. (Red arrows is the excitation photons, Blue is the emission energy), Courtesy of (Xu, 2001).

1.3.2 Two-photon fluorescence microscopy

Non-linear optics refers to unconventional interactions between light and matter. It refers to any interaction that resulted in a response or output from the illuminated materials that is altered in a nonlinear way depending on the intensity of the applied light (Boyd, 2003). Non-linear behaviour is a property of certain materials when excited with a very high intensity light sources, such as a pulsating laser.

Based on non-linear excitation, two photon microscopy imaging has emerged as an advanced imaging technique. The fluorophore within the examined samples is excited through a simultaneous absorption of two consequent photons which promote the transition of their energy to an excited state. In this technique, an intense laser with an excitation wavelength twice that required for the fluorophore emission is used. Two photons are used to excite the fluorophore resulting in a non-linear fluorescence, (see Figure 1-3- e). Two photon excitation only occurs within the volume of the specimen that has the highest photon intensity which limits the excitation within a specimen volume to be at the focal plane of the objective lens.

When compared to confocal microscopy, this imaging technique provides superior three-dimensional optical sectioning as the microscopic field is confined to the area irradiated by two consequent photons. No pinhole is required to suppress the out of focus fluorescence. Accordingly, it offers deeper penetration up to 500 μm with lower photo-toxicity to the specimen. In addition, it provides wider separation between the excitation and emission spectra and reduces the background scattering (So, 2008; Becker, 2008).

- **Autofluorescence**

Fluorescence is a radiative process that results in the emission of light with a lower frequency range following optical excitation with a higher frequency light that leads to electronic transition of energy states. This process requires a characteristic excitation frequency called the “excitation wavelength” that leads to light being emitted in a certain frequency known as the “emission wavelength”. These characteristic wavelengths are dependent on the nature of the fluorescent molecules. Molecules that have the ability to fluoresce are called fluorophores. Each fluorophore exhibits distinct optical characteristics:

- *Excitation and emission spectra*: are particular energy levels required by the molecule to be able to fluoresce and its correspondent wavelength of the emitted light (Karlsson, 2010).
- *Quantum yield energy*: represents a quantitative measure of fluorescence emission efficiency. It is expressed by the ratio of emitted to absorbed photons (Learmonth et al., 2009).
- *Fluorescence life-time*: the time that a fluorescent molecule spends in the excited electronic state prior to its return to the ground state, this will be discussed below (Learmonth et al., 2009).

These characteristics are dependent on the fluorophore structure as well as other environmental factors and are useful in identifying different fluorescent molecules. Fluorophores differ in their origin, they are either internist or extrinsic fluorophores. In living tissues certain molecules have the ability to fluoresce when excited with a definite “excitation wavelength”, these molecules are called intrinsic fluorophores and the process is defined as “auto-fluorescence”. Although auto-fluorescence may be undesirable as it generates background noise especially when examining samples labelled with an extrinsic fluorophore, AF detection is a very valuable technique to provide information about examined specimens (Billinton and Knight, 2001).

Regarding dental tissues, AF detection has been an area of interest in the past decade triggering numerous investigations that aimed to characterise the fluorescence behaviour of sound and carious tissues and to detect the origin of this natural fluorescence (Luciano Bachmanna, 2006). Many studies indicated the role of organic components in the generation of AF signals, others suggested that inorganic compounds themselves or molecules attached to them are responsible for the characteristic AF signal. Regardless of the anonymity of the AF origin in dental tissues, all these studies agreed that it is an intrinsic fluorophore which is affected by the health and integrity of the dental tissues. Accordingly, as caries causes changes in both organic and inorganic components of dentine, it has been found that caries has a major and clinically valuable effect on the fluorescence behaviour of dental tissues. Carious dentine exhibits higher fluorescence intensity that decreases gradually towards sound dentine (Terrer et al., 2016). When these changes in AF intensity were observed with blue-green excitation, researchers

attributed them to the breakdown of structural proteins by means of bacterial invasion and certain proteases (McConnell et al., 2007; Almahdy et al., 2012). Other studies attributed AF signal to the production of Protoporphyrin IX by bacterial decomposition and other oral bacterial metabolites as they used excitation in the red region (König et al., 1999).

The effect of in-vitro dentine demineralisation could be considered rather “confusing”. If we agreed on the organic origin of the AF signal, then in demineralised dentine, where no changes in the organic components are expected, the AF signal should remain unaffected. However, AF changes have been detected within these samples as two opposite observations. Some studies found an increased AF signal intensity within demineralised dentine, encouraging the claim that chromophores responsible for the AF signal must be organic in nature. As a result of the demineralisation process these chromophores are assumed to be modified, de-quenched or become concentrated as the tissues shrink (Van der Veen and Ten Bosch, 1996; Banerjee and Boyde, 1998). It is worth noting that the increased fluorescence intensity was detected only after four days of demineralisation as no changes were detected before that period (Van der Veen and Ten Bosch, 1996). This could be an indication that in order for the fluorescence signal to be enhanced, a considerable amount of mineral loss should take place exposing the organic matrix and causing concentration of the chromophores. In contrast, another study reported a significantly weaker or no signal from the demineralised dentine when compared to a significant fluorescence increase which was detected in the bacterial demineralised group (Shigetani et al., 2008).

Such discrepancies in the AF detection should be studied to achieve a better evaluation of the examined samples by combining this technique with other stain-free imaging techniques, such as, FLIM and SHG imaging. These techniques also depend on the behaviour of the intrinsic components when optically excited providing characteristic examination of the living tissues with minimal intervention.

- **Auto-Fluorescence lifetime**

As explained in the Jablonski diagram, (Figure 1-3), when a molecule absorbs photons of a certain energy (wavelength) it undergoes a series of photo-physical events. The decay constant (k) of each of these processes characterises the probability of a process to occur. When radiative decay of the excited fluorophores takes place (as in Figure 1-3- d, e) the time that excited molecules need to reduce

their gained energy is proportional to this decay rate $1/k$ and is known as the mean lifetime. Fluorescence lifetime is also defined as the time required by a population of excited fluorophores (N) to exponentially (e) decrease their energy (to a more favourable ground state) via loss of energy through fluorescence (Berezin and Achilefu, 2010). It is a characteristic optical feature for each molecule and has become widely used for various biological and medical diagnostic applications.

Unlike auto-fluorescence intensity, lifetime is not dependent on any initial excitation conditions, such as wavelength, single or multiphoton excitation. It is also not sensitive to the fluorophores concentration or AF intensity. However, lifetime is affected by a number of internal and external factors that can be advantageous when investigating the tissues' biological status and differentiating healthy from diseased. Internal factors are mainly described as the fluorophore structure while environmental influencers may include oxygen concentration, pH values or the presence of a fluorescence quencher. These unique independent characteristics introduce fluorescence lifetime imaging as an additional distinct microscopic marker and encourage its integration into the family of molecular imaging tools.

Auto-fluorescence lifetime imaging (FLIM) can be performed either in a steady-state or time-resolved mode depending on the aim of monitoring lifetime changes. In steady-state fluorescence measurements, lifetime imaging is directly performed by measuring the fluorescence intensity and averaging its value over time then a lifetime map of the sample is generated. Using this method is beneficial for monitoring the sample's functional changes due to environmental factors and to gather information about its morphology and status (Lakowicz, 2013). Time-gated fluorescence lifetime measurements use a pulsating laser source with a high speed fluorescence detection system to measure the fluorescence lifetime in real time without averaging. This method provides a recorded lifetime value for each excited fluorophore. In the displayed image the intensity of each pixel in the created image represents the fluorescence lifetime of the fluorophore rather than its fluorescence intensity. In contrast to the steady-state method, time-resolved imaging offers the elimination of background fluorescence which enhances the image contrast. This is possible because this method is able to differentiate between the fluorophores that have similar excitation and emission spectra depending on the difference in their fluorescence lifetime. Therefore, FLIM provides valuable information about changes in the fluorophore's structure at the molecular level as well as the effect of

the environment surrounding them such as temperature and pH (Chang et al., 2007). All of these advantages make FLIM a very useful technique to monitor treatment responses and delineate healthy from diseased tissues. Regarding dental research, the application of FLIM has been performed in few studies that revealed fluorescence decay of the carious tissues distinct from healthy (Alfano and Yao, 1981; McConnell et al., 2007; Lin et al., 2011). These studies were consistent in their observations as shorter lifetime values were detected from carious dentine, although an inverse effect of caries has been reported (Koenig et al., 1993). However, further applications of FLIM in dentistry have the potential for more investigations in order to implement this technique for the evaluation of dental tissues.

- **Second harmonic generation**

Second harmonic generation microscopy (SHG) is another type of non-linear interaction between light and matter. It is an inherent property of some materials that are non-centrosymmetric. The production of an SHG signal requires a high intensity laser source to produce an additional frequency component with double the frequency (2ω), half the wavelength, of the illuminating light, which is the SHG signal. This signal is generated in addition to the usual linear component that results in Rayleigh scattering (Boyd, 2003). Structures that are able to produce an SHG signal are limited, for example collagen. Therefore, the detection of such a signal offers a highly specific stain-free evaluation technique of living tissues (e.g. connective tissues). Conditions like heat and enzymatic cleavage cause changes within the structure of proteins and were found to reduce the produced SHG signal (Kim et al., 2000). Consequently, this technique provides efficient identification and monitoring of such conformational changes within collagen.

Upon examining dental tissues, an SHG signal was detected mainly in sound dentine and to a lesser extent in enamel, which initiated speculation that collagen is the main source of this signal and not HA crystals, thus being confirmed in later studies (Altshuler et al., 1995; Chen et al., 2007; Elbaum et al., 2007). Second harmonic generation microscopy was suggested as appropriate to study the changes in dentine structure as a result of caries attack or due to the effect of applying restorative materials (Altshuler et al., 1995; Lin et al., 2011; Atmeh et al., 2012; Terrer et al., 2016).

1.3.3 Raman spectroscopy

The micro-Raman spectroscopy technique is a non-destructive spectroscopic technique that identifies the chemical content of tissues or materials by detecting the characteristic vibrational energy modes of certain chemical bonds within their molecular structure. The Raman spectra is released with an energy representing the difference between the incident and inelastically scattered photon which is dependent on the energy of the molecular vibration (see Figure 1-3- b,c). The obtained Raman spectra are then represented as spectral charts with the use of a charge-coupled device (CCD). These charts consist of multiple characteristic peaks that can be allocated to their wave-number as each peak represents a unique vibrational mode in the molecule. This characteristic Raman spectrum map can be considered as a molecular fingerprint of the material by which it can be identified. In addition, each peak intensity is proportional to the number of the molecules it represents within the volume of the scanned area which provides quantitative information about the structure of the tested sample (Penel et al., 1998).

- **Streamline™ technology**

Renishaw plc (Wotton-under-Edge, UK) has developed this novel Raman imaging technique with an integrated distinctive hardware and software. It is a dynamic Raman mapping combining line-laser scanning of the sample with sample movement in a vertical and horizontal direction facilitated by placing the sample on a motorized movable stage. This combination enables Raman mapping performance to be 200 times faster than the conventional point by point mapping where these steps are carried out in sequence and not simultaneously (www.renishaw.com). After Streamline Raman scanning, the scanned area of interest is represented as a series of points producing a chemical Raman image. Each point has its own Raman spectrum identifying the chemical structure of the sample at that point.

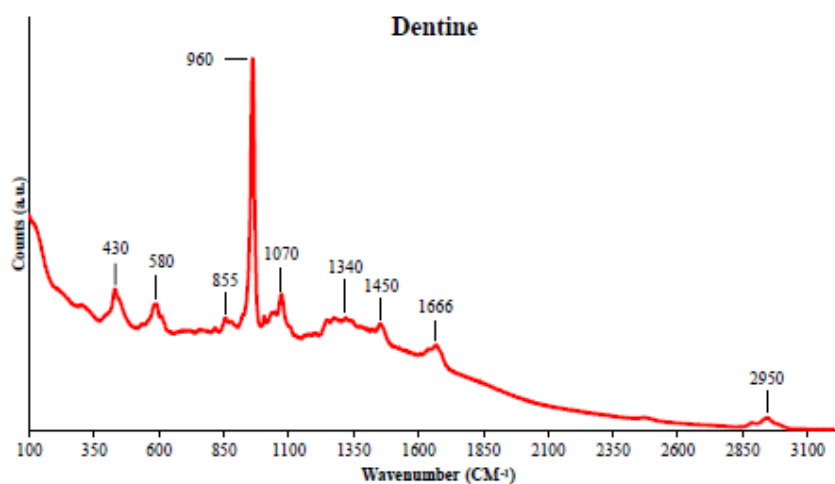


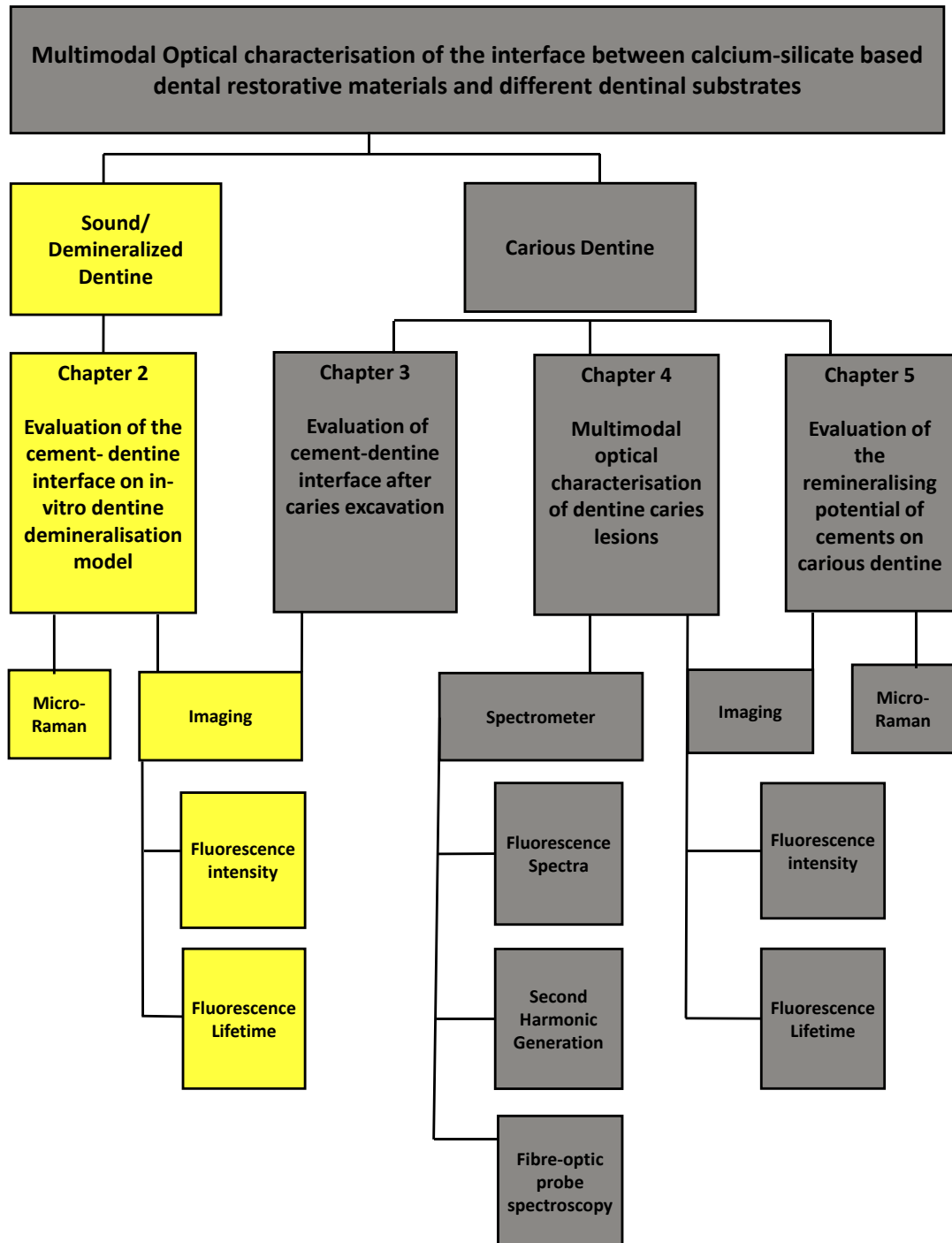
Figure 1-4 Raman spectra for sound dentine between 100-3100 cm^{-1} wavenumbers presenting the observed peaks, the assignments for these peaks are summarised in Table 1-2

Featured Peak wavenumber (cm^{-1})	The assigned band and histological representation
430	(v2) of PO_4^{3-} (O–P–O bond), Hydroxyapatite
580	(v4) of PO_4^{3-} (O–P–O bond), Hydroxyapatite
855	C–C, organic material
960	(v1) of PO_4^{3-} (P–O bond), Hydroxyapatite
1070	(v1) of CO_3 , Hydroxyapatite
1340	Amide III, Protein
1666	Amide I, Protein
2950	C–H banding, Organic material

Table 1-2 The common featured dentine peaks with their tentative assigned bands and correlated histological components (Spencer et al., 2000).

Raman spectroscopy provides many advantages including; easy and non-destructive sample preparation, direct representation of chemical concentration and relatively simple and reliable analysis of the produced spectra. These advantages encouraged the use of Raman spectroscopy in dental research. This technique was found valuable in evaluating the microstructural variations in sound and carious dental tissues (Figure 1-4) (Tramini et al., 2000; Sakoolnamarka et al., 2005b; Almahdy et al., 2012). Raman analysis has been also widely used to characterise the chemical composition of some dental materials and detect chemical changes associated with the materials' setting and maturation, such as calcium silicate cements and GIC and the nature of their interaction of the underlying tissues (Martinez-Ramirez et al., 2006; Atmeh et al., 2012). Quantitative information about the mineral distribution within dental tissues was achievable using Raman spectroscopy. As the phosphate peak at ($959\text{ cm}^{-1}\text{ v1}$) represents the apatite minerals (Spencer et al., 2000), it has been employed to detect mineralisation and to monitor the changes in its intensity that provides evidence about the dynamic mineral changes (Sauer et al., 1994; Parker et al., 2014; Milly et al., 2014).

2. Chapter Two: Evaluation of an In-vitro dentine demineralisation model and assessment of the remineralisation potentials of dental cements



2.1 Introduction

The concept of minimal intervention dentistry (MID) was first introduced in 1997. It then evolved as a result of the increased understanding of the caries process, methods of caries prevention and the new advances in adhesive restorative materials. For an effective implementation of MID clinically, a full understanding of the physico-chemical interaction between the available materials and the remaining dental substrate in the cavity is required. This interaction was formerly thought to be passive simple infiltration within the dental tissue. However, a more aggressive chemical interaction was recently elucidated with either resin or water-based cement materials (Atmeh et al., 2012; Yoshida et al., 2012). The mechanism of these interactions is believed to promote “bioactivity” where the materials exhibit the ability to use, stimulate, or supplement a natural regenerative response at the interface and form a chemical bond between the material and the substrate. This unique interaction will consequently result in achieving an optimum therapy with a long-term successful outcome under the umbrella of MID (Watson et al., 2014).

Remineralisation is a natural repair process that occurs to counterbalance demineralisation of the teeth caused by caries. The relative balance between these two actions determines whether destruction (caries) or repair (remineralisation) occurs (Featherstone, 2009). Natural remineralisation is a simple inorganic process that requires the presence of calcium and phosphate ions to recrystallize on the surface of the remaining crystals in enamel or dentine. The newly formed minerals may be more resistant to dissolution by acids especially if fluoride is available to be incorporated in the new crystal formation. Therefore, developing new materials that can induce this natural process is an important requirement in restorative and preventive dentistry (MID).

Several techniques have been used to assess changes in the mineral contents of different in-vitro dentine models as a result of their interaction with dental restorative materials. These techniques include microscopic assessment using scanning and transmission electron microscopy (SEM) & (TEM), evaluation of the density using x-rays and spectroscopic analysis such as: Micro-CT (Neves et al., 2010) and X-ray diffraction (XRD) (Saito et al., 2003), energy dispersive X-ray spectroscopy (EDX), Raman spectroscopy (Vollenweider et al., 2007) and Fourier transform infrared spectroscopy (FTIR). These techniques are of significant use for mineral quantifications; however, many do not provide sufficiently high resolution to effectively record the morphological changes within the structure of the mineralised dentine matrix. Multi-photon microscopy is known to provide detailed observation of

the dentine matrix with high resolution and without the need for extensive sample preparation. Our division hosts a multiphoton microscope which is capable of auto-fluorescence intensity and lifetime imaging in addition to second harmonic generation imaging SHG and spectroscopy. Using these imaging techniques would be valuable in assessing changes within the dentine matrix (mineralisation and organic matrix integrity) and their effect on the fluorescence properties of the examined tissues.

Glass ionomer cements (GIC) are water-based restorative materials. The setting of GIC is an acid-base reaction between polyalkenoic acid and the glass particles which are responsible for leaching ions (Aluminium, fluoride, and calcium or strontium). The release of these ions from the cement increases the potential for remineralisation of the affected tissues (Watson, 1999).

Mineral trioxide aggregate (MTA) was first introduced by Torabinejad in 1993 as a root-end filling material (Torabinejad and Chivian, 1999). Then studies indicated its potential uses in many other clinical settings such as a pulp-capping treatment (Paranjpe et al., 2010). Recently, Biodentine™ has been introduced as a new tricalcium silicate-based cement by Septodont (SaintMaur des Fosses – France), and has been presented as a bioactive dentine replacement and pulp capping agent to be placed on dentine under definite restorations. This new material shows several benefits over other similar products:

- It has a shorter setting time (12 minutes compared to several hours with MTA).
- Better physical and biological properties
- Bioactive with antimicrobial effect.
- Higher release and deep incorporation of calcium ions.

Biodentine's dehydrated powder weight is formed mainly of tri-calcium silicate and di-calcium silicate. Additionally, it consists of calcium carbonate and zirconium dioxide as a radiopacifier (Biodentine scientific file). This cement is dispensed as a powder capsule to which a fixed amount of hydration liquid is added. Upon mixing, Biodentine sets through a complex hydration reaction, in which the liquid dissolves the calcium silicate granules producing calcium silicate hydrate and calcium hydroxide offering the high alkalinity of the cement. The alkaline caustic effect of Biodentine stimulates a pulpal regenerative response and degrades the collagenous dentine components which facilitate the transfer of Ca^{2+} , OH^- , and

CO₃⁻² ions, providing higher mineralisation within the dentine matrix (Atmeh et al., 2012; Han and Okiji, 2013).

In-vitro dentine demineralisation has been extensively applied in dental research to study its biomimetic interactions with new materials through chemical exchange (Cao et al., 2013) or to evaluate the adhesion properties to dentine (Farge et al., 2010; Garcia et al., 2010) and assess the physical and mechanical properties of human dentine (Gopalakrishna, 2009; Bertassoni et al., 2011). Different demineralisation protocols were applied to develop either partial or totally demineralised dentine samples. Using EDTA, phosphoric acid and acetate containing solutions are the most common protocols. Acid etching is often used in dentistry to facilitate bonding to dentine and enamel. When the dentine is acid etched after caries excavation, it helps removal of the smear layer, causes partial removal of minerals within the intertubular and peritubular dentine and exposes the collagen fibres. The extent of the effect of acid etching is influenced by many factors, mainly the etching time, the acid concentration and pH (Marshall et al., 1997; Perdigão and Lopes, 2001). Partially demineralised dentine samples often aim to resemble caries affected dentine in terms of mineral content and physical properties and is used to study the effect of different restorative materials on dentine.

Raman micro-spectroscopy is a valuable quantitative chemical assessment method. Each Raman peak represents a certain vibrational mode for a single chemical bond in the molecule of a given material, which can therefore be considered as a unique fingerprint to identify that material. The intensity of this Raman peak is related to the number of molecules within the scanned area representing a quantitative value of that molecular presence in the examined area of interest (Penel et al., 1998; Tramini et al., 2000). In this study we were interested in quantifying the changes in the mineral content within the dental tissues. The Raman phosphate peak at 959 cm⁻¹ is characteristic for the tetrahedral PO₄³⁻ group that represents the P-O bond within the hydroxyapatite structure (Spencer et al., 2000; Bulatov et al., 2008). This peak has been previously identified and used to assess the potential chemical changes during enamel (Milly et al., 2014) and dentine (Atmeh et al., 2015) remineralisation.

In the current study, a multimodal non-invasive optical assessment of the effects of these cements was carried out to study the changes in dentine fluorescence properties after demineralisation as well as after its interaction with dental cements

and possible tissue remineralisation. A dentine demineralisation model that provides dentine samples with partially demineralised dentine and sound control dentine segments in the same tooth sample was also made. The model was tested for the effectiveness of the dentine demineralisation protocol. Afterwards, the efficacy of Biodentine™ and GIC (Fuji IX™) on different parts of the created model was compared. This evaluation was facilitated by providing control segments that allows an improved analysis method and better comparison under the same environmental and biological conditions.

The aims of this experiment were: First, to optically evaluate a dentine demineralisation model that provides internal control segments with a relatively simple demineralisation protocol. Second, assessment of the interaction between this model and two water based cements: Biodentine™ (Septodont, Saint Maur des Fosses- France) and a glass ionomer cement (GIC) Fuji IX (GC Corporation. Tokyo, Japan) in terms of mineral deposition and dentine fluorescence properties.

2.2 Materials and methods

Ten extracted sound molar teeth were used in this study. Teeth were collected using an ethics protocol reviewed and approved by the NRES Committee London - Stanmore (Reference 12/LO/0290). The roots of all teeth were sectioned to create a horizontal reference. Each tooth was sectioned into two halves. Seven teeth were used for cement evaluation and the other three teeth were left without restoration to act as negative controls.

2.2.1 Preparation of demineralised dentine samples

All teeth were prepared to include demineralised and sound sections within the same half as elucidated in Figure 2-1. Teeth were prepared using a diamond bur creating a perpendicular angle that was used as a reference point during imaging. Each half was then polished using 2400-grit carborundum paper under running water, and then it was covered with dental wax to protect the dentine surface leaving a marked 2mm width window. Dentine windows were demineralised using 37% phosphoric acid were used applied for 60 seconds to create a partially demineralised dentine segment (Cao et al., 2013). This protocol resulted in a model including the lesion in the middle surrounded by sound dentine from each side. After demineralisation, samples were rinsed with deionised water and then cleaned in an ultrasonic bath for 3 minutes.

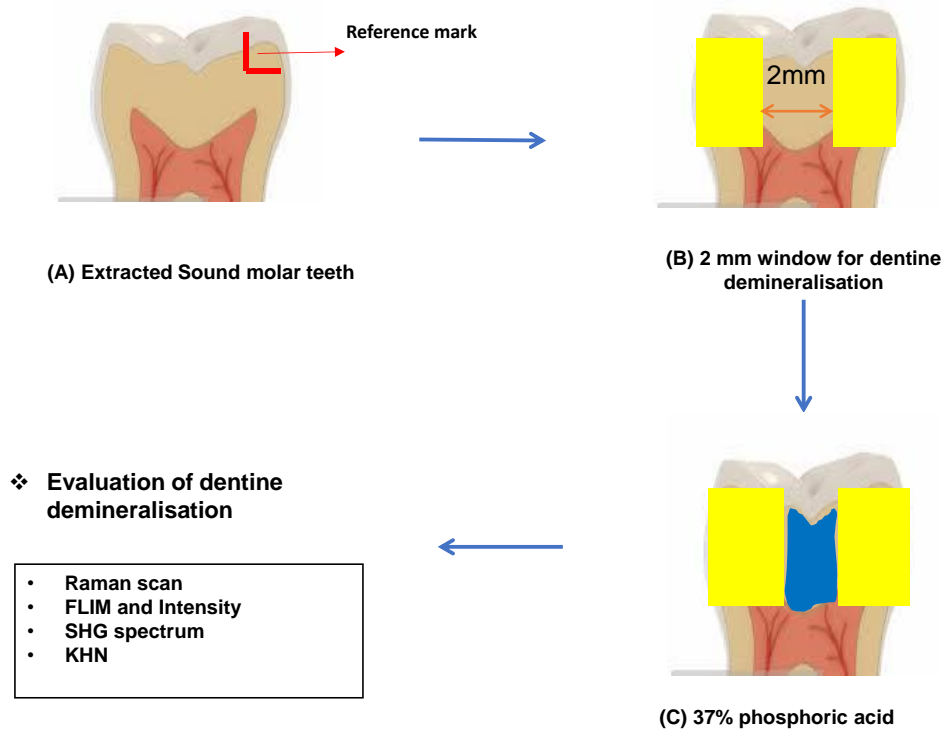


Figure 2-1 Sample preparation: **(a)** 10 extracted sound teeth sectioned into two halves with a right angle reference mark. **(b)** Part of the dentine was covered using dental wax leaving 2 mm window for dentine demineralisation. **(c)** Demineralisation is carried out using an acid etching protocol with 37% phosphoric acid for 60 seconds. Then evaluation of the demineralisation protocol is made by assessing changes in mineral peak, changes in fluorescence intensity and lifetime, measuring the difference in Knoop hardness number and assessing the SHG signal.

2.2.2 Assessment of the demineralisation protocol

• Optical characteristics

Immediately after demineralisation, each half was imaged using a two-photon fluorescent microscope to obtain: auto-fluorescence images, fluorescence lifetime images and then SHG signal. Nine areas from each half were imaged and the spectrum was detected at the same time. To ensure that the laser power was kept constant throughout the study, laser power was measured at the beginning of each session using a power meter (PM30, Thorlabs GmbH, Germany). Also the intensity of a previously prepared reference bead (PeakFlow™ Orange flow cytometry, 6 μm , Invitrogen, USA) was measured.

Both auto-fluorescence and fluorescence lifetime images (256 x 256 pixels), were obtained from each point using a 20x 0.75 NA air objective lens used with 854 nm excitation wavelength and a 550 ± 20 nm emission filter. The spectrum was then obtained from each point using a fibre-optic spectrometer (AvaSpec-ULS2048L, Avantes Ltd, Netherlands) installed within the same microscope apparatus, at a range of (400-700nm) recording both fluorescence and SHG signals.

- **Mineral peak**

A Renishaw inVia Raman microscope (Renishaw Plc, Wotton-under-Edge, UK) running in Streamline™ scanning mode was used in the study to evaluate the changes in the phosphate mineral peak between sound and demineralised areas within the samples. Samples were first focused using a 20x 0.40 NA air objective and a montage image was created for the area to be scanned including both areas of sound and demineralised dentine within the scan. Scans starting at the marked reference point were obtained using a 785 nm diode laser (100% laser power) through the 20x air objective. The signal was acquired using a 600 lines/mm diffraction grating centred between 849 cm^{-1} and 1603 cm^{-1} , and a 2 seconds CCD exposure time. The inter-spectrum distance was $50\text{ }\mu\text{m}$ along the axis parallel to the enamel-dentine junction (EDJ) and $2.7\text{ }\mu\text{m}$ along the axis perpendicular to the EDJ and crossing the sound-demineralised-sound areas (Figure 2-2).

For the analysis of Raman peaks, the maps were transferred to an in-house program designed to fit the spectra and then generate grey-scale images together with depth profiles of phosphate peak intensity at 959 cm^{-1} (PO_4^{3-} (v1)) across the sound and demineralised areas. The minimum energy value of the phosphate peak was selected at 939 cm^{-1} and its central energy value was set at 959 cm^{-1} . The exported results were in the format of 32-bit TIFF grey-scale images, the intensity of the peak at each position is represented by the 32-bit value of the corresponded pixel at that position. The resultant images representing peak height was opened using ImageJ, image processing software (ImageJ, Maryland, USA) and the mean peak height intensity was calculated for both sound and demineralised areas separately. The values were then averaged from all the samples for sound and demineralised dentine respectively.

• Tissue Hardness

The Knoop hardness number was used to evaluate the changes in tissue hardness due to decreased mineral content. The hardness was tested using a Struers Duramin (Struers Ltd., Denmark) microhardness tester. It produces a diamond-shaped indentation after applying a 10g load for 15 seconds. Later, these indentations were assessed by a 40× 0.65 NA objective by adjusting the software cursors at the indentation ends. Then, the manufacturer's software automatically calculated the hardness number which was recorded for each tested area.

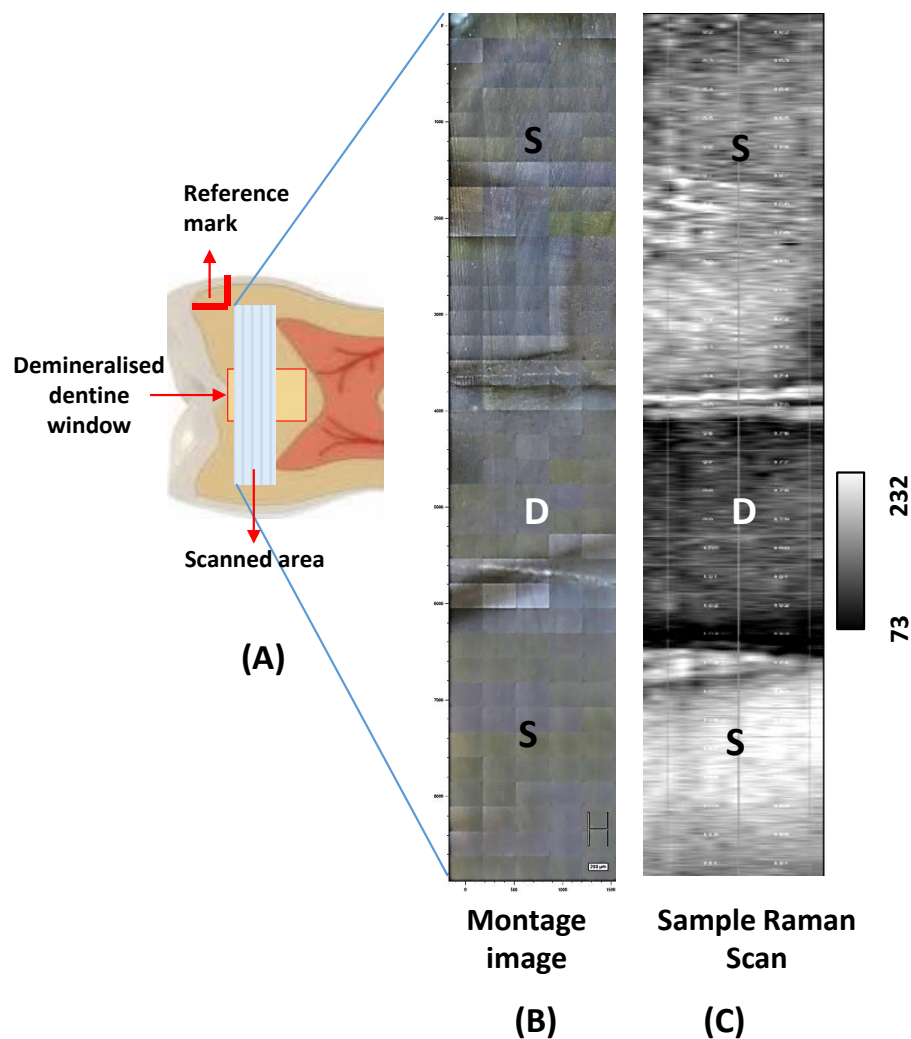


Figure 2-2 Sample preparation for Raman spectroscopy. (A) A diagram of a sample showing the demineralised dentine window and the selected area for Raman scan. (B) An example of a montage image created to include both sound and demineralised dentine. (C) The representative grey-scale image of Raman phosphate peak intensity at 959 cm⁻¹ of sound (S) and demineralised (D) dentine areas.

2.2.3 Sample preparation for the evaluation of dental cements

After each sample had been imaged and scanned for the evaluation of dentine demineralisation, they were rinsed with deionised water and cleaned in an ultrasonic bath for 3 minutes. Then, dental cements were prepared as per manufacturer's instructions. For calcium silicate cement Biodentine™ (Septodont, Saint Maur des Fosses- France), the liquid was added to the water and triturated for 30 seconds. The cement was applied using a plastic instrument on one half of each of the 7 test samples. The other halves were stored with glass ionomer cement (GIC) Fuji IX (GC Corporation. Tokyo, Japan) as per the manufacturer's instructions. Each sample was then stored for 30 minutes in a 37°C temperature incubator with continuous wetting to allow setting of the cements. Afterwards, each half was stored in a separate glass vial containing 7.0 ml of phosphate buffered saline (PBS) solution (Oxoid Limited, Hampshire,UK) for four weeks as shown in Figure 2-3

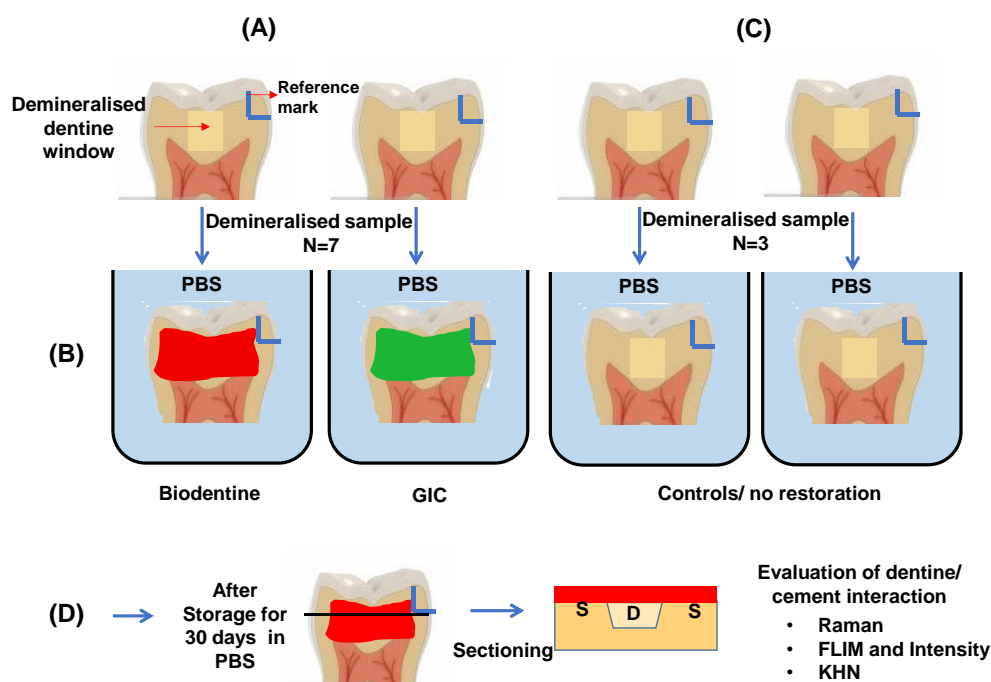


Figure 2-3 Sample preparation for cement evaluation. **(A)** Seven demineralised samples were selected as test samples. **(B)** for each sample, one half was stored with Biodentine and the other half with GIC for future comparison, all samples were stored in PBS containing storage media. **(C)** An additional three samples were used as controls and stored in PBS solution without restoration. **(D)** After storage, samples were sectioned at the reference mark and the interface was evaluated for changes in mineral peak, fluorescence intensity and lifetime and hardness number. (S) denotes sound dentine and (D) demineralised lesion.

- **Two photon imaging and Raman spectroscopy**

After four weeks storage, all samples were retrieved and placed in an ultrasonic bath for 10 minutes in order to remove any surface debris. Using a water-cooled diamond wafering blade (Benetec Limited, London, UK) at a low speed, each sample was sectioned at the reference mark to allow further evaluation of interfacial dentine. The sectioned surface was then polished using 1200-grit carborundum paper and cleaned in an ultrasonic bath for another 3 minutes.

Samples were then transferred to be examined using the in-house manufactured two-photon fluorescence microscope with the same settings as previously described in section (2.2.2/ Optical evaluation) to enable comparison. The same nine points from each half were imaged again and positioned at the previously recorded distance from the reference point. Auto-fluorescence intensity and lifetime images (256 x 256 pixels) were obtained from each area after setting the laser power to match the previous imaging setup.

For all images, before and after storage, Image analysis of the fluorescence intensity was carried out using ImageJ software (ImageJ, Wayne Rasband, NIH, USA) calculating the average intensity from each area. TRI2 FLIM analysis software (courtesy of Paul Barber, Grey Cancer Institute, Oxford) was used to calculate the average lifetime from FLIM images. The values for the average intensity and lifetime before and after storage were then used to calculate the percentage change for each measured area using the equation below:

$$((Xa - Xb) / Xb) \times 100\%$$

Where Xa is the value after storage, Xb is the initial value before storage.

Afterwards, a Raman spectrometer was used again with the equivalent previous settings to evaluate changes in the mineral peak in both sound and demineralised dentine areas. Similar analysis protocols for the mineral peak were performed and the percentage change between the initial values and after storage values was calculated to be used in the statistical analysis using the above formula.

2.2.4 Statistical analysis

To evaluate the effectiveness of the dentine demineralisation protocol, the differences between sound and demineralised dentine were compared using an independent samples t-test separately for different techniques (auto-fluorescence

intensity, fluorescence lifetime, SHG, Raman-mineral peak and Tissue hardness KHN) as the data followed a normal distribution.

These values were used later as the initial “before storage” values to be compared with the “after storage” results by calculating the percentage change in both sound and demineralised tissues. The percentage change was then used to investigate the significant differences between different material groups (Biodentine™, GIC and No restoration) for each used method. Linear models were fitted for each technique (fluorescence Intensity, FLIM, Raman and tissue hardness) separately to find out the significance difference between groups (sound and demineralised dentine) and materials (Biodentine, GIC and control). If overall significance was found then further PostHoc analysis was performed to find out which particular group or material was significant. All the P values were adjusted for multiple comparisons.

2.3 Results

2.3.1 Assessment of dentine demineralisation model

The model showed significant differences between sound and demineralised areas when assessed for changes in mineral content, tissue hardness and optical characteristics. The ratio of SHG signal to AF signal in the spectra was calculated and showed no differences between the sound and demineralised areas which indicate the integrity of collagen fibres that is essential for the remineralisation processes.

Figure 2-4 displays the results of the evaluation of the demineralisation protocol. Statistical analysis data are presented in appendix 2, there was a significant difference between sound and demineralised (lesion) dentine regarding all parameters except when comparing the SHG signal as there was no statistical significant differences between the sound and demineralised dentine.

The average intensity dropped significantly in the demineralised tissues ($p = 0.003$) from $34.2 \text{ A.U} \pm 1.5$ to $23.6 \text{ A.U} \pm 0.3$ which was confirmed in the representative fluorescence intensity images. Similarly, the average lifetime results indicate a drop from $1.6 \text{ ns} \pm 0.01$ in sound tissues to $1.0 \text{ ns} \pm 0.02$ in the demineralised dentine ($p = 0.001$). The produced lifetime images represent this difference as the images from demineralised dentine tend to shift towards the blue-green scale that corresponds to lower lifetime values. The average SHG signal intensity showed no difference

between demineralised and sound dentine ($p= 0.34$). This is displayed also in the spectrum which represents the intensity of SHG signal without any change while at the same time shows a decreased intensity of the auto-fluorescence signal.

The change in the mineral content was assessed by two techniques, the analysis of the mineral peak from the Raman spectrum and tissue hardness (KHN) as they both directly represent the mineral content. There was a significant decrease in the Raman mineral peak intensity value ($p= 0.003$) in the demineralised dentine compared to sound. The produced mineral peak spectra also represent a decreased mineral intensity in the demineralised tissues. The hardness number compares well with the Raman results as the average KHN for demineralised dentine (30.6 ± 3) is significantly lower than the sound tissue (48 ± 4) ($p= 0.001$). These results indicate that using 37% Phosphoric acid for 60 seconds as a demineralisation protocol is effective in removing a significant amount of minerals from dentine without affecting the integrity of its collagen fibres, which presence is vital for remineralisation to take place.

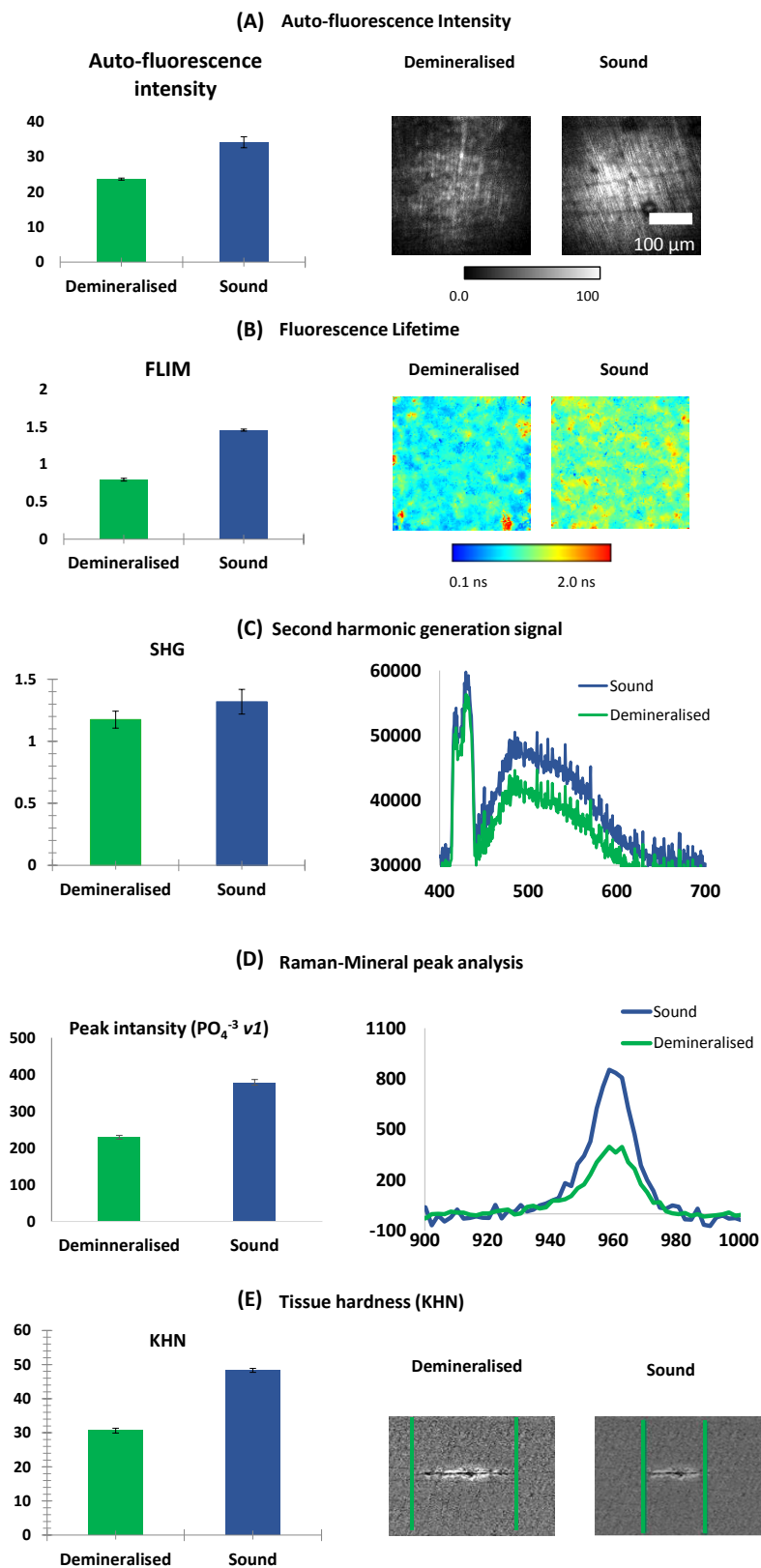


Figure 2-4 Multimodal assessment of dentine demineralisation. (A) Autofluorescence intensity. (B) Fluorescence lifetime. (C) Second harmonic generation signal. (D) Raman spectroscopy. (E) Tissue hardness (KHN).

2.3.2 Assessment of dental cements' interaction with sound and demineralised dentine

Two-photon microscopy imaging

Figure 2-5 displays representative auto-fluorescence intensity and lifetime images of sound and demineralised dentine with three different groups: Biodentine, GIC and control (no restoration) group. Regarding sound dentine, there was a comparable decrease in the intensity images after storage with Biodentine and GIC groups while no changes were noted in the control group. On the other hand, lifetime images showed almost no changes in the lifetime values regarding all groups.

For demineralised dentine the effects of BiodentineTM and GIC were compared together and assessed against the control group where no restoration was applied. The auto-fluorescence intensity images showed an increased intensity after the cement application. This change was greater with Biodentine than GIC. The control group showed no changes after storage. For the FLIM images, with Biodentine there was an increase towards the longer (yellow-red) lifetime components. Likewise, but to a lesser extent, the lifetime increased after storage in the GIC group. No changes in lifetime were seen in the control group.

- **Analysis of fluorescence intensity images**

The changes seen in the images among all groups were statistically analysed by calculating the percentage change before and after storage. Figure 2-6-(A), shows the differences in fluorescence intensity among the three groups. Comparable with the changes seen in the intensity images, samples stored with Biodentine exhibited a highly significant increase in the intensity of the demineralised tissues by 39.3% ± 2 compared to the control ones (1.4% ± 2.7), ($p = 0.001$). Samples also showed decreased intensity in the sound tissues by -15% which was significant when compared to the no restoration sound group 1.1% ± 0.8 , $p = 0.001$. The changes between the sound and demineralised tissues stored with Biodentine were highly significant as $p = 0.001$.

For the GIC group, the intensity also increased by $19.5\% \pm 1.4$, which was significant when compared to the demineralised control group ($p = 0.001$). The sound tissues with GIC showed a significant decrease in the intensity by $-16.8\% \pm 0.1$, as $p = 0.001$. The changes between the sound and demineralised tissues stored with GIC were highly significant as p value = 0.001 . For the control group there was almost no change in the intensity for both sound and demineralised tissues ($1.1\% \pm 0.8$, $1.3\% \pm 2.7$) respectively. It was also found that the changes in intensity between Biodentine and GIC were non-significant for sound ($p = 0.34$) but significant for demineralised tissues ($p = 0.001$).

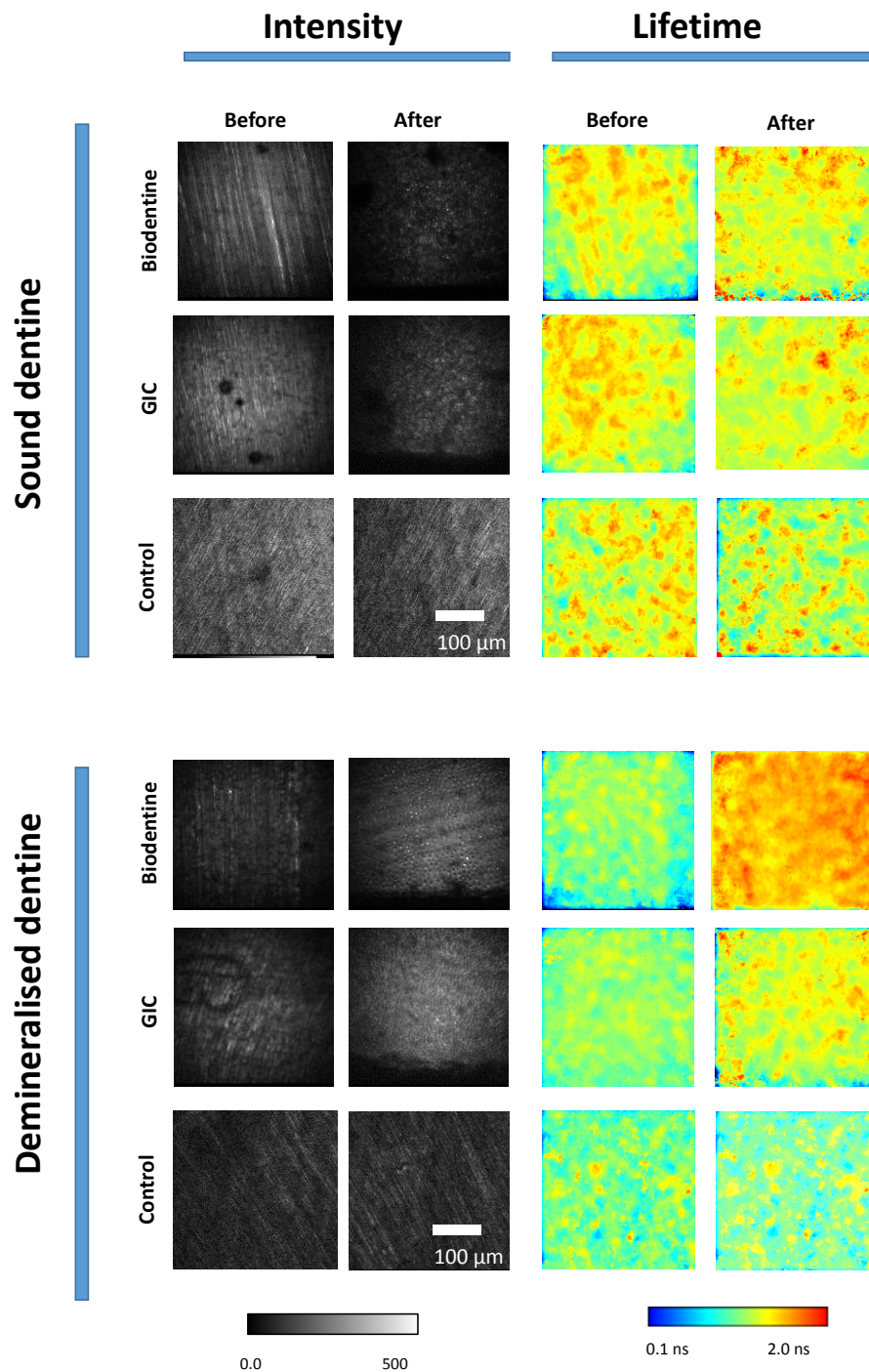


Figure 2-5 Representative Two photon images before and after cement application and storage for sound and demineralised dentine. Sound dentine showed decreased fluorescence intensity only with both cements. No change was recognised in the control group. Demineralised dentine groups show enhanced fluorescence intensity and longer lifetime with both cement groups.

- **Analysis of fluorescence lifetime images**

Fluorescence lifetime changes were also analysed and represented in Figure 2-6(B). It was found that, with Biodentine, the demineralised group had increased lifetime by 69.4% \pm 3.6 which was highly significant when compared with Biodentine/sound (2.1% \pm 0.4, $p= 0.001$) and when compared with the demineralised control group (0.8% \pm 0.9 as $p= 0.001$). Similar changes were seen in the lifetime values for the GIC group. Demineralised tissues stored with GIC had increased lifetime by 59.6% \pm 2.9; this was a significant increase when compared to changes in the GIC/sound (0.6% \pm 0.8, $p= 0.001$), and with the demineralised control (0.8% \pm 0.9, $p= 0.001$).

Differences in lifetime between Biodentine and GIC were insignificant for sound $p= 0.4$, but significant within the demineralised dentine, $p= 0.001$.

- **Tissue hardness (KHN)**

For the differences in tissue hardness, the change in the Knoop hardness number before and after storage was averaged for each group. The tissue hardness recovered to normal values in the demineralised tissues stored with both Biodentine and GIC as the average KHN mean value was 44.3 and 44.27 respectively which lies within the range of normal sound tissue hardness values. The changes in the hardness number before and after storage is displayed in Figure 2-6- (C). All sound dentine groups showed insignificant changes. The demineralised dentine groups showed an increased by 43% \pm 3.3 with Biodentine and 47% \pm 4.1 with GIC. These changes were significant when compared to the demineralised control group as $p= 0.001$ for both cements.

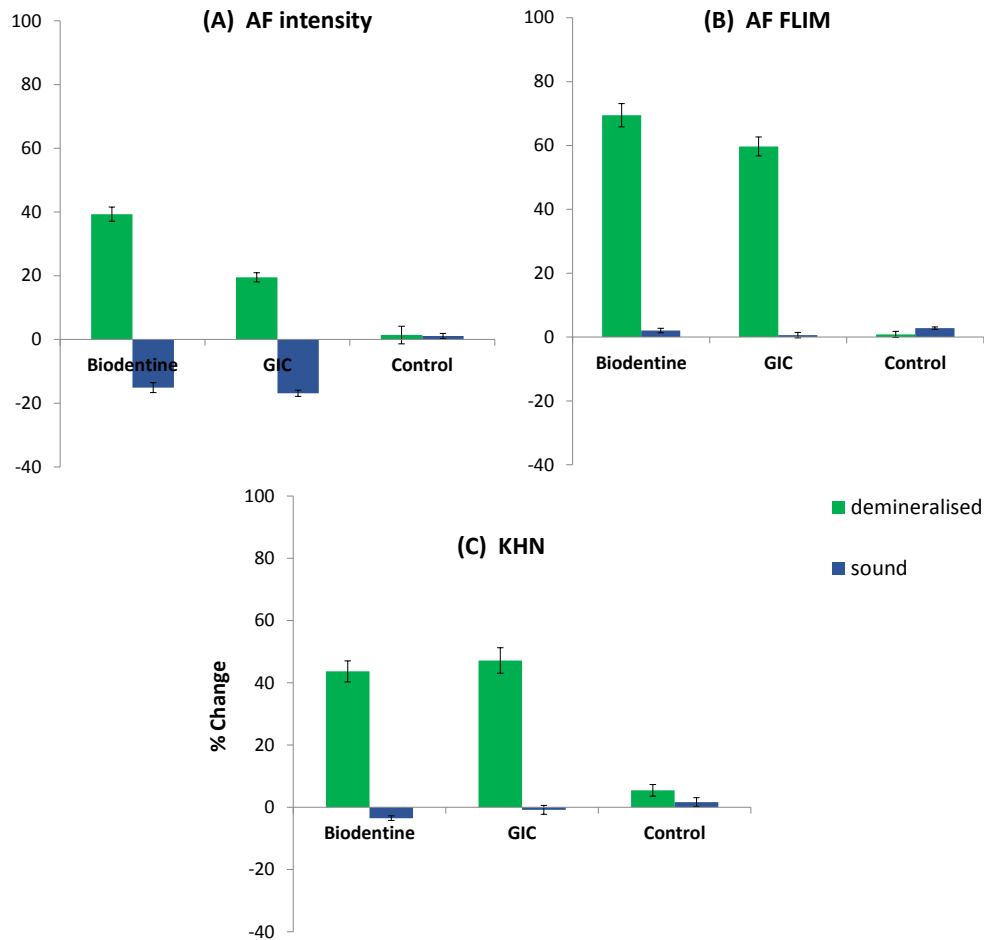


Figure 2-6 Percentage change before and after storage in the (A) Auto-fluorescence intensity, (B) Fluorescence lifetime and (C) KHN regarding each group for both sound (blue) and demineralised (green) dentine. The results show a greater change in the demineralised dentine with both cements regarding all parameters with no change in the control group. Sound dentine shows decreased fluorescence intensity with the cements with no change in the control group. In addition there were no changes in the FLIM or KHN regarding all groups of sound dentine.

• Raman spectroscopy

Figure 2-7-(A) shows the percentage change in the mineral peak intensity from the Raman analysis. Mineral content did not change within sound tissues in all groups. On the other hand, the demineralised dentine show a highly significant increase in the intensity of minerals when stored with Biodentine ($257.2\% \pm 24.5$) and with GIC ($241.5\% \pm 14.5$). When compared with the demineralised control group the $p=0.001$ for Biodentine and GIC. The results were also significant when comparing the demineralised and sound dentine stored with Biodentine and GIC ($p=0.001$).

However, these changes were not significant when comparing Biodentine and GIC groups as $p = 0.07$.

The statistical analysis of the results comparing different groups stored with Biodentine and GIC indicates that changes in the optical properties as a result of changes in the mineral content of demineralised dentine are caused by the dentine's interaction with different cements. These changes were not significant in sound dentine or control samples. Results also showed that despite the difference in the chemistry and the type of interaction of these cements with dentine, there were no significant differences between the effect of Biodentine and GIC when assessed by optical properties, Raman spectroscopy and tissue hardness. See statistical analysis tables in appendix 3, 4, 5.

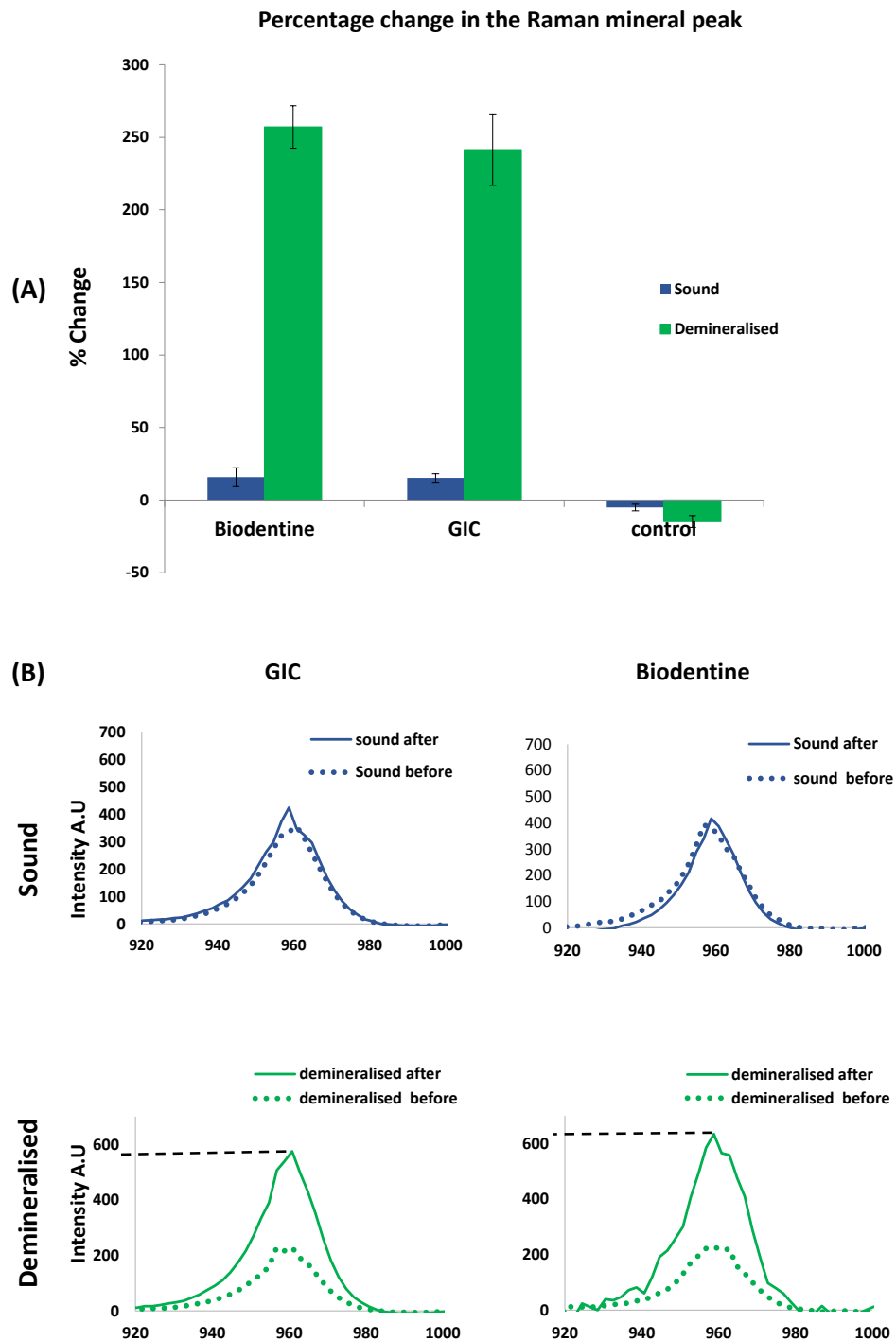


Figure 2-7 Raman analysis for mineral peak intensity. **(A)** Results of the percentage change in the mineral peak intensity before and after restoration and storage for both sound and demineralised dentine. The highest change is seen in the demineralised dentine stored with Biodentine and GIC. **(B)** Representative Raman spectra for the measured phosphate peak intensity from sound and demineralised dentine before and after restoration with dental cements.

2.4 Discussion

2.4.1 Sample preparation

Natural caries lesions in dentine exhibit a wide variety in depth, degree of organic matrix destruction and loss of mineral content. All of which have their effect on the tissue response to different applied therapeutic materials in an attempt to repair and remineralise the damaged tissue. In order to control these variations and properly investigate the remineralisation effects of such therapeutic materials, dental research has utilised in-vitro artificial dentine lesions in which the minerals are removed by means of acidic demineralisation with better control over the dentine's organic contents as there is no bacterial by-products. Initial pilot study for demineralisation protocol and cements assessment was performed on three teeth and significant results were found, therefore, sample size of ten teeth were decided to be sufficient for this study.

One of the aims of this study was to create a model for dentine demineralisation that has an almost identical mineral content and optical properties to that of caries affected dentine with the presence of an internal control sound dentine to allow for accurate future assessment of the dental cements' effect. The model was tested to ensure that the demineralisation protocol is effective in removing an adequate amount of minerals that does not affect the collagenous proteins as these play an important role in the remineralisation process. Acid etching with 37% phosphoric acid gel for 60 seconds, was used in this study to partially remove the minerals and create a dentine demineralisation model (Cao et al., 2013). This protocol had an immediate demineralisation effect compared to sample emersion in EDTA (Garcia et al., 2010), acetate or lactic acid containing demineralisation solutions which require the samples to be placed in the solutions for few days (Ngo et al., 2011). The produced lesion was measured by way of analysis of Raman scans on the cross section of demineralised samples (Figure 2-8). This depth was calculated by comparing the phosphate peak intensity within the demineralised dentine with the deeper sound dentine within the same sample. It is presented as a drop in the plotted depth profile extended to approximately 400 μm (Milly et al., 2014). Earlier studies have reported a wide range of lesion depth (between 10-2000 μm) in partially demineralised dentine, depending on the exposure time to the demineralisation solutions (Van der Veen and Ten Bosch, 1996; Tay and Pashley, 2008; Bertassoni et al., 2011). Furthermore, peak intensity evaluation has been documented as a suitable method to detect the differences between sound and demineralised areas (Ko et al., 2005).

Similarly, the degree of mineral loss using this protocol was assessed by analysing Raman scans to measure the change in phosphate peak intensity at 959 cm^{-1} (PO_4^{3-} ν_1). The detection of this peak has been reported before and used to assess the degree of demineralisation in artificial (Tramini et al., 2000) and natural carious enamel and dentine (Kinoshita et al., 2008; Almahdy et al., 2012). In this study, the intensity of the peak dropped significantly by -39.4% in the demineralised dentine when compared to the sound areas within the same sample.

For changes in the optical characteristics between sound and demineralised dentine, evaluation of the fluorescence intensity and fluorescence lifetime has been undertaken. Few studies have correlated the changes in these fluorescence properties to mineral content. In tests on natural caries, indirect correlation between the fluorescence and the mineral content has been done. However, the fluorescence intensity has always been higher in carious tissues than sound dentine. This increased fluorescence signal intensity is generated as a result of structural proteins' breakdown by means of bacterial invasion and certain proteases (McConnell et al., 2007; Almahdy et al., 2012). The current study was conducted under aseptic conditions thus, the results showed a decrease in the dentine fluorescence intensity after loss of minerals that is caused neither by direct nor indirect bacterial effect (Koenig et al., 1993). This implies the role of dentine's inorganic components in the generation of natural dentine auto-fluorescence and supports that the origin of the increased intensity in carious dentine may be organic in nature. An earlier study investigated the effect of acid etching on dentine fluorescence over different periods of exposure to demineralising solutions. They observed an increase in fluorescence from the demineralised dentine areas that was noticeable only after four days of demineralisation and onward as no changes in the fluorescence had been detected at day zero despite the considerable loss of minerals (Van der Veen and Ten Bosch, 1996). Another study compared the fluorescence changes of dentine between biological (bacterial) and acid induced artificial lesions with the results indicating a significantly weaker or no signal from the acid induced demineralised dentine while a significant fluorescence increase was detected in the bacterial demineralised group (Shigetani et al., 2008). The results of AF intensity imaging in this study also coincide well with analysis of the AF spectrum of the same samples. The spectrum in Figure 2-4 shows a decreased AF signal intensity but no change in the SHG signal which confirms the intact collagen components as there is a strong correlation between SHG signal and the collagen status as well as its concentration (Kim et al., 2000).

Fluorescence lifetime, on the other hand, displayed a significant decrease in the demineralised dentine. This has not been investigated previously in an artificial dentine lesion but the correlation between the lifetime and mineral content has been investigated in carious dentine using micro-CT evaluation (Lin et al., 2011) also in chapter four of this thesis. In the current study, the minerals have been partially removed and not eliminated, suggesting the involvement of other environmental factors, possibly pH changes; may affect the lifetime measurements (Gannot et al., 2004; McConnell et al., 2007).

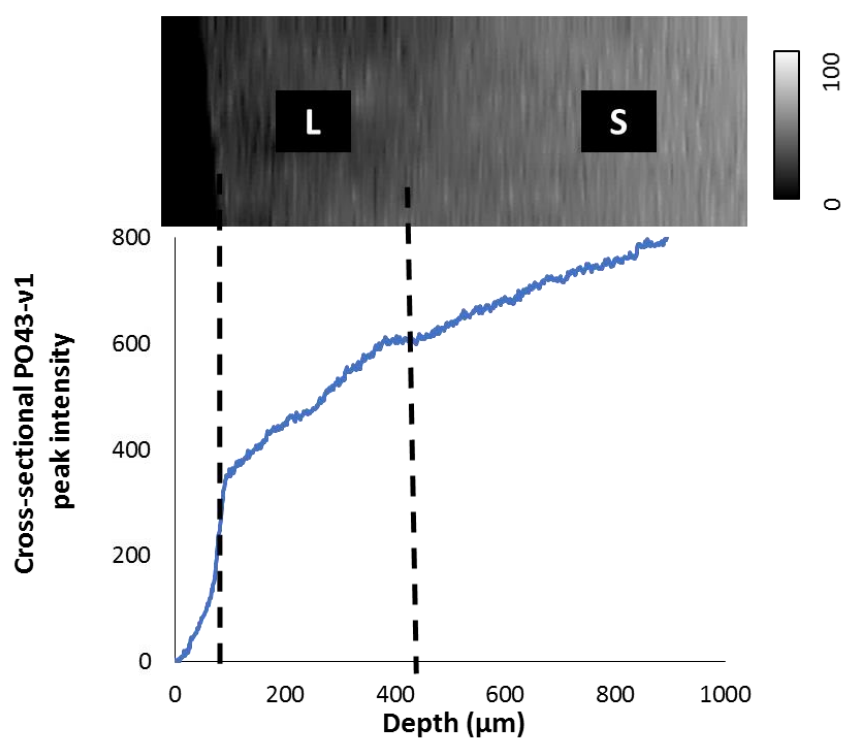


Figure 2-8 Representative grey-scale image and the depth profile of phosphate peak intensity of Raman phosphate peak at 959 cm^{-1} including the lesion of demineralised dentine (L) and sound dentine (S).

2.4.2 Evaluation of dental cements interaction and remineralisation potentials

In the current study both Biodentine™ and GIC have been used to compare their interaction with the created dentine demineralisation model. Various optical techniques have been used to evaluate their potentials in developing biomimetic remineralisation of the demineralised tissues and to examine their effects on sound dentine as well. Previous studies have investigated the effects of both cements on other dentinal substrates. It was confirmed that mineral transfer and apatite formation took place with variable mechanisms as a result of the dentine interaction with GIC (Lee et al., 2008; Ngo et al., 2011) and calcium silicate cements (Tay et al., 2007; Watson et al., 2014; Atmeh et al., 2015). This interaction was evaluated in this study using multiple non-invasive optical approaches to confirm mineral-hydroxyapatite formation and to study the effect of this mineralisation on the inherent optical properties of dentine.

Raman micro-spectroscopy provided quantitative information about the mineral concentration within a substrate reliant on the proportion between the PO peak intensity and the number of molecules within the volume of the scanned area (Tramini et al., 2000). It is a non-destructive, label free technique with a direct response to chemical variations within the sample (Tsuda and Arends, 1997). In this study the StreamLine™ scanning technique was used, which enabled the analysis of a large number of spectra in each samples and produced a more representative dataset of the examined tissues. In this system, the sample is moved along an illuminating laser line while data is read out. This gives the system the advantage of being 3-7 times faster than the conventional point-by-point serial scanning as the dead time between sequential data points is considerably reduced (Hutchings et al., 2008; Hédoux et al., 2011). Scanning dentine tissues normally produces background fluorescence. This was considered during peak analysis in each Raman spectrum, the PO peak was fitted using a Gaussian function and a first order polynomial background function, using an in-house analysis software. It is well-documented in the literature involving Raman analysis to fit the spectrum peaks prior to any subsequent measurements (Salehi et al., 2013; Toledano et al., 2014; Milly et al., 2014).

The detected Raman phosphate peak ($\text{PO}_4^{3-} \nu_1$) at the exact position on the Raman spectrum (959 cm^{-1}) has been reported in earlier studies which assessed the degree of demineralisation in dentine (Almahdy et al., 2012) and was also

reported as an indication to confirm HA formation on a calcium silicate pill (Parker et al., 2014). The current study used measurements of this peak to detect the mineral changes in dentine after being subjected to therapeutic dental cements.

The statistical analysis of (PO_4^{3-} ν_1) at 959 cm^{-1} intensity changes revealed a significant increase in mineral/ phosphate content within demineralised dentine under both Biodentine and GIC when compared to the control group (see appendix 3,4). A similar increase in the Raman phosphate peak has been previously reported to indicate biological mineralisation in cartilage and in teeth as a sign for HA formation (Sauer et al., 1994; Parker et al., 2014). Therefore, it can be suggested that biomimetic remineralisation has occurred as a result of the interaction with the Biodentine and GIC cements.

For Biodentine samples in this study, detecting the characteristic hydroxyapatite peak (Figure 2-7) is indicative of the nature of dentine remineralisation in the presence of Biodentine and a phosphate rich medium and confirms the cement's bioactivity (Sarkar et al., 2005; Tay et al., 2007). The apatite peaks in both sound and remineralised dentine were detected at a similar position. Thus, the probability of forming other calcium phosphate minerals can be excluded. The characteristic Raman peaks of other possible minerals such as; octacalcium phosphate (OCP), dicalcium phosphate dehydrate (DCPD), tricalcium phosphate (TCP) or amorphous calcium phosphate (ACP) show the absence of the ν_1 band that was used in the analysis of samples in this study (Sauer et al., 1994; Koutsopoulos, 2002; Tay et al., 2007).

Fluoride ions are found to be released in large amounts by glass ionomer cements (Ngo et al., 2006; Trairatvorakul et al., 2009). With the presence of phosphate ions in the storage solution and the release of phosphate and calcium ions from tooth structure, fluoroapatites are believed to be formed, thereby inducing remineralisation in demineralised tissues (Tsanidis and Koulourides, 1992; Ten Cate et al., 1995). The fluoroapatites have ν_1 band in Raman spectra similar to the one present in hydroxyapatite which was considered in the peak analysis within this study (Williams and Knittle, 1996). Although a significant increase in the mineral content is detected within demineralised tissues under Biodentine and GIC, comparing the results of both cements interestingly revealed an insignificant but higher percentage change with Biodentine than GIC.

Using an in house manufactured multiphoton microscope provided various optical data that can be obtained from the same position in the sample at the same time. For optical evaluation, AF intensity images and FLIM were used to examine the interface. After storage with both cements, samples showed improved optical properties in the demineralised dentine towards normal values in both AF intensity and FLIM. This may not be an absolute indication that remineralisation have had occurred but the present study shows a clear relation between mineralisation and dentine's fluorescence characteristics for the first time. Moreover, these optical changes certainly show signs for tissue repair that meet the optical values closer to that of normal dentine. This observation can be explained by the combined effect of calcium silicate cement during its setting and maturation which involve firstly, a "caustic etching" and degradation of the underlying dentine's collagen caused by the high alkaline calcium hydroxide (pH=13), followed by mineral transfer in the form of calcium phosphate. Upon setting of the calcium silicate cements, the hydrated cement releases calcium in the form of calcium hydroxide and a poorly crystalline calcium silicate hydrate (Bensted, 1976; Taylor, 1997). The calcium hydroxide ions with their high pH values are able to diffuse into the water filled spaces within the cement structure. In addition, these ions along with unset cement particles are responsible for the cement's high alkalinity, causing degradation of inter-tubular collagen fibrils and also induces apatite formation (Tay et al., 2007). An SHG evaluation of the interface under Biodentine cement was conducted recently in our laboratory and a significant reduction or even absence of the signal was noticed, which may indicate collagen degradation. However, an absence of SHG signal was not detected under GIC (Atmeh et al., 2012). The continuous release of calcium hydroxide with the presence of phosphate ions from (PBS) results in the formation and precipitation of calcium phosphate compounds on the exposed collagen (Tay and Pashley, 2008).

GIC cement displayed optical changes in sound and demineralised tissues similar to Biodentine (Figure 2-5, Figure 2-6). However, the significant increase in the fluorescence intensity and lifetime which was also detected under GIC is believed to be due to the demineralisation of the inorganic dentine component as an effect of the cement's PAA and tartaric acids (Sennou et al., 1999) which adds to the effect of acid demineralisation and may result in a total increase in the fluorescence intensity. These acids cause etching of the underlying dentine surface and trigger ion exchange at the interface. The ionic flow includes releasing fluoride ions in high

concentration plus aluminium and strontium from the glass particles of the cement and calcium ions from the tooth. This ion supply helps to tip the balance towards the apatite formation and remineralisation and therefore, enhances the fluorescence intensity and lifetime.

Direct correlation between the fluorescence intensity and biomimetic remineralisation was confirmed in this study for the first time. A high fluorescence signal has been reported previously in remineralised dentine and was attributed to apatite deposition within the matrix under calcium silicate cements (Atmeh et al., 2015) and when the hydrated cement was stored in PBS (Tay et al., 2007). The apatite formation has been validated by Raman analysis and may suggest that this change in the fluorescence intensity could be associated with mineral incorporation into the demineralised dentine. The percentage change in the mineral content in demineralised dentine before and after restoration has increased in both Biodentine and GIC samples by almost 200%. This high percentage must have an effect on the overall tissue fluorescence intensity.

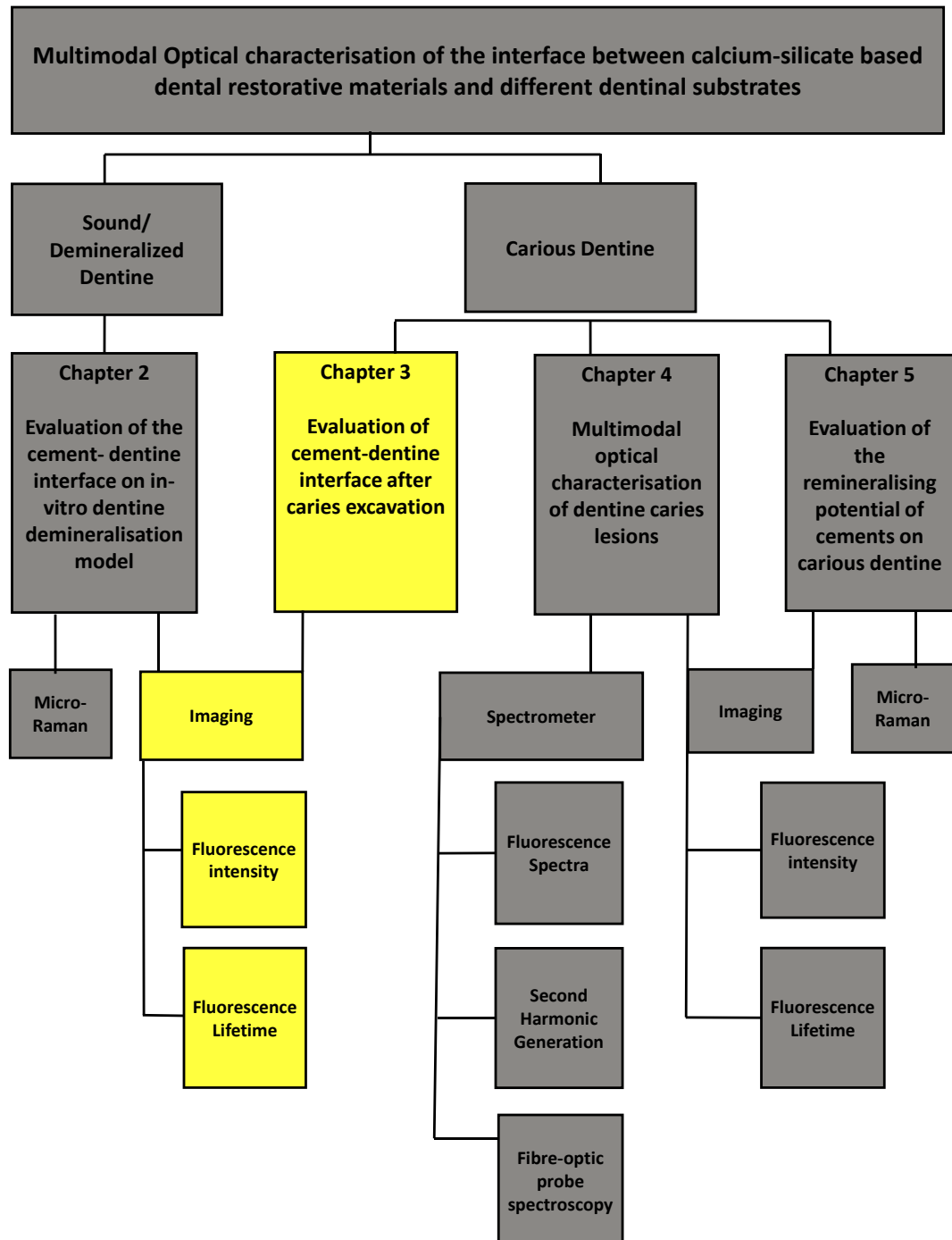
Detecting the changes in sound dentine, the cement's effect is seen as a significant decrease in the fluorescence intensity with minimal changes in the mineral peak and tissue hardness (Figure 2-6). This suggests that surface degradation of the matrix collagen may have occurred in the sound dentine (Leiendecker et al., 2012) with minimal effect on the mineral content of these tissues (Figure 2-7).

The comparable changes in the lifetime that were found in the dentine under Biodentine and GIC cements have not been evaluated previously without mineral labelling (Watson et al., 2014; Atmeh et al., 2015). In the present study, direct correlation between the natural dentine fluorescence lifetime and changes in the mineral content has been achieved. In previous research on carious dental tissues, it has been demonstrated that longer lifetime values are associated with higher mineral content within sound dentine (McConnell et al., 2007; Lin et al., 2011). The demineralised dentine samples in this study showed a shorter lifetime compared to the sound. After storage with Biodentine or GIC, these tissues significantly increased their fluorescence lifetime values. Such changes in the lifetime can be correlated with the massive increase in mineral content and tissue hardness (Figure 2-7). Overall comparison between the cements was critical for future clinical applications. The results suggested that there were significant differences between Biodentine and GIC regarding their effect on the different optical parameters within the demineralised dentine only. However, the Raman analysis results of the

demineralised tissues indicated higher percentage change in the mineral content with Biodentine but the difference was non-significant ($p= 0.065$). These results are in agreement with a recent In-vivo clinical evaluation of the same cements. The study also concluded that no overall difference was observed in the clinical response between Fuji IX™ and Biodentine™ with the latter showing a better therapeutic effect on the pulpal tissues (Hashem et al., 2015).

In conclusion, this study has introduced a dentine demineralisation model that met all optical and biological requirements to facilitate the proper evaluation of biomimetic dental materials. The demineralisation protocol is simple and is not time consuming. In addition, it provides internal control segments that allow future comparison with demineralised tissues. Both Biodentine™ and Fuji IX™ exhibited a high potential to induce mineralisation and apatite formation in partially demineralised dentine which confirms the cement's biomimetic interaction with dentine. These changes in mineral content have an effect on the optical properties of the dentinal tissues demonstrated as an increase in both fluorescence intensity and lifetime, thereby defining the direct relation between the mineral content and natural dentine fluorescence. The optical evaluation techniques with two-photon microscopy and FLIM provide a potential alternative non-invasive in-vitro method that facilitates reliable evaluation of dentine de/ remineralisation. However, Raman spectroscopy remains the absolute representation of changes in the mineral peak, thus, the most valued technique for remineralisation assessment.

3. Chapter Three: Evaluation of cement-dentine interface after caries excavation: Tetracycline labelling and two-photon fluorescence microscope



3.1 Introduction

There has been a growing body of research on dentine remineralisation mediated by restorative materials. This is encouraged by the new approach of minimally invasive dentistry in managing carious lesions. In the clinical situation, dentists are often instructed to confine caries excavation to the superficial infected tissues and leave the discoloured but partially affected dentine. The latter is believed to be potentially reparable and exhibit better adhesive and mineralisation potentials. Therefore, advances in dental restorative materials have also been directed towards biologically active materials that will affect the tooth repair positively and enhance the chances for tissue remineralisation.

Biodentine™ (Saint Maur des Fosses- France), was introduced as a coronal restorative material with a wide range of clinical applications. Being of a relatively short initial setting time, and a rich source of calcium ions, Biodentine™ could have a potential application for the management of dental caries by encouraging the remineralisation of caries affected dentine. In the previous chapter we investigated the effect of calcium silicate cements and glass ionomer cements on partially demineralised dentine. Our results confirmed the cements' bioactivity; such a highly significant increase in the mineral content was found with an accompanying change in the fluorescence characteristics of dentine due to this mineralisation.

In the current study, carious lesions were excavated to an appropriate end point leaving caries affected dentine in the cavity to promote remineralisation and assessment of the cement interaction with the remaining dentine. Using carious dentine to study the remineralising potential of Biodentine™ should be more representative and closer to the clinical situation, although it could be associated with some challenges, mainly due to the varying nature of dentine caries.

Caries excavation can be undertaken with many techniques but most of them are not selective in removing caries infected dentine and often require additional discrimination by the operator. Chemo-mechanical excavation, however, is a technique that may be self-limiting in selectively removing caries infected dentine. The enzymatic solutions (either hypochlorite-, pepsin or papain based solutions) is believed to cause further breakdown of the remaining collagen fibres to facilitate its removal with a hand excavator. Carisolv (Carisolv, MediTeam Dental; Sävedalem, Sweden) a caries removing system, based on hypochlorite, was developed for the concept of minimal invasive caries excavation. The gel contains 0.5% w/v sodium

hypochlorite, 0.1M of an amino acid mixture (glutamic acid, leucine and lysine), and water. The hypochlorite acts as a deprotenising agent and although it is not selective on its own, the selectivity of the gel to remove the infected tissues is attributed to amino acid mixture. The amino acids act as a buffering agent that reduce the aggressive effect of the sodium hypochlorite on sound dentine in addition to enhancing its effect on disrupting the degenerated collagen (Tonami et al., 2003). The resultant collagen fibrils are friable and can be easily removed by a specific noncutting hand instrument. The use of such instrument also benefits MI caries removal by offering a high tactile sensitivity to the operator and therefore permits selective caries removal. The efficacy of the Carisolv system has been proven to establish the optimal caries excavation endpoint. In a confocal microscopy study, the remaining tissue after Carisolv excavation was assessed by the natural caries auto-fluorescence signature and resulted in adequate caries removal when compared to other excavation methods (Watson, 2000). This also has been validated using Micro-CT, examining the remaining tissues after excavation resulted in a mineral density level that is at the cut-off point for dentine caries (Neves et al., 2010). However, more effective caries removal was achieved when Carisolv was activated with a metal excavator (Neves et al., 2011c). The Carisolv system also showed other benefits such as acceptable bond strength and a bactericidal effect due to chloramine compound formation (Neves et al., 2011b; Lager et al., 2002).

The evaluation of a dental cement interaction with the tissues can be carried out using a variety of methods, especially when assessing the mineralisation potentials. The use of auto-fluorescence imaging has been reported to be effective for evaluating the structure of the mineralised dentine matrix (Atmeh et al., 2015), (Chapter. 2). Deep tissue imaging which provided valuable information about tissue changes after cement application was achieved by using two photon fluorescence microscopy with FLIM. In this study, a similar imaging technique was performed combining the advantages of two photon imaging with mineral labelling which could provide a powerful technique for the study of the mineralisation process.

Tetracycline is a familiar labelling agent that has been previously used to evaluate mineralisation changes in bone (Wesseling-Perry et al., 2009) as well as in teeth (Moseley et al., 2003; Atmeh et al., 2015). It is composed of four carboxylic rings that allows it to chelate calcium ions from the mineralised tissues with no major alterations to its structure. This interaction results in increased yellow green

fluorescence under ultra-violet (UV) excitation which can be detected using multi-photon illumination in a fluorescence microscope (Schneider et al., 2003).

Tay and Pashley recognised the ability of calcium silicate cements to form apatites in the presence of phosphate rich media such as a solution of phosphate buffered saline (PBS) (Tay and Pashley, 2008). As the cement releases calcium in the form of calcium hydroxide (Camilleri, 2011) and in the presence of high concentrations of phosphate ions, remineralisation of the organic matrix is assumed by the formation of calcium phosphate which precipitate on the exposed collagen fibrils (Tay et al., 2007; Tay and Pashley, 2008). If tetracycline is added to the storage medium, incorporation of this fluorophore within the calcium forming minerals is expected and changes in the fluorescence characteristics will be detectable with the use of two-photon imaging.

The aims of this study were: 1. To investigate the effect of two water-based dental cements, Biodentine™ and GIC on the optical properties of excavated natural caries lesion, aiming to mimic the clinical situation. 2. To evaluate the novel imaging technique, combining two-photon microscopy and tetracycline labelling to assess the cements' mineralisation potentials.

3.2 Materials and methods:

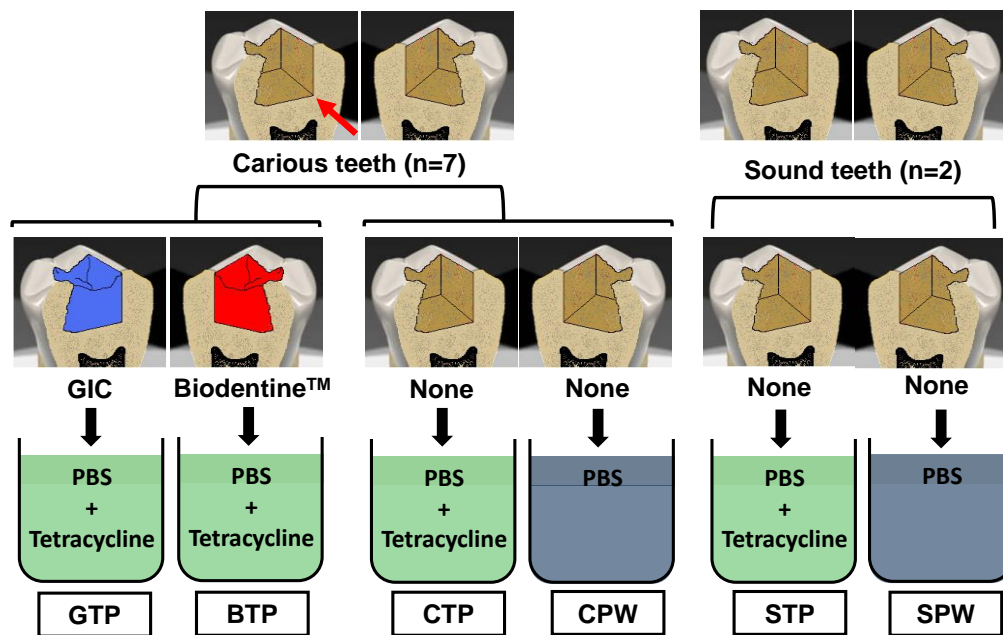
3.2.1 Sample preparation

Nine human molars were collected after extraction using an ethics protocol reviewed and approved by the NRES Committee London - Stanmore (Reference 12/LO/0290). Seven carious teeth were selected with deep lesions that contained soft carious dentine. Caries infected dentine was excavated chemo-mechanically using Carisolv® gel (MediTeam Dental. Göteborg - Sweden) with a special stainless steel, non-cutting hand instrument. Excavation was performed after preparing occlusal cavities to access the carious lesions. For both sound and carious teeth, one of the proximal walls of the cavity (see Figure 3-1) was prepared using a diamond cylindrical bur to create a flat proximal wall for the cavity with a right angle to its floor; this angle was used later as a reference point during imaging. The root of each tooth was then cut and the crown was sectioned through the middle of the lesion along its long axes into two halves using a water-cooled diamond wafering blade (Benetec Limited, London, UK) at a low speed. Sectioned

teeth were subsequently polished using 600, 800, and 1200-grit carborundum papers and cleaned in an ultrasonic bath with deionised water for 10 minutes.

The sectioned cavities of five excavated caries-teeth were filled with two different restorative materials; one was a calcium silicate based dental cement, Biodentine™ (Septodont, Saint Maur des Fosses- France) and the other was glass ionomer cement Fuji IX™ (GC Corporation, Tokyo, Japan). Before applying the cements, each sectioned tooth was mounted using a specially designed small device, with which the sectioned surface of the tooth was tightened against a plastic matrix to prevent any leakage of the cement. Cements were applied directly after correct mixing according to the manufacturer's instructions using an amalgam condenser and adapted with a plastic instrument. Samples were stored for an hour in an incubator at 37°C temperature and 100% humidity to allow natural setting of the cements. Another two carious teeth and two sound teeth were used as controls with no applied cement but stored in different storage media as shown in Figure 3-1. For ageing, samples were divided into groups with different storage solutions, either in a 0.015% tetracycline solution (87128 Sigma-Aldrich, Dorset, UK) and phosphate buffered saline (PBS) (Oxoid Limited, Hampshire, UK) at 37°C for 8 weeks, or in phosphate buffered saline (PBS) (Oxoid Limited, Hampshire, UK) and deionised water. Solutions were replaced every 2 days. All samples were stored separately in glass vials containing 7.0 ml of the storage media. Samples were distributed into groups as follows:

- 1- (GTP n=5): GIC, 0.015% tetracycline, and PBS.
- 2- (BTP n=5): Biodentine™, 0.015% tetracycline, and PBS
- 3- (CTP n=2) Carious teeth in 0.015% tetracycline, and PBS.
- 4- (CPW n=2): Carious teeth in PBS and water only
- 5- (STP n=2) Sound teeth in 0.015% tetracycline, and PBS.
- 6- (SPW n=2) Sound teeth in PBS and water only



3.2.2 Imaging and image analysis

Two-photon fluorescence microscope was used to image the samples using a 10 x 0.25 NA objective lens, 800 nm excitation wavelength, and 500 ± 20 nm emission filter. Using both fluorescence and fluorescence lifetime imaging (FLIM), the dentine-cement interface of each sample was imaged at six points before ageing and the XY coordinates of each point from the reference point were saved. After 8 weeks of ageing, samples were polished with a 2400-grit carborundum paper and cleaned in an ultrasonic bath for 10 minutes; the same points were re-imaged for evaluation.

Auto-fluorescence intensity (AF) was calculated for each image using ImageJ

Figure 3-1: Extracted human teeth were prepared, a right angle between the mesial wall and pulpal floor of the cavity (Red arrow) was created using a cylindrical bur. Teeth were divided to six experimental groups. Five teeth to be restored with either GIC (GTP) or Biodentine (BTP) and stored in tetracycline and PBS. Four teeth were left without restoration to act as controls and stored in either PBS alone (CPW,SPW) or with tetracycline storage solution (CTP, STP).

analysis software (ImageJ, Wayne Rasband, NIH,USA). The fluorescence intensity

(AF) of the interfacial dentine underneath the restoration was measured and normalised to the AF intensity measured for the dentine away from the interface. The ratio between the intensities in these two areas was calculated for each image and averaged for each sample. The average percentage of the change in AF before and after aging was calculated for each group. The change in AF was calculated using the following equation:

$$((Xa - Xb) / Xb) \times 100\%$$

Where **Xb** is the value before aging and **Xa** is the value after aging.

For the fluorescence lifetime (FLIM) measurements, data were analysed using TRI2 software (courtesy of Paul Barber, Grey Cancer Institute, Oxford). The decay curves were well fitted using a double exponential model. The analysis was conducted in the same manner as for the fluorescence intensity, where an area of interfacial dentine just below the interface was selected while another area was selected away from the interface to represent the sound dentine as shown in Figure 3-2. The change in the (FLIM) after aging was calculated using the above equation, and values were averaged for each sample and each group. One-Way ANOVA test was performed to compare the groups. Tukey's test was used later to detect the differences between any two groups.

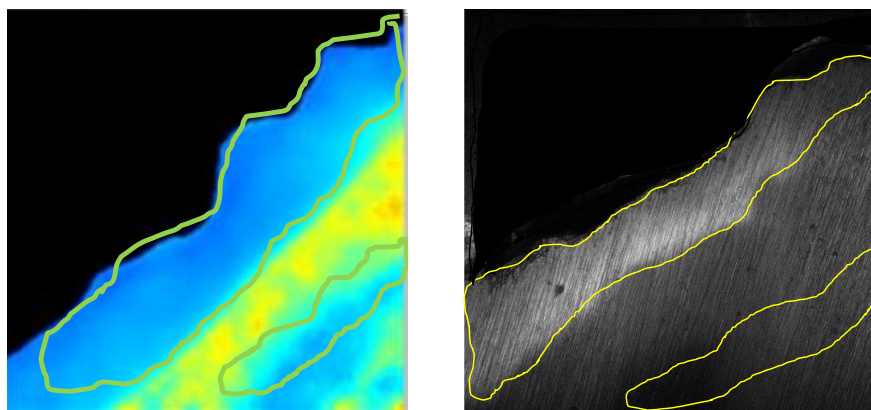


Figure 3-2 Image analysis. Florescence lifetime (left) and Fluorescence intensity (right) images where analysed by calculating the average intensity and lifetime ratio between two areas in each image. One area just below the interface and the other away from the interface representing unaffected dentine.

3.3 Results

Representative fluorescence intensity and lifetime images of each group before and after aging are shown in Figure 3-3. The short lifetime is presented by the blue colour in the images. The reduction in the FL of the dentine could be explained by the absorption or incorporation of tetracycline, which has a very short fluorescence lifetime compared to that of dentine. However, in the Biodentine group as well as the GIC filled samples, the area of reduced fluorescence lifetime appeared in the form of a well-defined band underneath the dentine–cement interface. In contrast, samples without restoration (CTP, CPW and STP), show scattered and more generalised changes in the FL with no changes detected in the sound samples stored in PBS alone. The appearance of shorter lifetime indicates that tetracycline incorporation was mainly concentrated in these areas, which could be explained by active mineral deposition and remineralisation of the matrix as a result of the cements effect. Comparable observations were detected in the fluorescence intensity images for different groups. Tetracycline intensity was much higher than normal dentine, so one could expect an increase in the FI where tetracycline is present (in BTP, GTP and DTP). An increased intensity was also noticed in the excavated caries group stored in PBS alone.

The effect of the aging of caries-affected dentine and sound dentine on the AF and fluorescence lifetime when stored in phosphate-rich media with or without the Biodentine or GIC is presented in Figure 3-4. The graph shows an increase in the FI in all of the samples. Biodentine-filled samples exhibited the highest increase ($71\% \pm 16.4$), while in the GIC samples the increase was around ($13\% \pm 5.6$). The intensity changes in the restoration-free carious samples stored in tetracycline-free media (CPW) was found to be higher by ($48.5\% \pm 26$), while it changed minimally in the sound samples stored in the same media (SPW) or in the carious sample stored with tetracycline. The fluorescence lifetime graph in Figure 3-4 shows a reduction in the normalised lifetime in all of the groups except for the restoration-free sound dentine stored tetracycline free (SPW). The reduction in the Biodentine filled samples was the highest ($-25.5\% \pm 4.1$), followed by the GIC-filled samples ($-16\% \pm 2.9$) compared to the minimal changes in the control samples ($-2\% \pm 5$). The statistical analysis showed no significant differences between samples stored in GIC and Biodentine in terms of fluorescence intensity or lifetime ($p= 0.065$, $p= 0.685$) respectively. For fluorescence lifetime there was a highly significant difference between the control group (CPT) and Biodentine group ($p= 0.004$) also

between this control group and GIC ($p= 0.012$). In addition, fluorescence intensity results showed significant differences between the (CPT) group and the cements groups as ($p= 0.040, 0.048$) for Biodentine and GIC. For FLIM results, both cements groups showed significant differences compared to other control groups (CPW and STP) as the P values for GIC group ($p= 0.044, 0.046$) and for Biodentine ($p= 0.041, 0.042$). However, comparing the differences in intensity results for these groups were not significant.

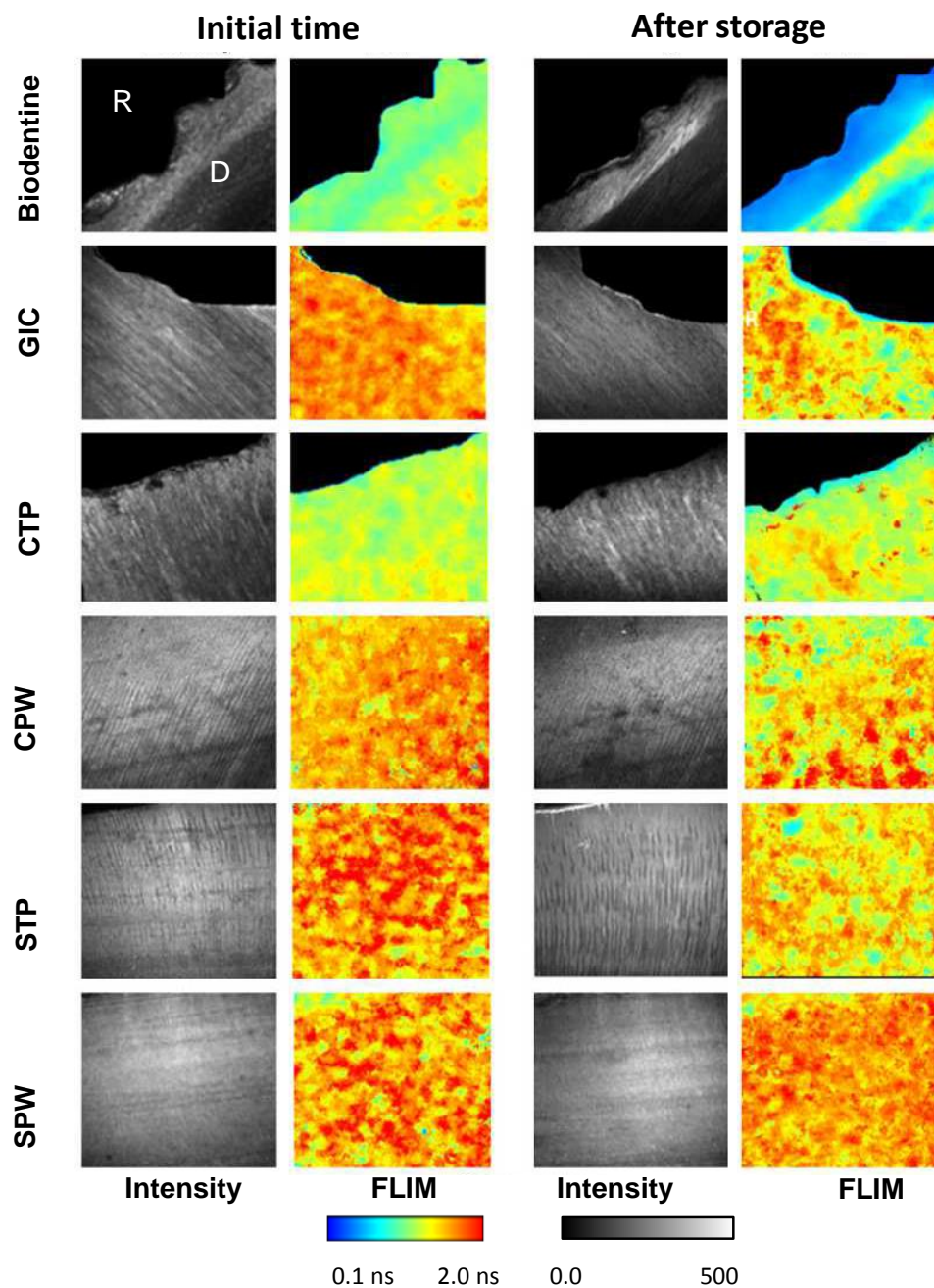


Figure 3-3 Representative fluorescence intensity (FI) and fluorescence lifetime (FLT) images for the dentine–cement interface of different groups before and after aging. A well-defined band of shorter fluorescence life-time was detected in the (BiodentineTM) filled samples. Reduction of the fluorescence lifetime was also detected in GIC filled samples as a band below the interface with more areas infiltrating the dentine matrix. The restoration-free samples (CTP, STP) that were stored in Tetracycline containing solution, showed minimal and more generalised fluorescence changes. Other controls stored in Tetracycline free solution (CPW SPW) showed non-significant changes in FLT (C = excavated caries, S = sound, T = Tetracycline, P= Phosphate buffered saline), R= Restoration, D= Dentine.

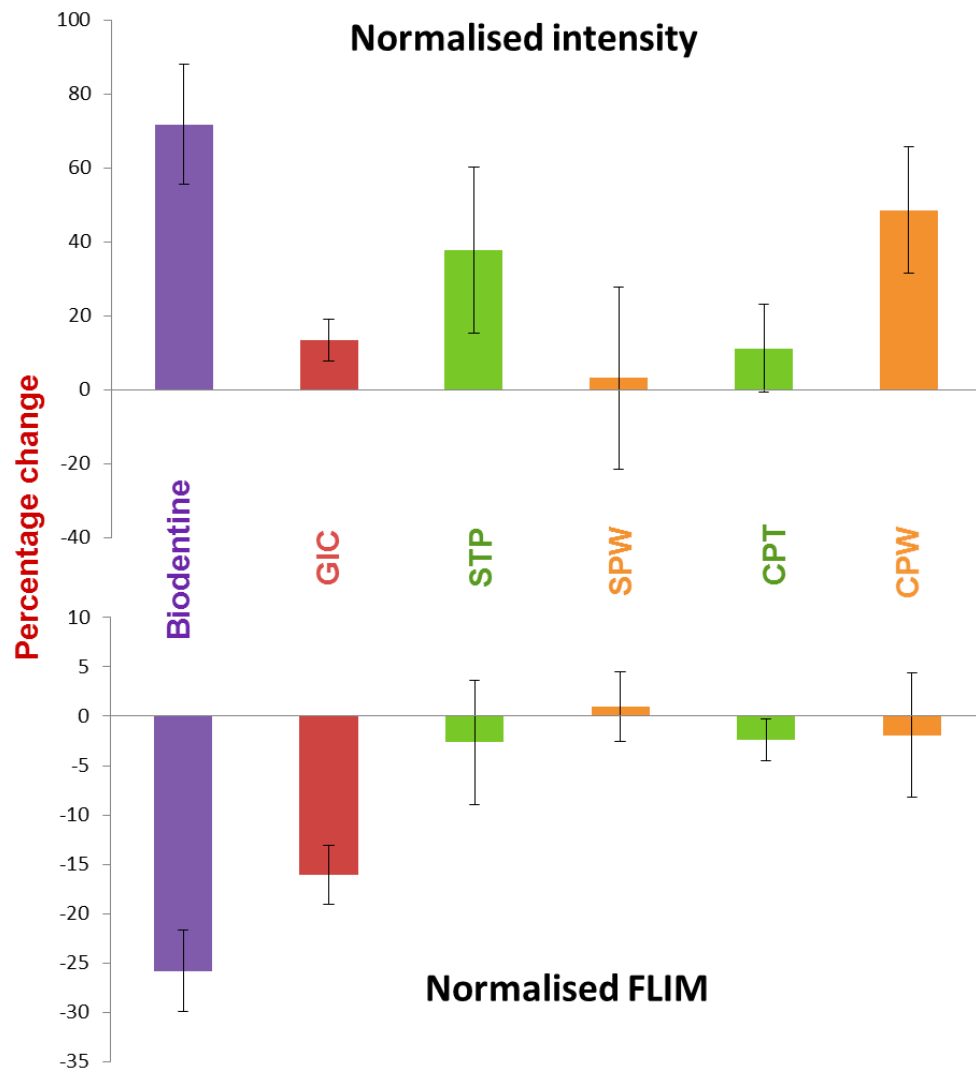


Figure 3-4 Normalised fluorescence intensity (FI) and fluorescence lifetime (FLT) presented as percentage differences of samples restored with Biodentine or GIC. Control samples of sound teeth with/ without Tetracycline and excavated carious teeth with and without Tetracycline.

3.4 Discussion

Understanding the nature of the calcium silicate cement interaction with natural caries lesions and the mechanism of potential remineralisation effects on the remaining caries-affected dentine requires studying the interfacial properties of the dentine underneath it. This has been possible with the use of novel imaging techniques promoting comparable optical evaluation of the interface before and after the application of the cement. Having used teeth selected with deep carious lesions, this study was associated with many challenges. Since these lesions occurred naturally, it was impossible to fully standardise caries excavation, which

may have led to a variation in the quality of the tissues left at the end of the caries excavation. Under or over excavation of carious dentine could have left caries-infected or sound dentine respectively despite the use of chemomechanical caries excavation that is believed to achieve a reproducible caries excavation endpoint. If infected dentine was left, fluorophores originating from the cariogenic bacteria or from the host might interfere with the fluorescence lifetime and intensity analysis. Moreover, residual infected dentine could interfere with the remineralisation process, as it is not expected to occur in this structure-less substrate. On the other hand, over-excavation would remove the caries affected dentine and leave a sound substrate, with no potential sites for remineralisation. However, the main aim was to mimic the clinical situation and perform caries excavation according to dentists' standards with expected variation in the actual tissue type left in the cavity. In addition, analysing images before and after storage gave the data a reliable comparison of the same tissue types at the same exact position on the sample. Using the combined multi-photon imaging and tetracycline labelling to study the dentine-cement interface had promising results in previous studies on demineralised dentine samples (Atmeh et al., 2015). Similar to our results, imaging both cements reflected the way that they interact with the underlying dentine upon their setting and maturation.

The tetracycline calcium complex is found to have fluorescence lifetime of (0.56 ns) (Atmeh et al., 2015), the BTP and GTP actual lifetime measurements falls close to this range (0.62 ns, 0.70 ns) respectively as shown in Figure 3-5. This indicates that the changes in the interfacial optical properties presented in these groups are due to the formation of tetracycline-incorporated minerals. These changes require the presence of calcium, phosphate and tetracycline to occur in this manner, which was confirmed by the minimal changes in the FL and FI within the control groups as one of these three elements was absent (see Figure 3-4).

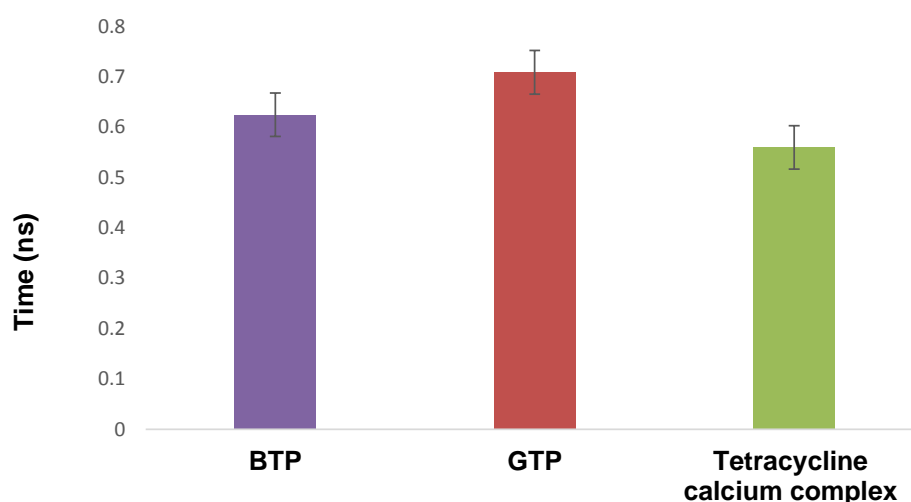


Figure 3-5 The actual fluorescence lifetime measurements of Biodentine group (0.62 ns), GIC (0.70 ns) and tetracycline calcium complex (0.56 ns).

Normalisation of the fluorescence measurements of the interfacial dentine to similar measurements obtained from areas of the tissue away from the interface made the results more comparable, where those areas of unaffected dentine could be considered as an internal control for the same sample, and samples of the same group. Increased fluorescence intensity and shortened fluorescence lifetime of the interfacial dentine under dental cements are both related to the incorporation of tetracycline fluorophore into the dentine at these areas (Schneider et al., 2003; Atmeh et al., 2015). Such incorporation could be mediated by the formation of calcium (or strontium in the case of the GIC) containing minerals such as hydroxyapatite, which is expected to form in the presence of calcium and phosphate ions under high pH conditions. These conditions were available in the Biodentine group, in which the hydrated cement was the source of calcium and hydroxyl ions, and the phosphate buffered saline was the source of the phosphate ions leading to the optical changes seen this group.

Images of the interfacial dentine under Biodentine showed a wide band of increased fluorescence intensity and shortened lifetime. These changes could be explained by the initial high alkalinity of the cement upon setting (pH=13), which may have caused degradation of the organic matrix and deformation of collagen

fibres. This resulted in optical changes similar to the ones caused by caries (Lin et al., 2011). In addition, the structural changes affecting the collagen fibres were also confirmed by Amre et al, as lower or absence of SHG signals was found in the dentine below Biodentine cement (Atmeh et al., 2012). The following ion release from the cement in the form of calcium carbonate enabled tetracycline incorporation into the mineral structure and may cause these optical changes as well. Earlier studies suggested crystal growth within dentinal tubules at the interface between Biodentine and dental surfaces (Santos et al., 2005). The formation of these apatite crystals allows tetracycline incorporation and results in the observed optical changes.

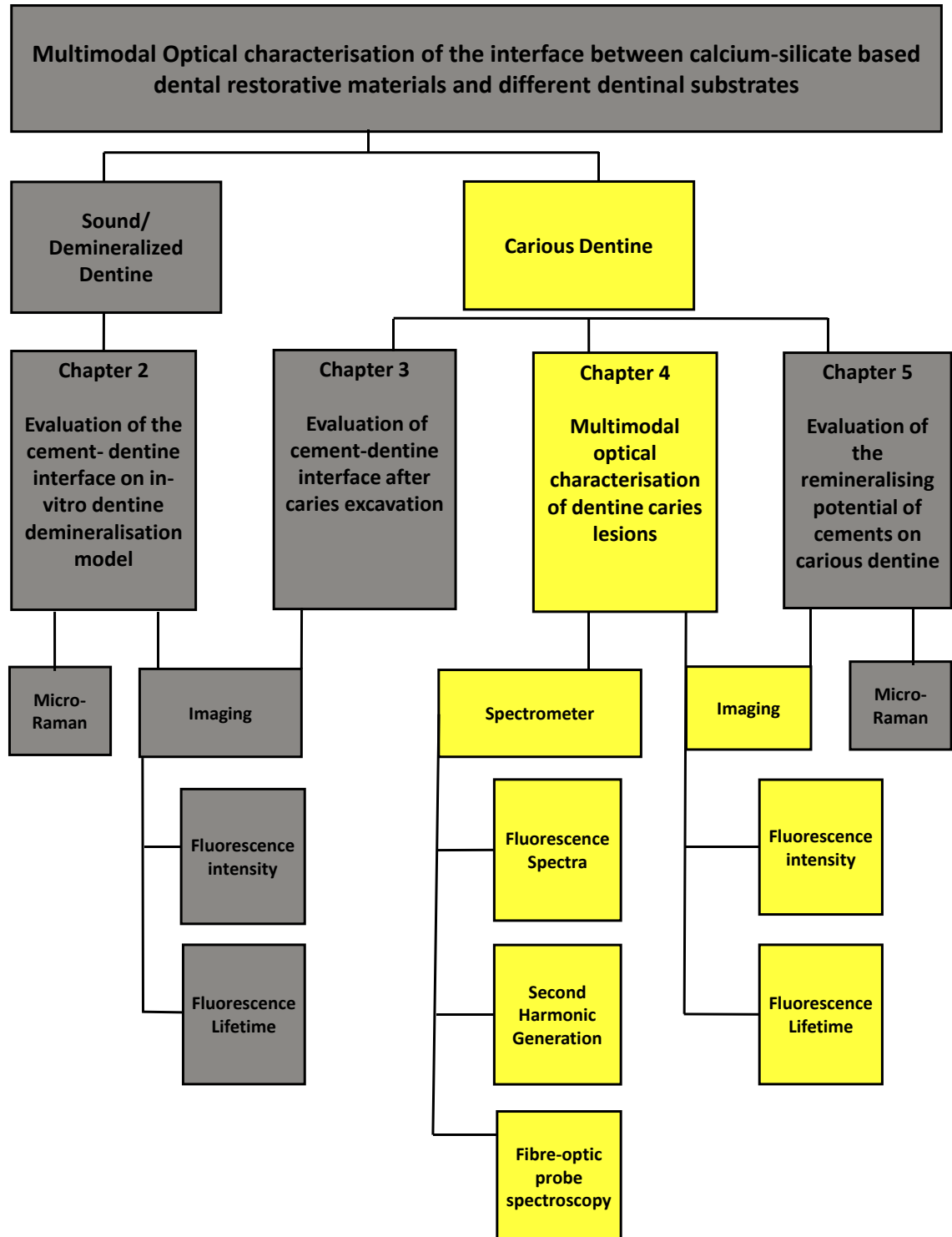
In the GIC sample images, there was a thin layer of decreased lifetime and increased fluorescence intensity along with the presence of these optically changed areas deeper within the dentine matrix rather than confined to an interfacial alteration. Changes within the dentine matrix are believed to result from the demineralising effect of the PAA and tartaric acids on the inorganic dentine component (Sennou et al., 1999). GIC acids target only the inorganic dentine components allowing the cement to infiltrate deeper through inter and peri-tubular dentine as seen within the dentine matrix in our samples. This eventually aids in the remineralisation process with the cement offering free fluoride ions that are incorporated in the fluorapatite formation. In addition, the free calcium ions that are released from the tooth binds to tetracycline and led to the increased fluorescence intensity and shorter lifetime of the GIC samples. The interfacial ion exchange layer that appears between dentine and GIC (Wilson et al., 1983) was visible as a thin layer of shortened fluorescence lifetime corresponding to tetracycline binding and therefore affecting the fluorescence properties of the tissue.

Comparing the optical changes between both cement groups (BTP, GTP) show differences in both the fluorescence intensity and lifetime. These changes occurred in a similar manner. However, they were greater in BTP which could be attributed to the nature of the minerals that are present and the difference in pH conditions as well. In the BiodentineTM- filled samples, the developed high pH favours the formation of hydroxyapatite while in the GIC filled-samples (GTP) the pH value was much lower. This low pH would be less favourable for apatite formation. However, it has its role in promoting deeper infiltration of the cement and acidic demineralisation of the dentine to free calcium and phosphate ions.

In the restoration-free samples (CTP), there was almost no change in the fluorescence behaviour before and after aging. While in the caries-excavated samples stored in tetracycline-free media (CPW), bacterial growth and further tissue destruction within the samples cannot be excluded with the absence of tetracycline, therefore this bacterial effect might have resulted in an increase in the fluorescence intensity after storage. With the sound dentine samples, as expected there were no changes in the samples lacking tetracycline (SPW). However, higher increase in intensity with (STP) samples was found and could be attributed to the tetracycline conditioning effect on sound dentine. This role of tetracycline was observed in periodontal studies using tetracycline for dentine conditioning to facilitate dental tissue healing (Frantz and Polson, 1987; Silverio et al., 2007).

In conclusion, the Biodentine and GIC samples showed an increase in the fluorescence intensity and shortened lifetime of the interfacial dentine after aging. This may indicate the formation of tetracycline-incorporated minerals, which could indicate remineralisation of the dentine substrate under the cement. This study suggests that fluorescence lifetime and fluorescence intensity imaging and measurements can produce a useful insight into mineralisation process, recorded over time, within the same carious tissues next to a bioactive restorative material.

4. Chapter Four: Multimodal optical characterization of dentine caries lesions



4.1 Introduction

Dentine caries displays histological and clinical changes that can be described as biologically intermingled zones of superficial highly infected dentine and a deeper layer of partially demineralised affected dentine (Fusayama and Terashima, 1972; Ogawa et al., 1983). Determining the caries excavation end point is always challenging for dentists especially when dealing with deep carious lesions. In respect to a minimally invasive approach in managing caries lesions, selective excavation is recommended to be limited to the infected layer when approaching the pulp during operative management of the cavitated lesion. This approach will prevent excessive tissue removal, preserves the pulp vitality and allow tissue repair. As for deep carious lesion, favourable results have been found when removing the heavily infected dentine while preserving caries affected tissues near the pulp and then use an indirect pulp capping material to promote tissue healing. One study has applied this technique on primary and permanent molars and resulted in a high 3-years success rate in both. The survival rate was 96% for 86 primary molars and 93% for 34 permanent teeth (Gruythuysen et al., 2010). Such conservative treatment will directly save the patients time and money by avoiding pulp exposure and consequent endodontic treatment improving the patients' attitude towards dental treatment in general. A recent study showed that only 53% of the patients chose to save the tooth while the rest would go for extraction due to the high cost and the unpleasant experience of endodontic treatments (Vernazza et al., 2014). Therefore, the differentiation between dentine caries zones is critical, both clinically and in laboratory investigations. It is an essential step in-vitro to allow the development of minimally invasive selective operative techniques and the investigation of biomimetic materials and their interactions with tooth surfaces (Banerjee and Watson, 2015). The current laboratory techniques available for caries characterization include bacterial analysis, autofluorescence measurement techniques, hardness measurement or chemical analysis techniques including Raman spectroscopy. Most of these methods are technique-sensitive and limited to surface characterization. They often require careful sample preparation and some may be considered invasive.

Auto-fluoresce is an inherent property of dental tissues and many other biological molecules as they have the ability to fluoresce when excited with a particular wavelength without the addition of other luminescent substances. Non-invasive auto-fluorescence signal (AF) detection has been used to study the detailed structure and the condition of the dental tissues (Banerjee and Boyde, 1998;

Stookey, 2005). As the unique AF signal is generated from natural or chemical compounds in normal dental hard tissues (fluorophores) any alteration in the dentine structure (such as that caused by caries) will cause changes in the AF characteristics of these tissues. The natural fluorescence from sound and carious tissues may vary in their origin. Sound dentinal tissues are believed to emit AF from the cross-linked chains of collagen or minerals attached to it. Carious dentine, on the other hand, shows increased AF that may be caused by denatured collagen breakdown products (hydroxypyridinium crosslinks), products of bacterial decomposition (protoporphyrins) or other bacterial metabolites (Banerjee et al., 2010a; Stookey, 2005). Another study suggested the role of inorganic components, either the mineral themselves or components attached to them (Björkman et al., 1991). Despite the possible multiple AF origins, the distinct AF signal from carious dentine has been proposed to be used as an alternative non-invasive marker in caries studies (Shigetani et al., 2003; Banerjee et al., 2010a).

Other optical signals may be detected from dental tissues. Second harmonic generation is an optical property that is generated only from certain materials including collagen, microtubules and muscle fibres (Abraham et al., 2010). When these molecules are excited with high laser intensity they have the inherent ability to generate an additional frequency component with half the wavelength and double the frequency (2ω) of the illuminating light. This is an additional signal to the usual linear component that results in Rayleigh scattering and is known as the SHG signal. In dental tissues, a strong signal is detected in sound dentine with a lesser extent in enamel due to the role of collagen as a source of SHG (Elbaum et al., 2007; Chen et al., 2007). As collagen destruction takes place during the caries process, a direct effect on the intensity of the SHG signal is expected. This effect has been studied and a significant reduction of SHG signals was detected in carious tissue when compared to sound (Kao, 2004; Chen et al., 2007).

The AF and SHG signals may be effective indicators for caries diagnosis. However, the optical techniques used to detect them are intensity-based and precise tissue characterization may be affected due to possible fluctuation in laser intensity, light scattering or fluorophore concentration. Fluorescence lifetime imaging (FLIM), on the other hand, is independent from the intensity and fluorophore concentration (Berezin and Achilefu, 2010). The fluorescence lifetime is defined as the average time that a molecule spends in the excited state before its return to the ground state. It is specific for each fluorophore and has been used widely to provide valuable information about the cellular and tissue structure of the

fluorophores at a molecular level (Ng et al., 2001). Each pixel's intensity in the displayed lifetime images represents the fluorescence lifetime of the fluorophore rather than the intensity of the fluorophore. Certain local conditions act as influencers of fluorescence lifetime including: oxygen level, hydration and pH (Kwak et al., 2001; Chang et al., 2007). These unique characteristics make FLIM a promising technique for the examination of dental tissues, as local conditions and disease will significantly change the fluorophore lifetime, providing accurate information about the status of the examined tissues. When examining dental samples, it has been found that the average AF lifetime is shorter in enamel than dentine and longer in sound than carious tissues (see Figure 4-1) (Lin et al., 2011). In addition, It was found to be effective in detecting structural changes in dental tissue, such as, mineralization (Webb et al., 2002; McConnell et al., 2007; Ferretti de Oliveira et al., 2010). The lifetime was recorded in this study via time-resolved fluorescence measurement, which calculates the lifetime intensity without averaging. It uses short pulsed illumination light source with high speed detection systems to measure the lifetime. This method prevents the loss of valuable information about the fluorescent molecule due to signal averaging that could result from using steady state mode measurements (Lakowicz, 2013).

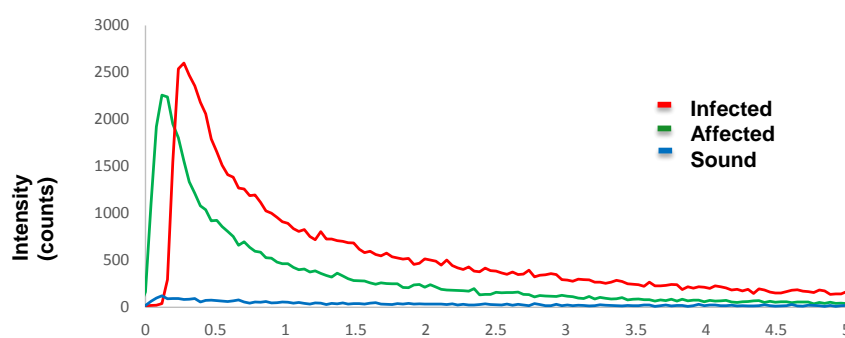


Figure 4-1 Representative Auto-fluorescence decay curve from caries-infected (red), caries-affected (green) and sound (blue) dentine.

A multiphoton fluorescence microscope was used in the current study to investigate the differences in fluorescence characteristics of carious dental tissues and enable this technique to be used later on to assess their interaction with dental cements within the same samples. This advanced imaging technique uses a pulsed laser source with double the excitation wavelength that is required for the fluorophore emission. Consequently this offers deep tissue penetration with high resolution and decreased photodamage (So et al., 2000; Helmchen and Denk, 2005). In

addition, it provides wider separation between the excitation and emission spectra and reduces the background scattering (So, 2008; Becker, 2008). Moreover, the need of using pinhole is no longer needed as multiphoton excitation reduces photo-bleaching outside the focal plane since only the fluorophores in the centre of the focal spot are excited. These advantages are of great importance when imaging thick dental samples. The present study was conducted using an in-house manufactured multiphoton fluorescence microscope that offers AF imaging with a FLIM option and a spectrometer also being connected to it to simultaneously spectrally analyse the optical signal from the same object area. These applied multimodal techniques are promising for in-vitro dental caries characterization as they are non-invasive, highly specific and provide point to point comparable measurements with relatively high resolution.

The aim of this study was to delineate objectively the zones of caries infected, affected and sound dentine by means of multimodal techniques based on the optical properties of these tissues. The use of single/two-photon microscopy and spectroscopy were validated by correlating the data from AF intensity and lifetime images, AF and SHG spectra with the current “gold standard” microhardness measurements. These techniques sensitivity and specificity were then further compared to determine the best methods that differentiates between caries zones. The null hypotheses investigated were that there are no significant differences in signals between different dentine caries zones using multimodal optical microscopy/spectroscopy techniques and that there is no correlation between these techniques and knoop microhardness (KHN) between the three histological zones tested.

4.2 Materials and methods

Twenty extracted carious human molar teeth were collected using an ethics protocol reviewed and approved by the NRES Committee London - Stanmore (Reference 12/LO/0290). The root of each tooth was sectioned to act as a horizontal reference. Each tooth was sectioned longitudinally into two halves through the lesion then the buccal and lingual surfaces were also cut to create a flat surface using a slow-speed (200 rpm) water-cooled diamond wafering blade XL 12205, (Benetec Ltd, London, UK). Teeth containing suitable dentine caries lesion surrounded by healthy dentine were selected for analysis. Each half was prepared with a diamond bur at the start of the lesion to create a perpendicular angle that was used as a reference point during imaging and data recording. Finally, a scaled clinical photograph was obtained using high resolution camera (Nikon D800E, Japan) for the visual 'clinical' evaluation and to mark the exact distance of points to be measured from the reference point depending on the overall size of the lesion. The samples were labelled and stored in a separate glass vials containing distilled water throughout the study.

4.2.1 Two-photon microscopy AF, SHG and FLIM imaging and AF spectrum detection

An in-house manufactured two-photon microscope was used in this study. Samples were rinsed with deionised water in order to remove any surface debris. At the start of imaging each sample, the laser power was measured using power meter (PM30,Thorlabs GmbH, Germany) and the intensity of a previously prepared reference bead (PeakFlow™ Orange flow cytometry, 6 µm, Invitrogen, USA) was measured. These two imaging references were used to calibrate the incident laser intensity as they were kept constant throughout the study in order to eliminate any effect of laser intensity fluctuation. Samples were rinsed with deionised water to remove any surface debris. When imaging each section, the sample was placed with the root surface parallel to the cover slip then the reference point was localised and recorded in the microscope controller software. The X and Y positions from the reference point was recorded for the first measured point, then subsequent points series were localised, separated by 500 µm towards the pulp chamber forming an imaginary vertical line to cross all histological zones of carious dentine. Further three or four parallel series of lines were imaged through the sample depending on the extent of the lesion and matching the points marked previously on the clinical

photograph, this gives data of approximately 42 tested points from each sample (Figure 4-2). Samples were examined using a two-photon fluorescence microscope with a 20x 0.75 NA air objective lens, 854 nm excitation wavelength and 550 ± 20 nm emission filter (McConnell et al., 2007; Banerjee et al., 2010a). A fluorescence intensity image, 256 x 256 pixels, was obtained for each point measurement. Using the FLIM option in the same microscope, fluorescence lifetime images, 256 x 256 pixels, were also obtained. The AF spectrum displaying both AF and SHG signals were transmitted to a fibre-optic spectrometer (AvaSpec-ULS2048L, Avantes Ltd, Netherlands) installed within the microscope apparatus. The obtained spectrum was detected at a range of (400-700nm) which included the wavelengths where SHG (427nm) and dentine AF (550 nm) signal exhibit strong peaks.

4.2.2 Single-photon spectrometer autofluorescence

After imaging, samples were transferred for AF spectrum detection using a single-photon fibre-optic spectrometer. A stereo microscope (MEIJI Techno UK Ltd., UK), was used to localise the reference point on each sample and the position on a movable stage was set to zero. Then the spectrum was detected from each point following the measurements recorded previously. The auto-fluorescence was stimulated with a 470 nm mounted LED, its beam was directed through a Dichroic long-pass filter (>505 nm), via a multimode optical fibre (200 μm) to the tooth surface. The excited fluorescent light was collected using the same fibre and transmitted to a fibre-optic spectrometer at > 488 nm (AvaSpec-ULS2048L, Avantes Ltd, Netherlands) as illustrated in Figure 4-3. The fibre was peroxide-bleached between each reading and subsequent readings were performed only when no fluorescence was detected from the probe in air (Banerjee et al., 2010a). To ensure high local resolution, the fibre end was placed end-on to the tooth surface. Measurements were transferred automatically and saved to Excel to be analysed, via the Avantes analysis software.

4.2.3 Microhardness measurements

The Knoop microhardness (KHN) from each tested point was measured using a Struers Duramin microhardness tester (Struers Ltd., Denmark). Diamond-shaped indentations were produced by applying 10g load for 15 seconds, after which they

were measured through a 40x 0.65 NA objective and the KHN was calculated using the manufacturer's software.

The reference point was spotted using the same objective and the movable stage was set to zero to allow further testing of the previously imaged points on each sample and crossing the different histological layers of carious dentine. The obtained data from other optical measurements (average lifetime, AF intensity, AF and SHG signals) were then allocated to the tissue type it represents depending on the KHN calculated. The points were considered caries-infected dentine if the Knoop hardness number (KHN) was <25 , while caries affected dentine had KHN ranging from 25 to 40 and the sound dentine KHN >40 (Ogawa et al., 1983; Banerjee et al., 1999; Banerjee et al., 2010a).

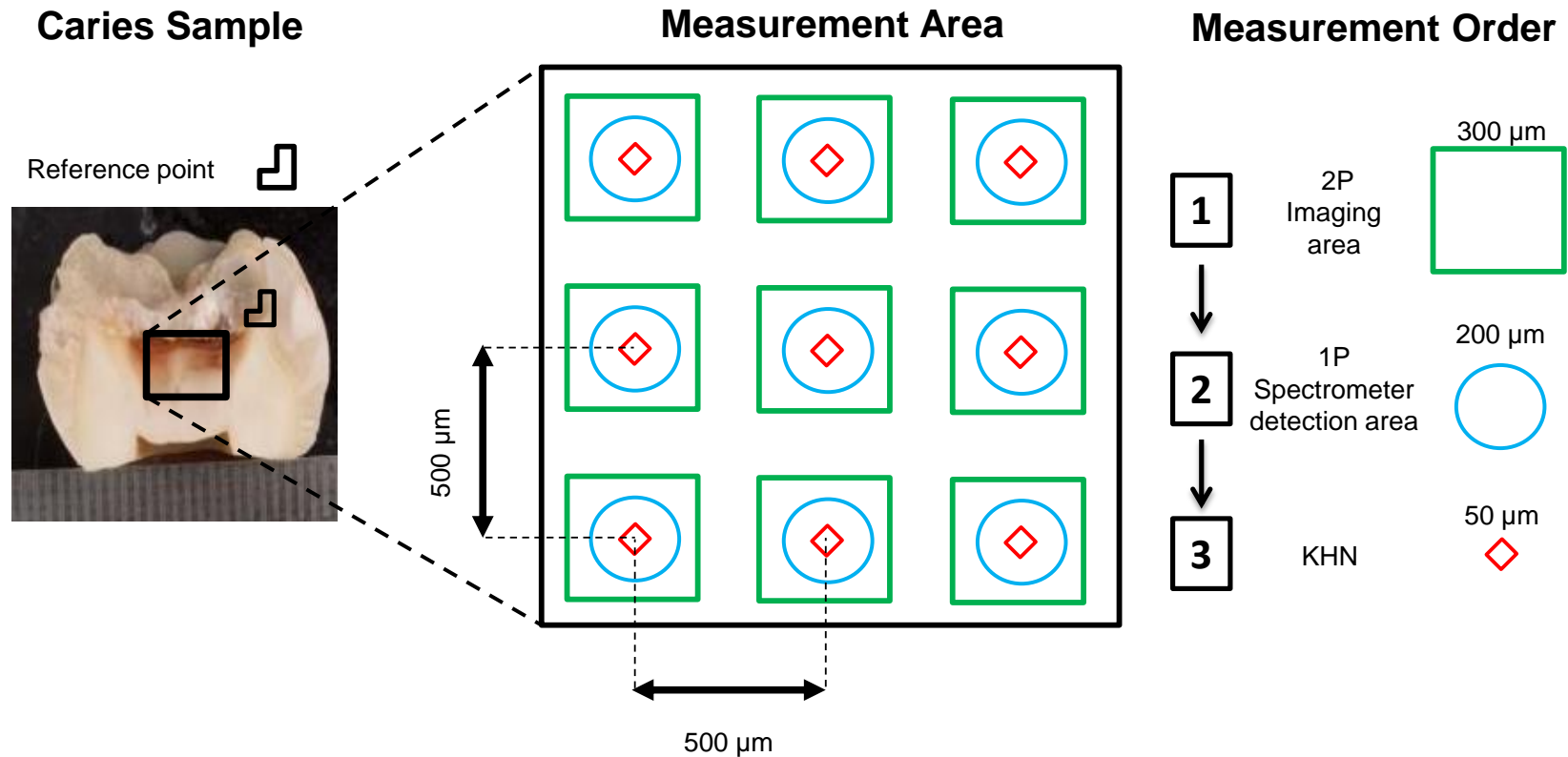


Figure 4-2 A calibrated photomicrograph of a sample with the reference point created and the test area selected. Geometric representation of the performed techniques, starting with two-photon imaging then single-photon fibre-optic spectrometry and finally Knoop microhardness testing.

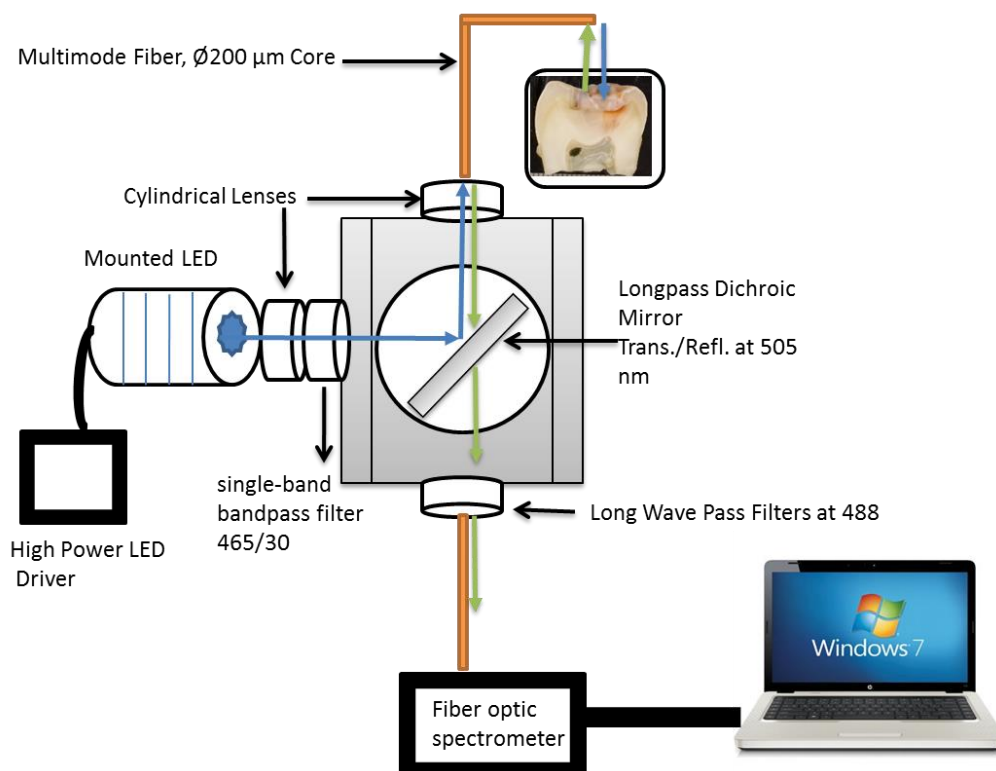


Figure 4-3 Single-photon spectrometer experimental apparatus. Excitation: Mounted high power blue LED (470 nm), Single excitation bandpass filter 465/30. A dichroic reflector (505 nm LP) positioned at 45° angle in the excitation beam permitting transmission of >505 nm wavelength. A long pass (488 nm) emission filter.

4.2.4 Statistical analysis

The obtained fluorescence lifetime (FLIM) images from two-photon fluorescence imaging were analysed to calculate the average lifetime using TRI2 FLIM analysis software (courtesy of Paul Barber, Grey Cancer Institute, Oxford). The fluorescence decay curves were fitted using a biexponential model and the lifetime values were then averaged for each tissue type (caries-infected dentine, caries-affected dentine and sound dentine). Likewise, using ImageJ analysis software (ImageJ, Wayne Rasband, NIH, USA), the fluorescence intensity of each image was calculated and the values were averaged for each tissue type. The obtained multiphoton spectra displayed three distinctive peaks; the SHG signal at (427 nm) and two autofluorescence signals that we refer to as AF1 and AF2. From each point measurement, we calculated the average intensity of SHG between (417-437

nm), for AF1 (440-510 nm) and (510- 630 nm) for the AF2 (see Figure 4-6-D). The ratio of SHG/AF2 and AF1/AF2 were used to display the results after it was averaged for each tissue type.

The spectra from the single-photon spectrometer were also analysed by calculating the average weighted wavelength and average intensity from the obtained spectra. The AF intensity data was then normalized by the intensity of a fluorescence reference slide measured at the start of testing each sample. Data from both weighted wavelength and normalised AF intensity were then averaged for each tissue type.

A one-way ANOVA test was performed to compare the significant differences between caries layers for each applied method, using IBM SPSS Statics Viewer 21 software (IBM United Kingdom limited, UK). The differences between any two tissue types were detected using Tukey's test. Sound dentine data located well away from carious dentine were obtained and used as positive controls regarding all parameters.

- **Statistical classification method to test and compare the applied optical techniques**

To create a robust statistical method which computes the probability of identifying caries tissues based on optical measurements, we implemented an algorithm which calculated density functions using variable-width kernels. In this statistical classification method, the width of the kernel function was set to be directly inversely proportional to the local density as described by Terrell and Scott (1992). In brief, both kernel width and density function were calculated using a recursive algorithm was the kernel width is given by:

$$\delta = \frac{1}{[nP(\vec{x})]^{1/D}}$$

As n = number of measurement and D is the dimension (number of techniques).

Due to the spares nature of our data, the original Gaussian function used by Terrell *et al* did not converge for low densities, as the width tends to go to infinity. Instead, we used a Cauchy/Lorentzian function for the Kernel as the function side lobes decay slower than a Gaussian function, making the algorithm more stable and faster to converge:

$$f(x; x_0, \gamma) = \frac{1}{\pi\gamma} \left[\frac{\gamma^2}{(x - x_0)^2 + \gamma^2} \right]$$

where x_0 is the location and γ is the width of the distribution. The relative probability of the different tissues is then given by the relative weight of their density function. A representative example for the fluorescence lifetime is shown in Figure 4-4 with the density function (A,B) and the probability (C) for infected, affected and sound dentine.

Finally, the sensitivity and specificity of each technique, or combined of techniques, were evaluated using the generic “leave-one-out cross validation” (LOOCV) method where each data point is evaluated using the rest of the dataset and the number of false positive and false negatives one recorded. **software and DR.festy**

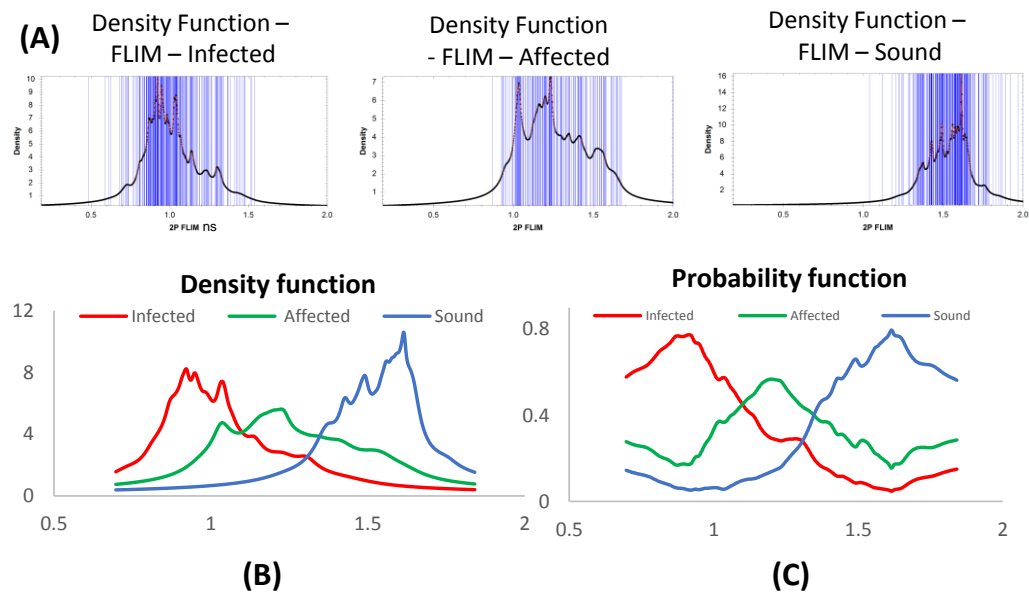


Figure 4-4 A representative example of the calculated probability density function with Variable Kernel Width using Lorentzian Kernel for FLIM data. (A) Density functions for infected, affected and sound dentine. (B) The density function for all carious zones. (C) The probability of all carious zones.

4.3 Results

4.3.1 Two-photon fluorescence microscopy

Multimodal optical techniques were verified using the laboratory gold standard method for caries characterization. Figure 4-5 summarizes representative data obtained from different dentine caries zones using the two-photon microscope. The FLIM images indicate that the average fluorescence lifetime decreased gradually from sound to carious tissues (red represents a longer lifetime for healthy tissues). In addition, the AF images show an increased intensity from sound to carious dentine as the images were darker in sound tissue and bright in carious dentine.

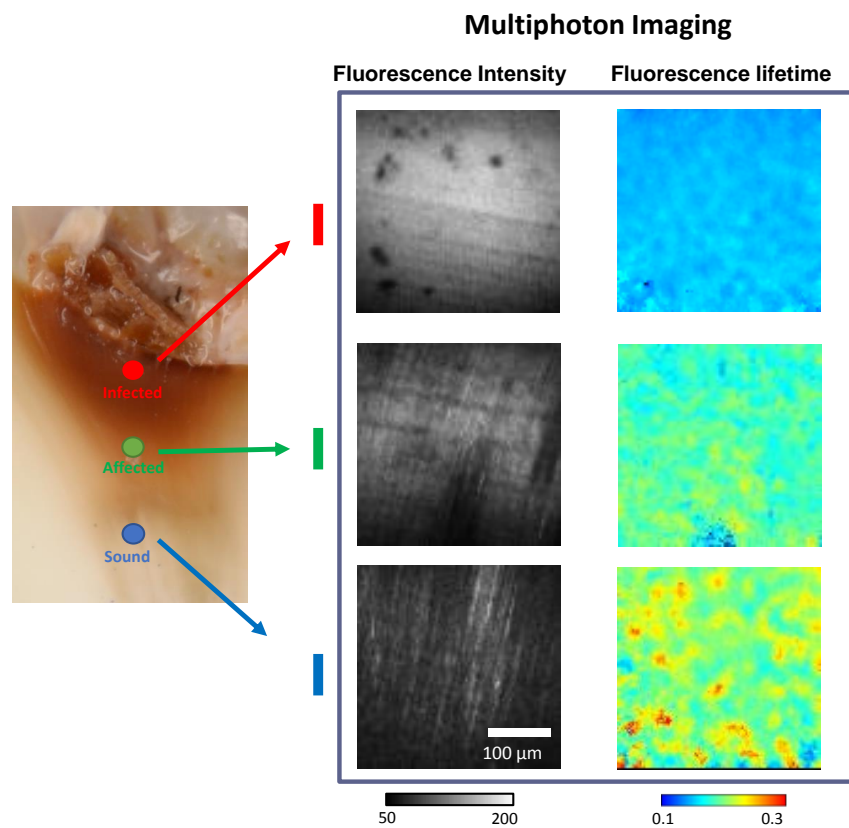


Figure 4-5 Representative multiphoton fluorescence images showing a decrease in the fluorescence intensity from infected to sound dentine and an increase in the fluorescence lifetime from (0.9 ns) for infected to (1.6 ns) for sound dentine.

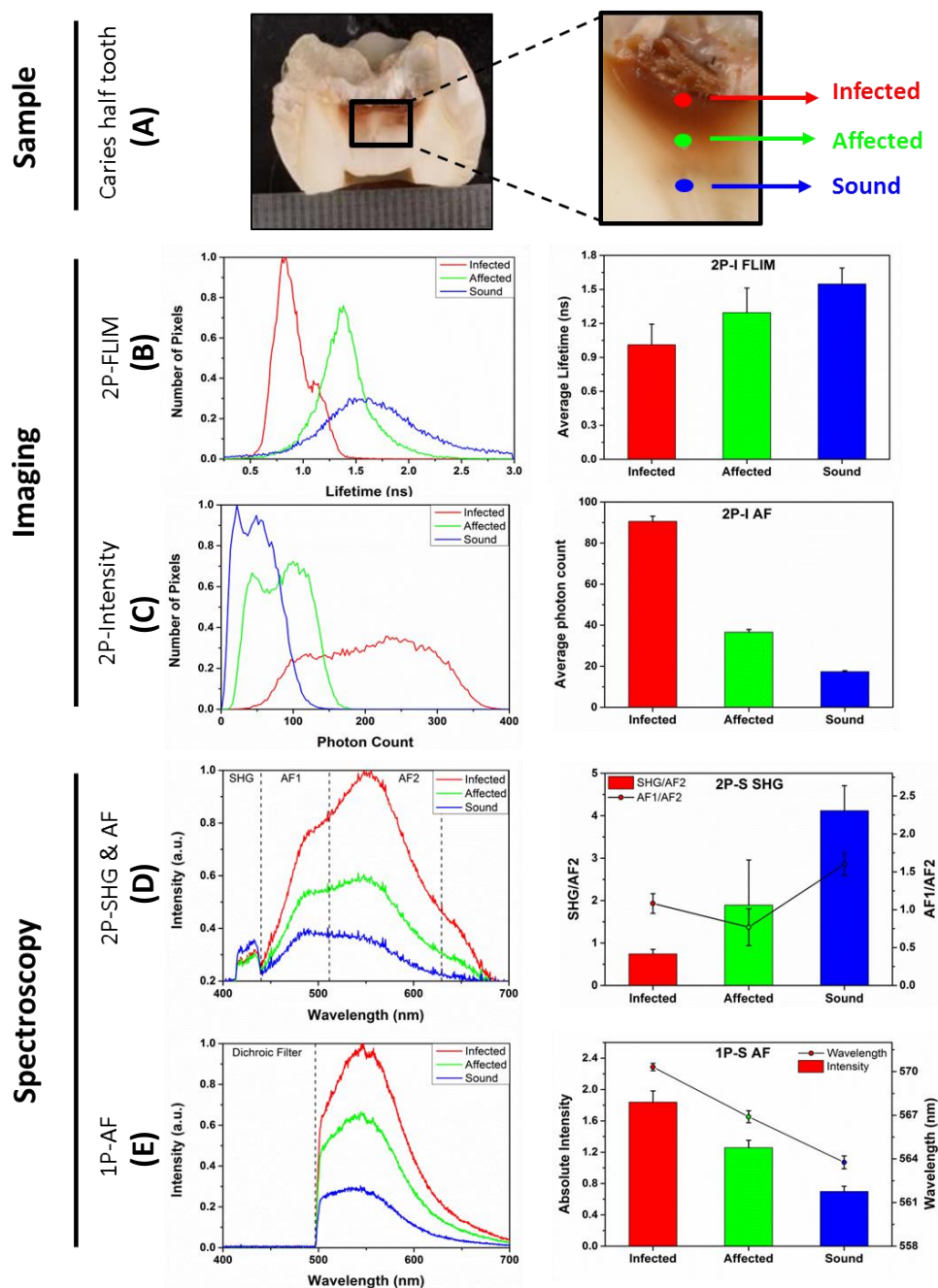


Figure 4-6 (A) a photograph of half a sample with an example of the selected caries lesion displaying caries zones (red) is for infected tissue, (green) for affected and (blue) is for sound. Multiphoton imaging results are presented in (B) for lifetime data. Representative histogram showing variations in the lifetime values and the average auto-fluorescence lifetime calculated for each tissue type. (C) Representative histogram of the AF intensity images and the calculated average AF intensity for caries zones. Multiphoton spectroscopy data are presented in (D) representative AF spectra obtained from the lesion. The bar graph represents the average SHG/AF2 ratio and the AF1/AF2 ratio. The averaged spectra from single-photon excitation are presented in (E) with a graph showing the averaged AF signal intensity and the average weighted wavelength for each carious dentine zone.

The analysis of fluorescence lifetime images (FLIM) showed significantly distinct average lifetime values for each dentine zone ($p= 0.001$). The auto-fluorescence decay curves were fitted by a double-exponential model. The yielded average lifetime recovered from ($0.9 \text{ ns} \pm 0.01$) in caries infected dentine to ($1.6 \text{ ns} \pm 0.01$) in sound dentine tissues, while in caries affected dentine it was calculated to be ($1.3 \text{ ns} \pm 0.01$) as shown in Figure 4-6-B. These results indicate that the reduction in auto-fluorescence lifetime induced by the caries process can be exploited to delineate caries infected from caries-affected dentine and to diagnose healthy and carious tissues. The obtained blue-green AF intensity decreased from infected to sound dentine tissues. Significant differences were found in the average intensity values ($p= 0.001$) between caries infected $90.6 \text{ AU} \pm 2.5$, affected $36.6 \text{ AU} \pm 1.3$, and sound dentine $17.3 \text{ AU} \pm 0.5$ (see Figure 4-6- C).

To monitor changes in the two-photon AF and SHG signals across the carious lesion, spectra were obtained from the samples and a representative average spectrum for each tissue type is presented in Figure 4-6-D. The ratio of SHG/AF2 was low in the caries-infected dentine $0.7 \text{ AU} \pm 0.1$ and showed an increase towards caries affected $1.9 \text{ AU} \pm 1$ and sound dentine $4.1 \text{ AU} \pm 1$. The statistical analysis resulted in significant differences between caries-infected and sound dentine ($p= 0.001$) and between caries-affected and sound dentine ($p= 0.03$) but was not significant between caries infected and affected dentine ($p= 0.39$). On the other hand, the ratio of AF1/AF2 intensity from two-photon spectra showed significant differences between infected and affected as $p= 0.021$, but was not significant to differentiate between affected and sound as $p= 0.97$. This ratio at the caries infected dentine was $1.08 \text{ AU} \pm 0.1$, and decreased in the caries affected $0.8 \text{ AU} \pm 0.2$ then was $1.6 \text{ AU} \pm 0.1$ in sound dentine.

Regarding the change in SHG signal, another ratio calculation was carried out based on previous study considering the total AF signal intensity (Terrer et al., 2016). The ratio of SHG/ (AF1+AF2) was calculated and showed significant results discriminating between the three carious zones as $p= 0.001$. The ratio of infected caries dentine averaged $0.2 \text{ AU} \pm 0.08$ for infected dentine, $0.5 \text{ AU} \pm 0.08$ for affected dentine and $1.4 \text{ AU} \pm 0.2$.

4.3.2 Single-photon fibre optic spectrometer

The obtained spectra display distinct AF intensity and weighted wavelength for each tissue type as shown in Figure 4-6-E. The average intensity values of carious dentine were found to be almost double the intensity of sound dentine. For caries-infected dentine it was $1.8 \text{ A.U} \pm 0.1$, $1.2 \text{ AU} \pm 0.9$ for caries-affected and $0.7 \text{ AU} \pm 0.6$ for sound dentine. Whereas for the weighted wavelength the peak emission was red-shifted from 545 to 556 nm. The average weighted wavelength was located at $563.7 \text{ nm} \pm 0.4$ for sound, at $567 \text{ nm} \pm 0.4 \text{ nm}$ for affected and $570.3 \text{ nm} \pm 0.2 \text{ nm}$ for infected dentine. Statistical tests revealed high significant differences between the three groups ($p = 0.001$) for both AF intensity and weighted wavelength.

4.3.3 Results from the statistical classification method

Calculated specificity and sensitivity of individual optical techniques are displayed in Figure 4-7-A. It shows that all methods have good specificity (all above 65%) while sensitivity got as low as 25% with single photon intensity (weighted wavelength) measurements. Figure 4-7-B displays the average sensitivity and specificity (for all tissue types) for each technique. Multiphoton imaging intensity showed the best results for both specificity and sensitivity regarding all tissue types. Therefore it was assessed in combination with all the others to evaluate the benefits of combining two optical techniques (Figure 4-8). We found that the best results were achieved when combining multiphoton intensity and FLIM imaging to characterise the dentinal tissues. The sensitivity test resulted in 88 %, 61% and 76% for infected, affected and sound respectively, while specificity results were 89.9%, 82.9% and 95.8%. Figure 4-9 represents a plot chart associating the average AF intensity and lifetime data. It shows the ability of both parameters to significantly distinguish between infected and affected caries tissues, with less evidence in discriminating caries-affected and sound dentine.

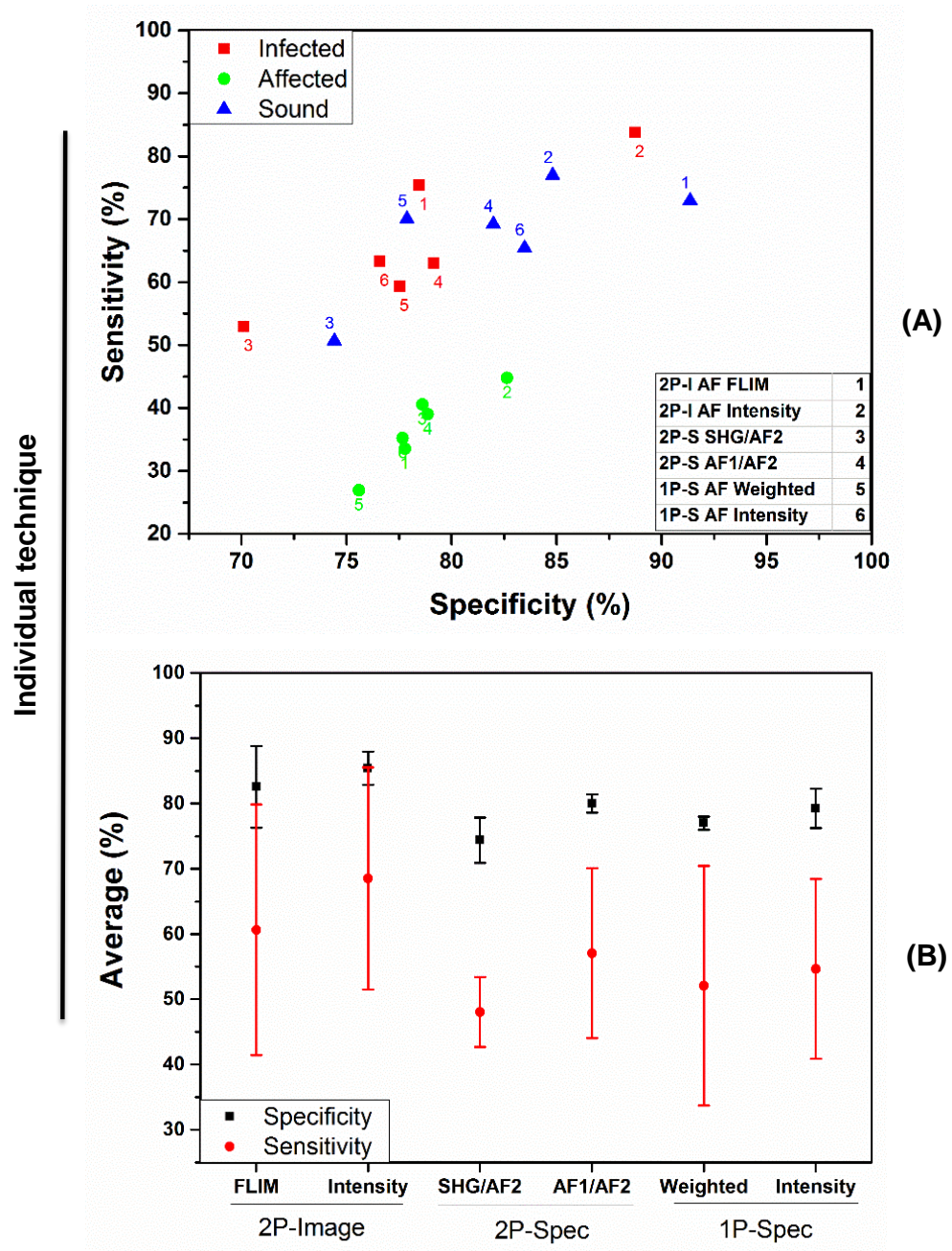


Figure 4-7 The sensitivity and specificity calculated for individual optical technique regarding each caries zone are presented in (A) and averaged for individual technique in (B) highlighting the superior sensitivity and specificity of the multiphoton intensity imaging technique.

Combined 2PI with other techniques

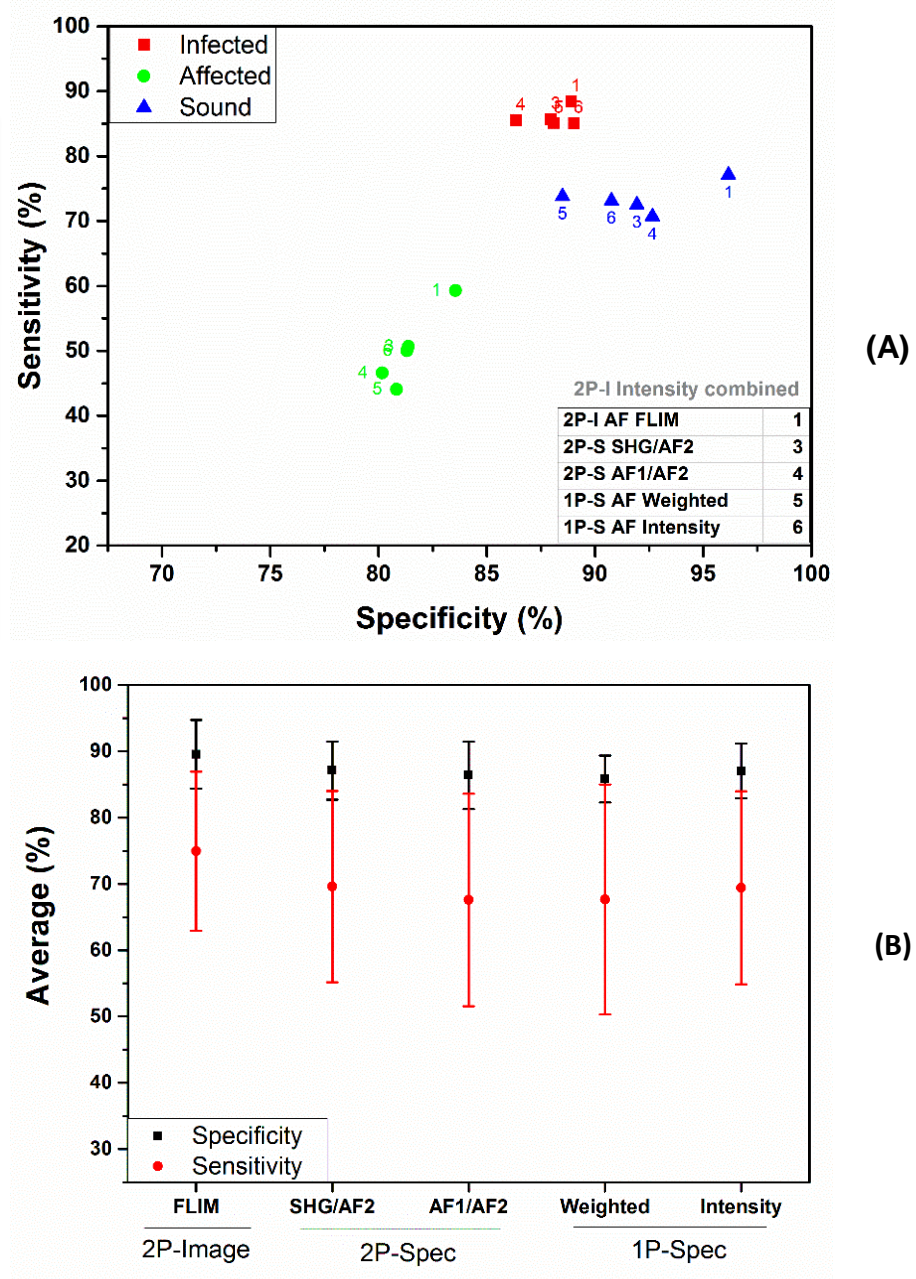


Figure 4-8 The sensitivity and specificity of each optical technique when combined with the two-photon intensity imaging (2PI). Regarding each tissue type in (A). The averaged sensitivity and specificity values for the combined technique in (B). The data shows that combining multiphoton intensity and lifetime imaging resulted in the best sensitivity and specificity values.

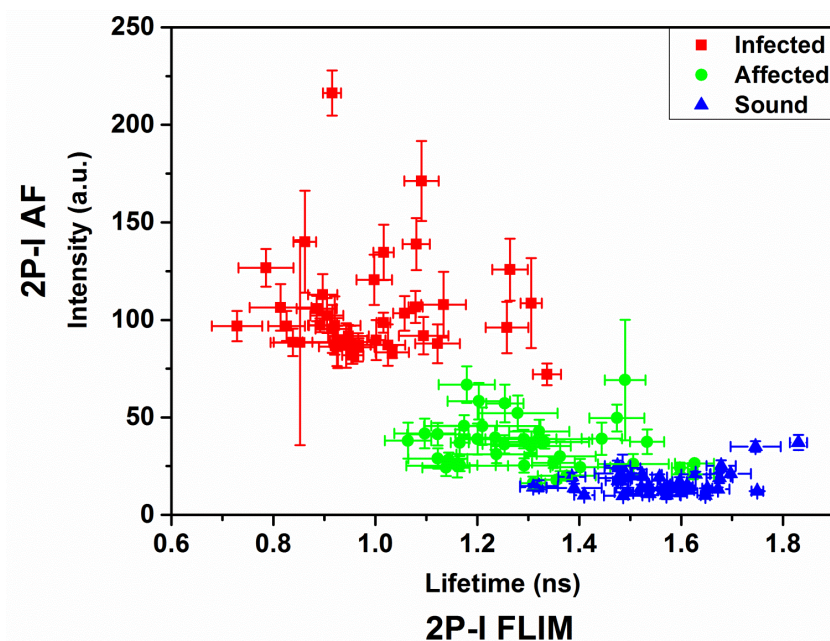


Figure 4-9 Plot graph showing the average intensity and lifetime data of caries infected (red), affected (green) and sound (blue) dentine. The graph represents the ability of both parameters to discriminate between infected and affected tissues with less significance regarding affected and sound dentine.

4.4 Discussion

This study introduced a multimodal non-invasive optical approach using multiphoton microscopy apparatus to correlate the optical data, and the KHN obtained from carious and sound dentine. In addition, the study presents the fibre-optic spectroscopy as a technique for direct auto-fluorescence measurement that can be detected with good accessibility and precise localisation within the examined tissues.

The progression of a natural carious lesion is a continuous histopathological transition with gradual histological and bacteriological alterations towards the pulp rather than separated distinct zones of caries-infected, caries-affected and sound tissues. Clinically the relative tissue hardness of the remaining tissues during caries excavation remains the most reliable but subjective method for dentists to determine the end of the excavation procedure. The relative dentine hardness measurements using a microhardness indenter (Knoop hardness indenter) is a direct in-vitro translational value for dental tissues relative mineral content and inherent physical properties (Ogawa et al., 1983; Banerjee et al., 1999). This relationship was further investigated in a previous study, in which a significant correlation between Ca:P ratios of caries-affected dentine and its microhardness

was found (Sakoolnamarka et al., 2005a). Therefore, Knoop indentation has been used to characterise different carious zones and to detect changes in dentine hardness after the application of therapeutic dental materials (Kirsten et al., 2010; Bresciani et al., 2010). It has been found that the Knoop hardness number for caries infected dentine is <25, while caries-affected dentine values are between 25-30 and sound dentine has KHN above 40 (Ogawa et al., 1983; Banerjee et al., 2010a; Almahdy et al., 2012). These values were used in this study as a reference to determine the tissue types after imaging and allow investigating the correlation between the obtained optical data and the KHN. However, there are many limitations associated with the use of the microhardness testing, the readings are rather subjective to the operators skills with may introduce some errors specially in relation to infected dentine where the tissues are too soft and it is rather difficult to produce a readable indentation. Moreover, the test is considered destructive, and so the KHN was obtained in this study only after other non-invasive experimental methodologies had been carried out and data collected. The disadvantages related to the use of hardness testing motivated the search for non-invasive objective method to delineate the zones of caries dentine.

The alternative non-invasive optical techniques presented in this study were further investigated to achieve quantitative comparisons. The evaluation was based on their calculated sensitivity and specificity to delineate the dentine zones within carious lesion. This is a valuable method to determine the future application of such techniques either clinically or in laboratory investigation. Multiphoton fluorescence imaging (intensity and lifetime) showed superior sensitivity and specificity in differentiating caries-infected from caries affected dentine, either individually or combined. This suggests the significance of applying this technique in-vitro to determine the endpoint of caries excavation as the technique is highly sensitive to caries infected dentine. It may also be beneficial to carry out studies investigating the efficiency of caries excavation techniques or assessing the interaction of dental materials with dentine and their potential remineralisation effects.

Previous studies reporting the use of FLIM to investigate dental tissue samples are limited (Table 4.1). One reason for this limitation could be that FLIM requires a high repetition rate pulse laser with an excitation wavelength that must be well-matched with the absorption wavelength of the tested sample. This is achievable by using either a pulsed laser diode for single photon excitation which provides a limited number of wavelengths or via multiphoton excitation (Berezin and Achilefu, 2010; Watson et al., 2008). In this study, the in-house manufactured multiphoton

fluorescence microscopy was used with the additional advantages of simultaneous AF imaging, FLIM and SHG signal generation from the same sample area.

Excitation/ Emission(nm)	FLIM (ns)				References
	Sound E	Sound D	Carious E	Carious D	
330	-----	5.7-6.3	-----	-----	(Matsumoto et al., 1999)
488/ 560 \pm 25	1.75- 1.9	2.3	-----	Infected=1.8 Affected= 1.9	(McConnell et al., 2007)
70/ 500	2.46	2.8	1.8	Infected= 1.9 Affected= 2.3	(Lin et al., 2011)

Table 4-1 a summery table representing previous studies that investigated the lifetime of dental tissues with the lifetime results for sound and carious tissues.

The current data showed a repeatable progressive increase in the fluorescence lifetime from carious to sound dentine tissues, reporting significant differences due to variations in environmental conditions and chemistry across the examined tissues. This compares well with the previous FLIM studies on carious dentine (König et al., 1999; McConnell et al., 2007; Lin et al., 2011). König et al.(1999), reported two lifetime components when examining carious tissue, a very long one (10-20 ns) which was due to porphyrins, as explained by the spectral analysis, in addition to other shorter lifetime components 0.5–0.3 and 3.2–2.3 ns due to porphyrin aggregates (König et al., 1999). In the current study, 550 \pm 20 nm bandpass filters were used and the long porphyrin lifetimes were not detected. This stimulates the investigation of other fluorochrome sources as the porphyrin contribution was minimized. A single-photon excitation with photonic crystal fibre (PCF) technology was used to perform TCSPC FLIM on dental samples (McConnell et al., 2007). This technology was successful to broaden the range of accessible excitation wavelengths that is not achievable with single-photon excitation but the low resolution and defocusing of the images produced in addition to the strong scattering were not well-resolved. These limitations were surmounted in the current study by the use of two-photon excitation that provides a wide range

of excitation wavelengths with optical sectioning capability. The analysis of the fluorescence lifetime images obtained by McConnell et al. in a similar band pass range 560 ± 25 nm showed comparable reduction in the lifetime accompanied with enhanced AF within the carious dentine as noticed in our study. The mineral content of the carious dentine has been related to the decreased fluorescence lifetime as shown in this study by the KHN measurements and in a previous study where it was correlated with mineral density using micro-CT evaluation (Lin et al., 2011). It was also demonstrated earlier in chapter two of this thesis as the lifetime was affected by aseptic acidic demineralization of sound dentine. However, sound enamel lifetime values were shorter than those of sound dentine despite the lower mineral content in the latter (McConnell et al., 2007; Lin et al., 2011). This suggests that the altered fluorescence lifetime in dental samples may be attributed to both organic and inorganic components. Other factors that are proposed as explanations of the change in lifetime may include any inherent dentine matrix fluorophore, possibly collagen, that has been altered due to the caries process; the quenching effect of local environments such as pH changes, oxygen level or local ion concentration (Kwak et al., 2001; Gannot et al., 2004) all of which suggest further investigations.

Two-photon emission spectra in this study are detected at a wide range (400-700 nm) which allows the analysis of both AF and SHG signals. Second harmonic generation is a non-linear interaction between light and matter. With high intensity laser illumination this interaction leads to the emission of light with double the frequency (half the wavelength) of the illuminating laser source (Boyd, 2003). Earlier studies showed strong correlation between SHG signal and collagen concentration (Kim et al., 2000; Kao, 2004). Therefore it has been found that dentine produces an intense SHG signal compared to cementum or enamel (Eichler and Kim, 2002). In the natural caries process, collagen destruction takes place, and one can expect the reduction or loss of SHG in the affected tissues. This has been demonstrated previously using ultra short pulsed lasers (Eichler and Kim, 2002) and multiphoton imaging (Lin et al., 2011). Similarly, for the laser excitation used in the present study (854 nm), the SHG signal was detected at (427 nm) and its intensity differs significantly across the carious lesion. Although SHG was found not to be dependent on the degree of mineralisation (Altshuler et al., 1995), its direct correlation with the collagen gives SHG detection a potential use in caries diagnosis and determination of caries removal endpoint.

The data variations of SHG signal intensity between caries zones in this study were not statistically significant. Contrarily, the ratio of SHG/AF2 was significant in differentiating caries-affected and sound dentine. A recent study has presented two-photon excitation spectra with SHG and AF data with similar spectral profile to the one in the current study (Terrer et al., 2016). They have also found insignificant variations of SHG and AF signals between sound and carious dentine. Therefore, a ratio of SHG/AF was used to conduct a comparison. This study differs from the current one in the recognition of two auto-fluorescence peaks in the obtained spectrum which we refer to as AF1 (440-510 nm) and AF2 (510-630 nm) instead of a single AF peak (475-700 nm) (Terrer et al., 2016). Moreover, in the current study, we are considering the differences between caries-infected and caries-affected dentine where more prominent variations in AF2 intensity was noted. This justifies calculating the ratio between SHG/AF2 and AF1/AF2 in order to present qualitative comparisons between all dentine zones.

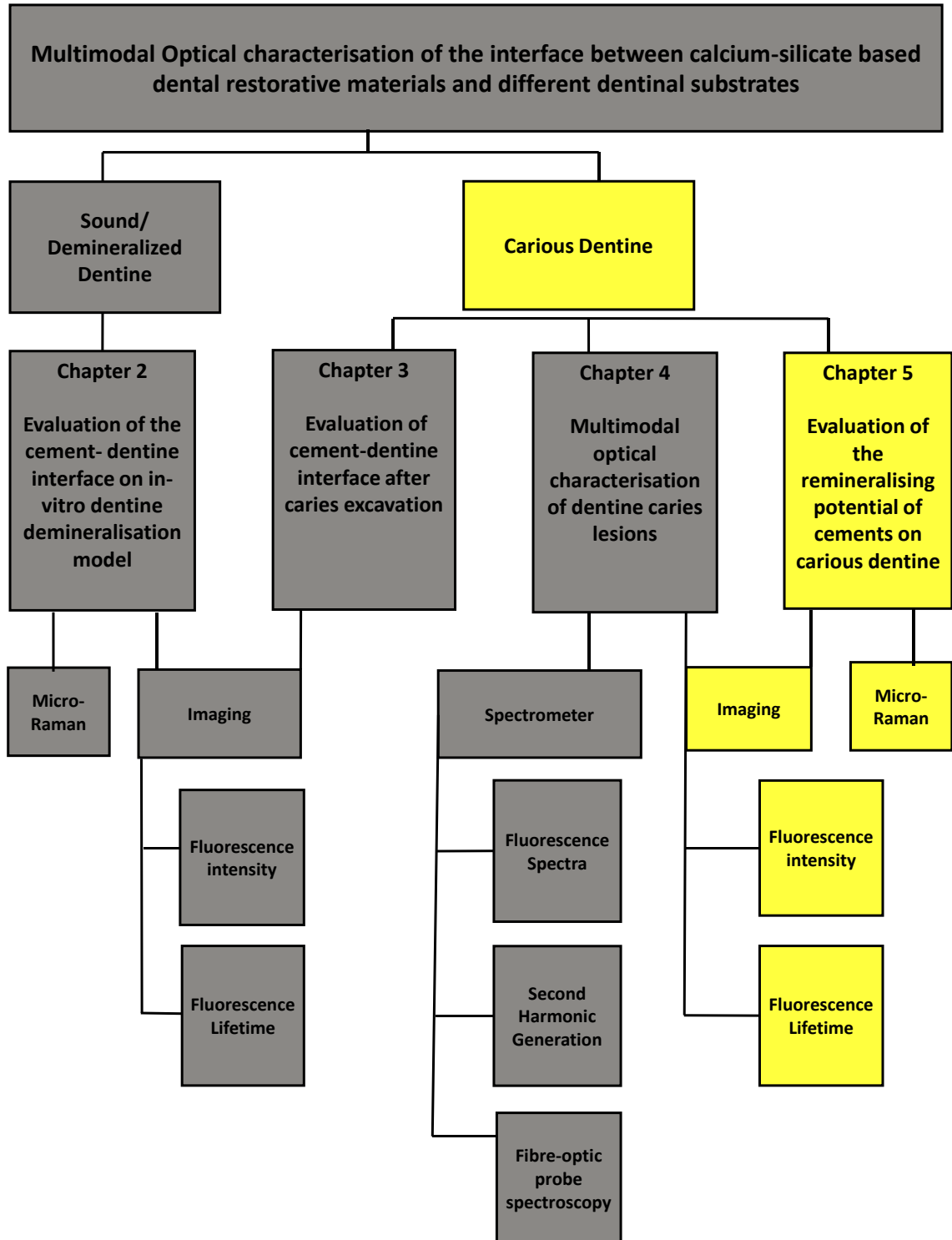
The differences in the average auto-fluorescence intensity for each caries zone seems to concur with previous studies which have found that the AF signature is prominent at the superficial, infected and pigmented carious dentine, then its value drops towards the pulp at sound dentine area (Banerjee et al., 1999; McConnell et al., 2007; Banerjee et al., 2010a). The AF signature of dentine as a result of blue-green excitation is referred to the breakdown of structural protein (Van der Veen and Ten Bosch, 1996; Banerjee and Boyde, 1998; McConnell et al., 2007). This suggests that for AF signal to be generated there must be either direct or indirect bacterial interaction with the dentine matrix. Thus, changes in the AF intensity reflect the degree of tissue destruction and the chances of tissue repair through remineralisation. At the superficial infected dentine, matrix degradation has occurred by means of bacterial input so the AF signal is enhanced. More centrally, tissues are still soft as they are affected by the acidic environment which causes inorganic structural changes followed by the activation of certain proteases (MMPs) that induces the defibrillation of unprotected collagen fibrils. This explains the detection of AF signal in this layer but to a lesser extent and the increased tissue hardness compared to infected tissues (Kleter et al., 1998; Carvalho et al., 2009).

Auto-fluorescence signal intensity obtained from single-photon excitation displayed recognisable emission AF peak around 550 nm from sound dentine tissues then the emission intensity gradually increased and red-shifted to 556 nm within caries-affected and infected tissues (detected >500 nm with single-photon spectroscopy). Signals at this range with excitation at wavelength of 488 nm have been detected

earlier and referred to bacterial molecule, as metallo- porphyrin, or to the breakdown of collagen molecules as a result of bacterial influence, which are suitable explanations for our experimental setup (Banerjee et al., 1999; Hibst et al., 2001; Ribeiro et al., 2005b; Banerjee et al., 2010a). Besides the significant results found from the single-photon fibre optic spectrometer, this technique has the advantages of point by point measurements with great accessibility to all examined surfaces and simple analysis of the acquired spectra. It has been successful on extracted teeth in the laboratory with future potential of developing a chair-side device based on fibre optic spectrometry for the assessment of caries excavation procedure.

In conclusion, the optical techniques used in this study offer a quantitative and reproducible definition of lesion zone transitions detected from a large number of samples with significant correlation to Knoop hardness number. They can be considered as alternative microscopic markers, non-invasive and objective in-vitro diagnostic techniques for dental caries with further consideration to bring these optical signals to clinical application. Furthermore, the imaging methodology used allow for sample examination without labelling nor preparation which permits future assessment of the samples after storage with possible evaluation of dental materials or advanced caries excavation techniques. The applied model in this study methodology allows for co-localized testing of the samples by means of multiple modalities. The results rejected the null hypothesis investigated in this study as the detected optical signals from different caries dentine zones provided distinct delineation between them. Also, there was a correlation between these optical signals (AF, F lifetime and SHG) and the relative tissue hardness KHN.

5. Chapter Five: Evaluation of dental cements' interaction with natural carious dentine



5.1 Introduction

A challenging mission for minimal invasive dentistry has been to develop a compatible material that can replace the lost part of the tooth and at the same time be able to induce tissue healing and minimize any further damage to tooth structure. The development of glass ionomer cement and, more recently, calcium silicate cements such as Biodentine™ (Septodont, Saint Maur des Fosses- France) has been a major step forward in this respect. The two cements have been shown to induce a sort of mineral deposition and promote tissue healing, both clinically (Koubi et al., 2013; Hashem et al., 2015) and in laboratory investigations (Atmeh et al., 2012; Han and Okiji, 2013). In clinical situations, they are used as indirect pulp capping restorative materials, where the caries infected dentine is selectively removed then the material is applied on the remaining affected dentine to promote tissue healing by enhancing remineralisation and preventing further destruction by the carious process (Hilton, 2009; Hashem et al., 2015).

The in-vitro remineralising capacities of these cements have been assessed in our laboratory using sound dentine and totally demineralised dentine samples (Atmeh et al., 2012; Atmeh et al., 2015). All of these confirmed the bioactivity of Biodentine cement and its ability to induce mineral deposition within the dentinal tissues. However, to date, no studies have been conducted to investigate the interaction of Biodentine with natural carious teeth. Despite the claimed similarity of artificially demineralised samples and natural caries in terms of mineral content, other biological components in carious lesions play an important role in rendering or enhancing the remineralisation process. Therefore, it is of great importance to evaluate the effectiveness of dental materials in such natural conditions.

A large number of researchers have studied the role of glass ionomer cements in remineralising carious dental tissues. A chemical exchange between the cement and demineralised dentine was reported in clinical trials (Ngo et al., 2006) and showed a satisfactory success rate as an indirect pulp capping treatment (Hashem et al., 2015). Also, it has been shown that the sustained release of fluoride ions may be responsible for the anti-cariogenic property of GICs (Forsten, 1998; Franci et al., 1999), as these ions could be taken up by the dentine matrix to form acid resistant compounds: fluoroapatites (Tsanidis and Koulourides, 1992). Other ions were also reported to be included in the ion exchange such as aluminium, strontium and calcium. On the other hand, (Biodentine™) has been recently introduced as a coronal restoration. It has a different mechanism in promoting dentine remineralisation. This has yet to be extensively studied but a few

researchers have suggested that the high alkalinities provided by the cement, in addition to the continuous calcium release, are the main influencers for tissue repair. Moreover, these cements are able to form apatite when placed in a phosphate rich media for example, phosphate buffered saline solution (PBS) (Tay and Pashley, 2008; Atmeh et al., 2015). This mineral deposition phenomenon is a result of the unique setting reaction of the calcium silicate cements (Tay et al., 2007). They release calcium in the form of calcium hydroxide and with the presence of phosphate ions it is believed to form calcium phosphate, which will precipitate on the exposed collagen and results in the mineralisation of the organic matrix.

Formerly in this thesis (chapter 3), chemomechanical excavation of carious lesion has been performed in an attempt to reach a reproducible caries excavation end point where affected dentine is left in the cavity (Watson et al., 2014). However, there were two major concerns raised from that study. First, despite the reliability of the use of Cariosolv as a self-limiting caries excavation technique, no test has confirmed the definite tissue type left in the cavity along the interface. In addition, one cannot predict the influence of Carisolv alkalinity on the interaction of the cements whether it enhances or hinders the cement's performance. Therefore in this study, cements were examined against the whole carious lesion without any intervention and with a precise tissue characterisation. This methodology provided a novel evaluation of the cement's interaction with all the carious dentine zones.

In the previous chapters of this thesis, optical fluorescence characteristics were significantly altered when characterizing carious tissues. These optical changes were also detectable as a result of the cement's interaction with sound and demineralised dentine. The dentine substrate used in this study includes carious lesions with unpredicted optical changes due to the effect of the applied cements. Therefore, due to the heterogeneity of the carious substrate and to allow a more reliable investigation of mineral changes in these tissues, tetracycline was suggested to be used as a mineral labelling fluorophore. Promising results in mineral evaluation have been achieved when tetracycline was used with caries affected dentine (Watson et al., 2014)- (Chapter 3) and in previous studies with demineralised dentine (Atmeh et al., 2015). With the presence of caries and bacteria remaining in the cavity, tetracycline will also be beneficial in preventing bacterial growth and further collagen hydrolysis as it is known by its antimicrobial and anti-matrix metalloprotease (MMP) effects although this will not be considered as a clinical treatment regimen (Ramamurthy et al., 1998; Osorio et al., 2011).

Raman spectroscopy is another valuable technique for the assessment of mineral content (Chapter 2). The Raman mineral peak intensity analysis used in this study has been effective for evaluating the mineralisation effect of different materials on cartilage and on dental tissues as well (Sauer et al., 1994; Milly et al., 2014). This analysis is a direct representation of the changes in the phosphate mineral peak (PO_4^{3-}) at 959 cm^{-1} which is characteristic for HA that are expected to form during tissue remineralisation induced by dental cements (Parker et al., 2014).

In this chapter, the potential of dentine remineralisation induced by the two classes of water-based cements, glass ionomer and calcium-silicate based cements, was evaluated through the examination of the interface between these cements and the natural carious dentinal tissues. Using previously analysed carious teeth, where the different zones of dentine caries have been characterised (Chapter 4), an assessment of the cement interaction with caries-infected, caries-affected and sound dentine is made possible. Comparing the mineralisation nature and other effects of both cements with and without mineral labelling was examined using a variety of microscopic techniques including two-photon auto-fluorescence microscope, FLIM and Raman spectroscopy.

Therefore, the aims of this study were: 1- to examine and evaluate the mineralisation effect of calcium silicate cement (Biodentine™) on the natural dentine lesion in terms of change in mineral peak and fluorescence properties and to compare these effects with those of another water-based cement, (glass ionomer cement Fuji IX™). 2- to investigate the use of tetracycline as a mineral labelling agent with carious dentine tissues.

5.2 Materials and methods:

5.2.1 Sample preparation

In the previous chapter, twenty extracted carious molar teeth were sectioned into halves through the carious lesion the teeth were selected with deep carious lesion that extend halfway through the dentine but without pulp exposure. Each half was individually examined and caries zones were characterised as elucidated, as it was mapped and presented as precisely measured points from a defined reference point. In this study the same samples were used. Teeth were divided into groups as shown in Figure 5-1 according to the restorative material and to the storage medium. Ten teeth were allocated for Biodentine evaluation, five of them were stored in tetracycline containing storage medium (0.015% tetracycline, PBS and water) while the other five were stored in PBS and water only. The other ten teeth were divided in the same manner for GIC evaluation.

Immediately after microhardness testing, which was the last test performed for caries characterisation; samples were rinsed with deionised water, and cleaned in an ultrasonic bath for 3 minutes to remove any surface debris. For Biodentine™ (Septodont, Saint Maur des Fosses- France) samples, the cement was prepared as per the manufacturer's instructions, the precise amount of liquid was added to the powder then the capsule was triturated for 30 seconds. The cement was then applied using a plastic instrument to one half of a carious tooth, leaving the other half to act as a control with no restoration. The reference mark was left exposed to allow future localisations of the examined points (see Figure 5-2). Similarly, for GIC Fuji IX™ (GC Corporation. Tokyo, Japan), following the manufacturer's instructions, the capsule was mixed and applied to one half of each carious tooth.

After the application of both cements, samples were allowed to set for 1 hour at 37°C temperature in a wet environment. Then, they were stored in different aging solutions for 4 weeks. Storage solutions were replaced every two days. The groups were as follows:

A. samples stored in PBS without labelling

1. **B+PW** (n=5 halves): phosphate buffered saline (PBS) solution alone (Oxoid Limited, Hampshire,UK).
2. **B- PW** for the other (n=5 halves): carious teeth no restoration in PBS alone.
3. **G+PW** (n=5 halves): phosphate buffered saline (PBS) solution alone (Oxoid Limited, Hampshire,UK)
4. **G-PW** for the other (n=5 halves): carious teeth no restoration in PBS alone.

B. Samples stored in PBS and Tetracycline containing solution

5. **B+TP** (n=5 halves): 0.015% Tetracycline (87128 Sigma-Aldrich, Dorset, UK) in a phosphate buffered saline (PBS) solution.
6. **B-TP** for the other (n=5 halves): carious teeth no restoration in 0.015% Tetracycline and PBS solution
7. **G+TP** (n=5 halves): 0.015% Tetracycline (87128 Sigma-Aldrich, Dorset, UK) in a phosphate buffered saline (PBS) solution (Oxoid Limited, Hampshire,UK).
8. **G-TP** for the other (n=5 halves): carious teeth no restoration in 0.015% Tetracycline and PBS solution.

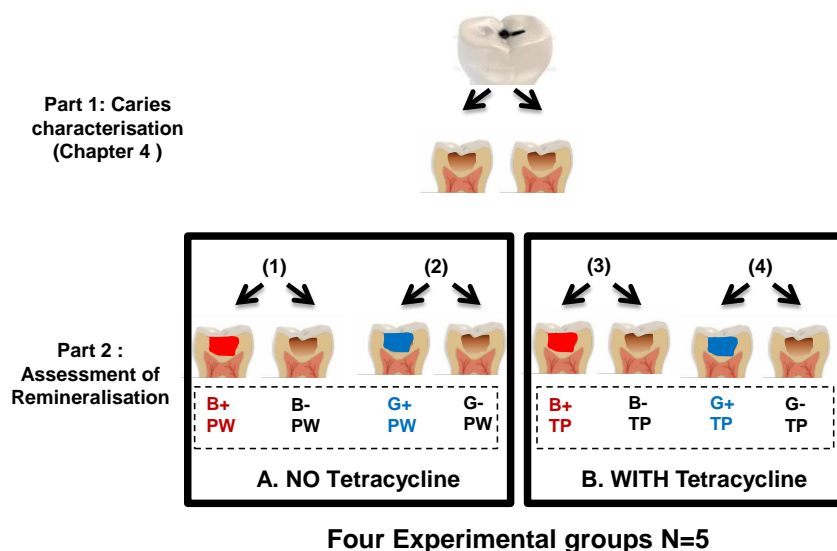


Figure 5-1 Diagram showing the experimental groups divided according to the restorative cement and the storage media.

5.2.2 Imaging

After storage, samples were retrieved and rinsed with deionised water. For each half, the best representative line of points including all three dentine caries zones was chosen according to the results of the caries characterisation from the previous study. Then the sample was cut at that certain position which was localised by a precise distance from the reference point using a water-cooled diamond wafering blade (Benetec Limited, London, UK) at a low speed. Afterwards, samples were gently polished using 1200-grit carborundum paper rinsed again and cleaned in an ultrasonic bath for 3 minutes (Figure 5-2- (C)).

A multiphoton fluorescence microscope was used to image the interface between the cement and different histological layers of caries. Imaging along the interface was undertaken from the side (see Figure 5-2-C, D), as localisation of each point on the Y-axis was feasible from the preserved reference mark. Identical microscopic settings were used as for the previous study, with a 20x 0.75 NA air objective lens, 854 nm excitation wavelength and 550 ± 20 nm emission filter were used for imaging to allow reliable comparisons (Banerjee et al., 2010a; McConnell et al., 2007). Both fluorescence intensity images and fluorescence life time images at 256 x 256 pixels were obtained from each point.

- **Image analysis**

Fluorescence intensity images were analysed using Image J analysis software (ImageJ, Wayne Rasband, NIH,USA). The average fluorescence intensity from each image was calculated then averaged for each tissue type (caries-infected, caries-affected and sound dentine) in each experimental group. In a similar way, the average lifetime was calculated from FLIM images using TRI2 FLIM analysis software (courtesy of Paul Barber, Grey Cancer Institute, Oxford). The fluorescence decay curves were fitted using a bi-exponential model and the lifetime values were recorded for each point then averaged for each dentine zone in each experimental group. The percentage change in both fluorescence intensity and lifetime were calculated for each point measurement using baseline values (before storage) from the previous study that corresponded to the same location on the sample. The following equation was used:

$$((Xa - Xb) / Xb) \times 100$$

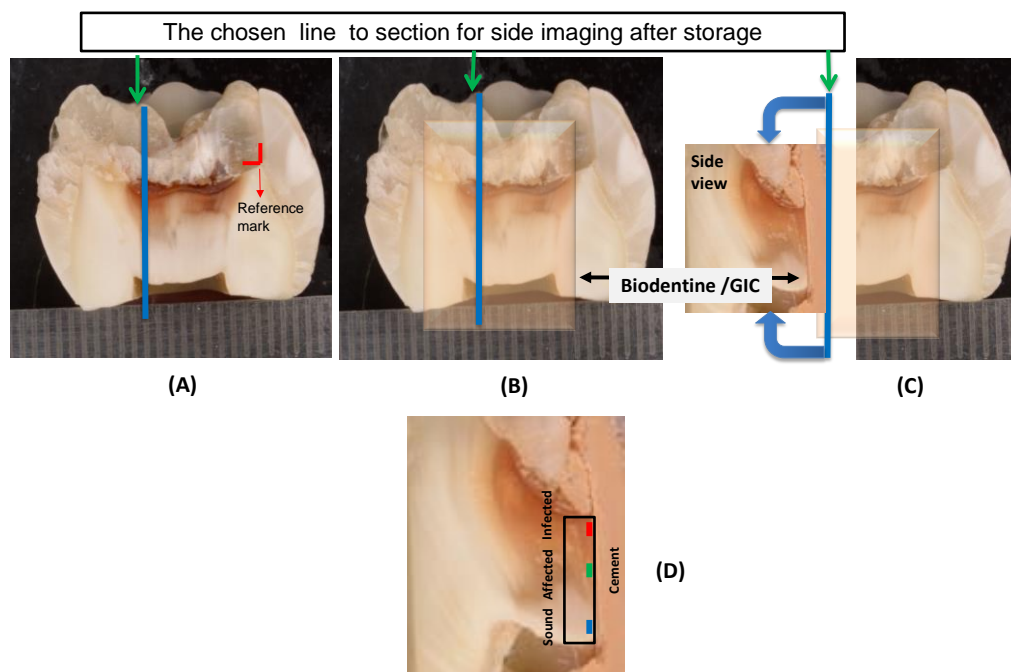


Figure 5-2 Sample preparation for cement evaluation. (A) Carious tooth before restoration with a chosen area of imaginary line including previously tested data and identified tissues (blue). (B) Application of the cement with exposed reference area. (C) Tooth sectioning at the chosen line to expose the carious tissues from the side. (D) Sample is ready for imaging the interface from the side including different dentinal tissues under the cement.

5.2.3 Raman spectroscopy

Raman scans were performed on the samples that were stored in PBS only, this included the following groups: (B+PW, B-PW, $n=5$), (G+PW, G-PW, $n=5$). A Renishaw inVia Raman microscope (Renishaw Plc, Wotton-under-Edge, UK) in StreamLine™ scanning mode was used with the same scanning parameters addressed in Chapter 2, Section 2.2.2.

Each sample was examined along the interface between the cement and dentinal tissues using 20x 0.40 NA air objective and a montage image was created. Using the same objective this interface was then scanned using a 785 nm diode laser (100 mW laser power) and the Raman signal was obtained using a 600 lines/mm diffraction grating centred between 849 cm^{-1} and 1603 cm^{-1} , and a 2 seconds CCD exposure time. Raman spectroscopy was used in this study to facilitate the detection of any changes in the mineral peak as an effect of the interaction

between the cement and carious dentine. Therefore, spectra from each sample was acquired with an inter-spectrum distance of 50 μm from the cement towards the dentine (X- axis), and 2.7 μm along the interface (Y-axis) covering the previously examined area that includes all recorded points of caries infected, affected and sound dentine across the sample. The scanning started at the position of the reference point, so further correlation with caries zones will be possible.

- **Raman analysis**

The acquired Raman spectra were displayed using Renishaw WiRE 3.2 software (Renishaw Plc, Wotton-under-Edge, UK). Then, they were exported into an in-house curve-fitting software to be analysed. After fitting the spectra, the software was used to generate grey-scale images and depth profiles of phosphate peak intensity at 959 cm^{-1} (PO_4^{3-} v1). Each sample encompasses different histological zones of dentinal tissue with natural caries; these tissues produce variable background auto-fluorescence signals that must be taken into consideration. Therefore, the spectra were fitted using a Gaussian function and a first order polynomial option in the analysis software.

The exported results were in the format of 32-bit TIFF grey-scale images where each pixel represents the mineral peak intensity at that position. Images were opened in image processing software ImageJ (ImageJ, Maryland, USA). Using a custom-written macro, the images were mapped by 500 μm squares and the mean intensity of each square was automatically calculated. These squares allow precise measurement from the reference point as they represent the points previously allocated to different zones of carious dentine. The value of peak height from each tissue type for each group was calculated to be statistically analysed (Figure 5-3).

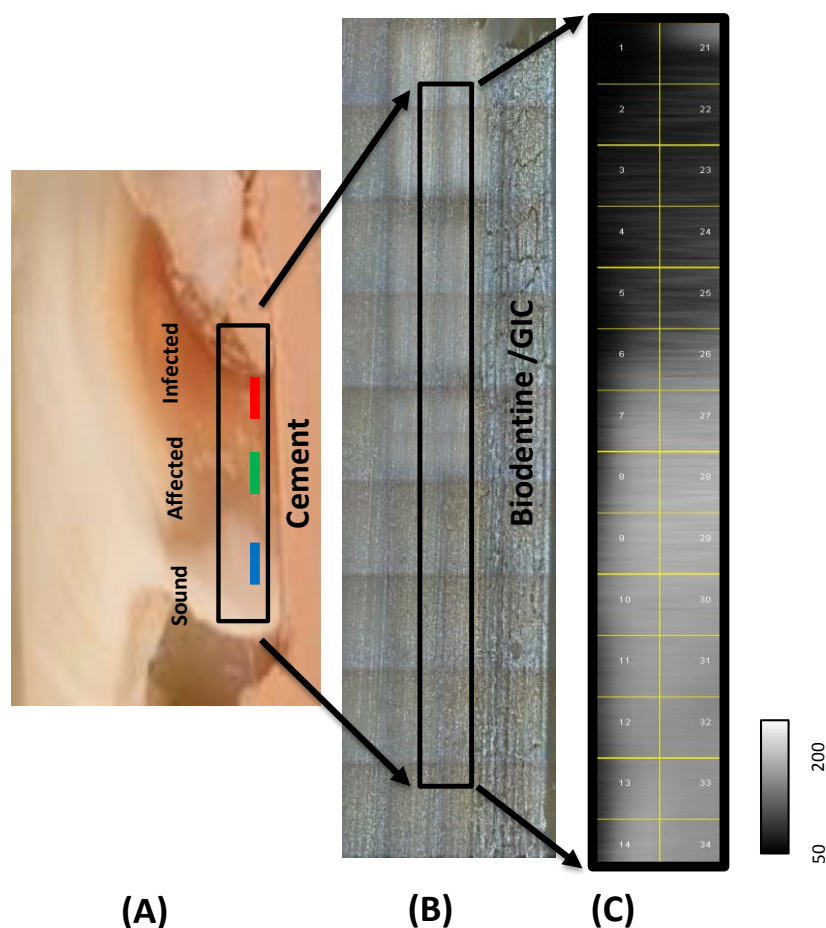


Figure 5-3 Sample preparation for Raman spectroscopy. (A) The selected tested area including all tissue types. (B) Montage image of the sample. (C) The Raman scan after mineral peak analysis starting at the first tested point.

5.2.4 Statistical analysis

Descriptive statistics were used to summarise the outcome measure for each group and materials separately. Linear regression models were used to test the effect of materials and tissue type on the intensity and lifetime measures after checking for the normality assumption. The model included the main effects of materials, storage media and the interaction effect between them. This analysis was undertaken for lifetime and intensity data separately for different tetracycline and no tetracycline groups. If the interaction between group and material was statistically significant in the model, then further post hoc analysis was carried out to find out which combination of material and group was significantly different. In such cases, the p values were adjusted for multiple testing. All the analyses were carried out using Stata version 12.0 (StataCorp LP, Texas, USA).

5.3 Results

5.3.1 Samples stored in PBS without Tetracycline labelling

A. Two- photon fluorescence Imaging

Representative images showing baseline intensity and lifetime images before storage compared to the images after storage with and without the application of Biodentine and GIC, are displayed in Figure 5-4 for experimental groups (No material-PW, B+PW, G+PW). In Figure 5-5, the calculated percentage change in both fluorescence intensity and lifetime after image analysis is displayed to show the differences before and after storage of each group regarding different dentinal substrates. These data were statistically analysed and presented in appendix 6.

A comparison of the effect of both cements on different tissue types with the control group (where no cement was applied) is described below in detail.

- **Caries Infected dentine:**

GIC cement had no effect on the fluorescence lifetime or intensity of the infected tissues as seen in the representative images (Figure 5-4). There was no significant difference between GIC and control groups as $p = 0.970$, 0.44 for intensity and lifetime respectively. On the other hand, Biodentine cement significantly increased the fluorescence intensity of the infected tissues ($p = 0.001$) when compared to the control group. However, it has minimal effect on the infected dentine fluorescence lifetime where $p = 0.281$. There was a significant difference between the GIC and Biodentine effect on infected tissues regarding fluorescence intensity measurement only ($p = 0.001$).

- **Caries affected dentine**

The affected dentine was more susceptible to optical changes in response to remineralisation effects of the applied cements. GIC samples exhibited a significant increase in both fluorescence intensity ($p = 0.031$) and lifetime ($p = 0.001$) of the caries affected tissues when compared with the control samples, as displayed in the images and statistical results (see Figure 5-4). Similarly, Biodentine significantly increased the intensity ($p = 0.001$) and lifetime ($p = 0.001$) of the affected tissues. Comparing both cements, there was no significant difference between the two groups regarding fluorescence intensity ($p = 0.064$) but the changes were significant between Biodentine and GIC in lifetime results of caries affected dentine ($p = 0.032$).

- **Sound dentine**

For both cements, there was an insignificant increase in the fluorescence intensity of dentine ($p= 0.513, 0.553$) for Biodentine and GIC correspondingly, when compared to the control group. Likewise, changes in the lifetime results were not significant for Biodentine ($p= 0.42$) or GIC ($p= 0.47$). In addition, when Biodentine and GIC were compared, their effect on the sound dentine was not significant for either intensity ($p= 0.91$) or lifetime ($p= 0.18$).

B. Raman spectroscopy

Comparing the intensity of the mineral peak at 959 cm^{-1} from different groups (Figure 5-6) promotes reliable detection of the cements' mineralisation effects on different dentinal tissues. The analysis revealed an increased mineral content of the infected tissues when Biodentine was applied ($137\text{ A.U} \pm 7.7$ to $154\text{ A.U} \pm 4.9$), ($p= 0.03$). However, no change in mineral content was detected in the infected tissues between the control groups ($137\text{ A.U} \pm 7.7$) and GIC group ($138\text{ A.U} \pm 4.5$) ($p= 0.12$). Likewise, no significant changes were detected in the sound dentine ($411\text{ A.U} \pm 16$) with GIC ($408\text{ A.U} \pm 21$) ($p= 0.96$) or Biodentine ($412\text{ A.U} \pm 5.7$) ($p= 0.84$). On the other hand, the affected tissues showed significantly increased mineral content when treated with Biodentine ($400\text{ A.U} \pm 16.4$), compared to the control group ($236\text{ A.U} \pm 9.2$) ($p= 0.001$). GIC also significantly increased the mineral peak intensity of the affected tissue ($349\text{ A.U} \pm 12$), ($p= 0.001$). Although the results suggested a greater mineralisation effect with Biodentine ($400\text{ A.U} \pm 16.4$) than GIC ($349\text{ A.U} \pm 12$), such a difference was not significant ($p=0.5$) (see appendix 7).

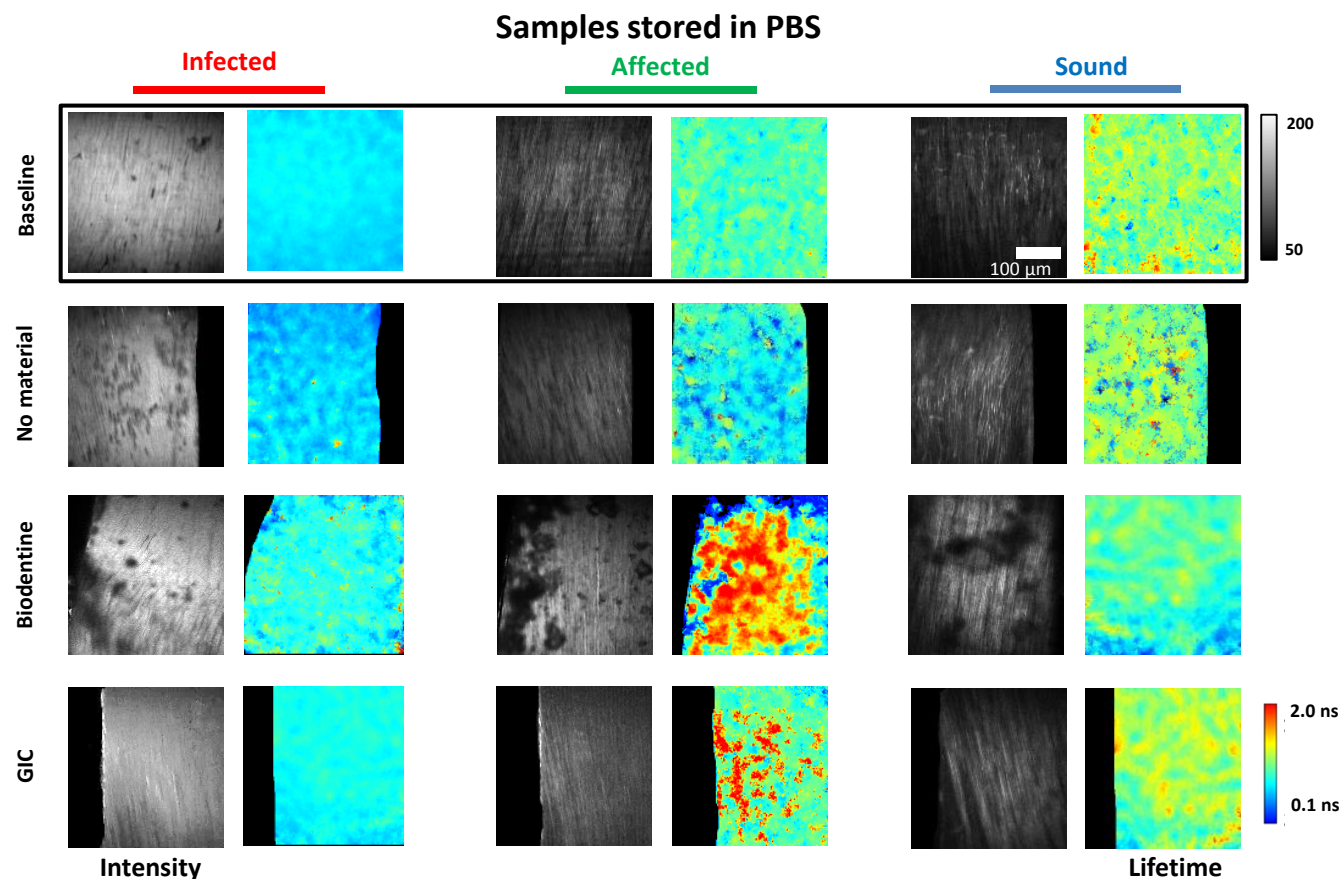


Figure 5-4 Representative Two-photon imaging of the interface between carious dentine/ Biodentine -GIC. The figure compares baseline fluorescence intensity and lifetime images for caries infected, affected and sound dentine before cement application with the after storage images for each group (Control (no material), Biodentine and GIC).

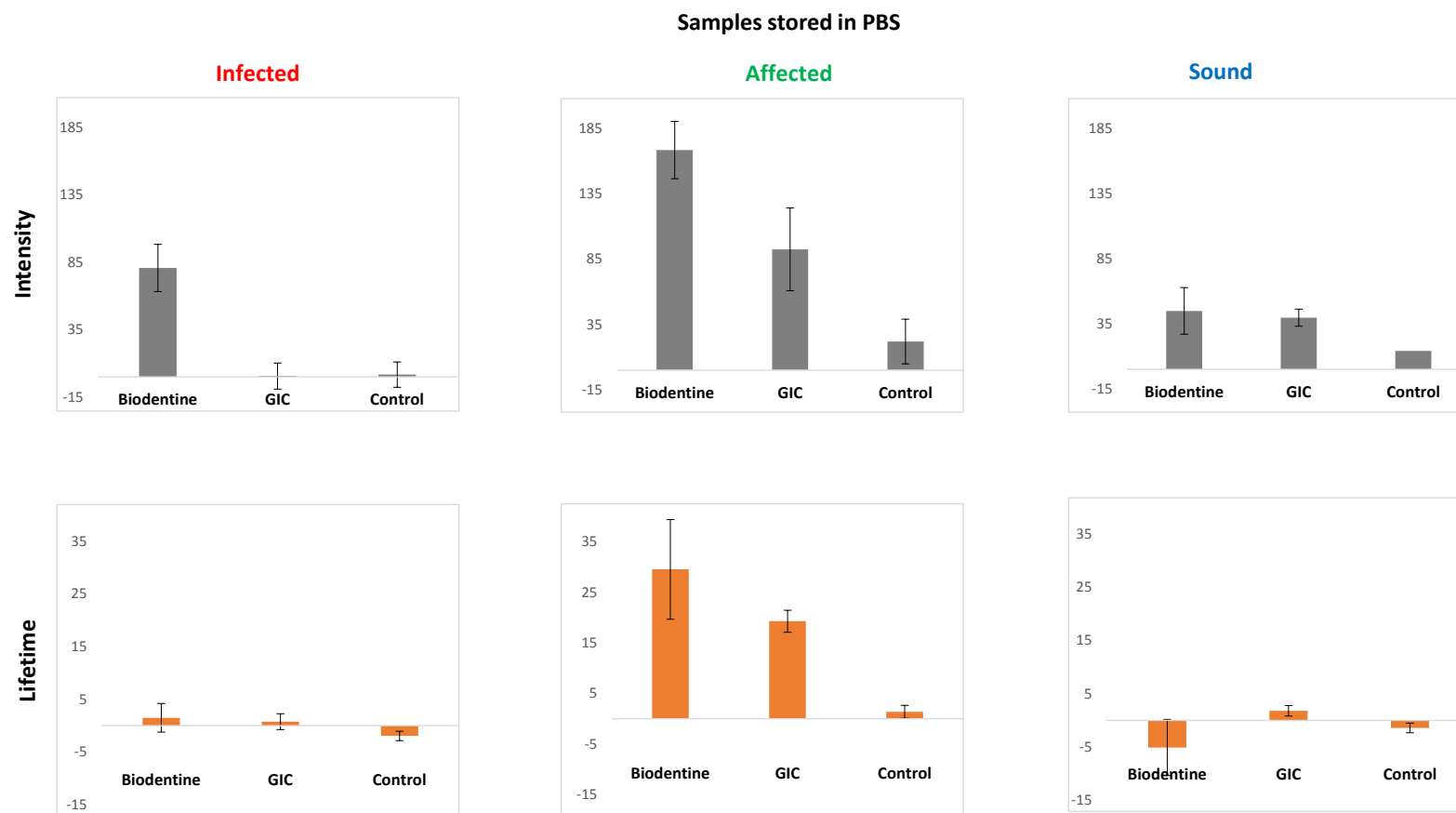


Figure 5-5 The calculated percentage change in both fluorescence intensity and lifetime after image analysis is displayed to show the differences before and after storage of each group regarding different dentinal substrates.

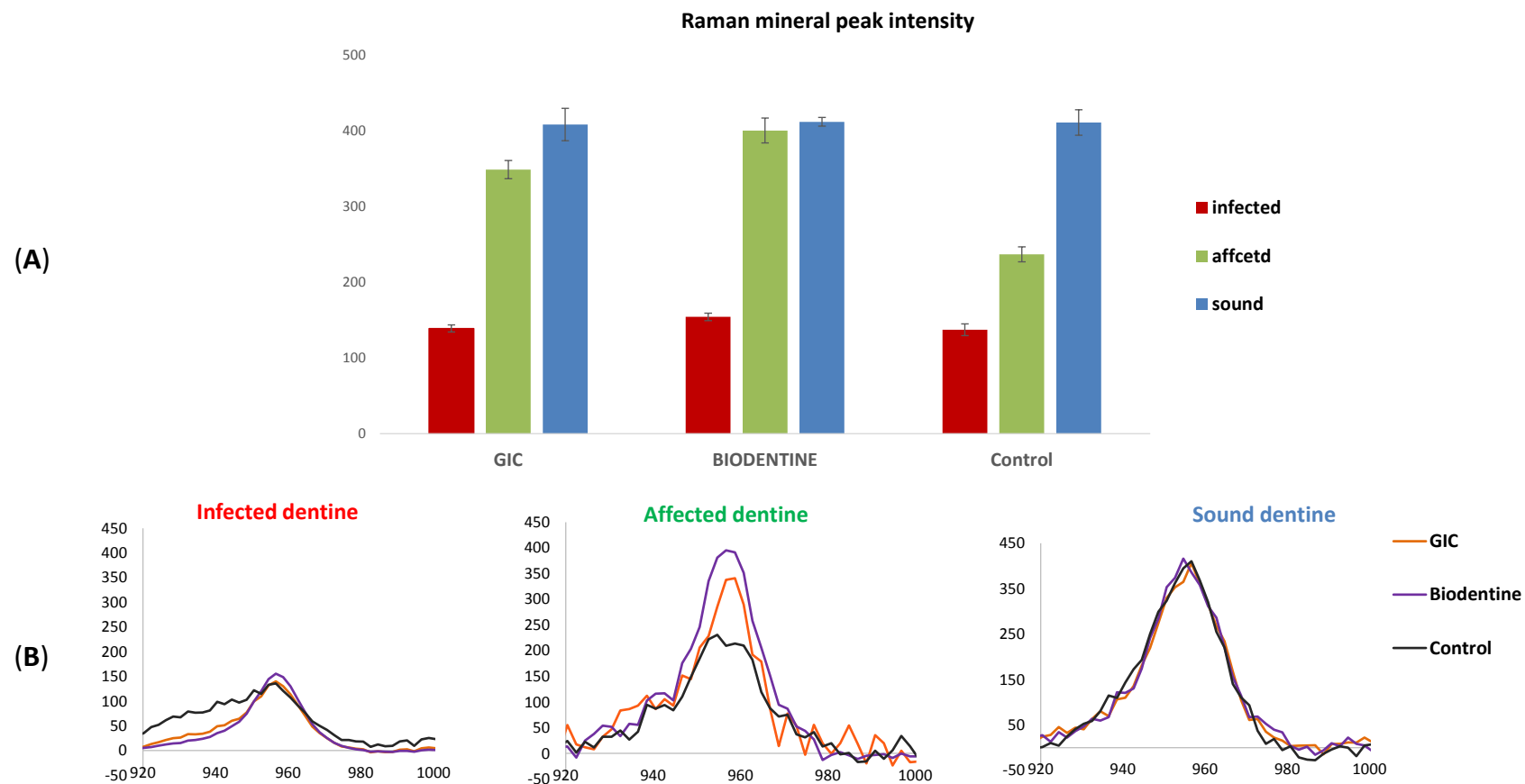


Figure 5-6 (A) Raman-mineral peak intensity for caries-infected (red), affected (green) and sound dentine (blue) for each experimental group. (B) Representative Raman spectra of the phosphate peak at 959 cm^{-1} for each tissue type, comparing GIC (orange), Biodentine (purple) and control group (black).

5.3.2 Samples stored in PBS and Tetracycline as a mineral labelling fluorophore

A. Two-photon fluorescence imaging

With tetracycline labelling, the fluorescence intensity is expected to increase while the lifetime decreases as a result of tetracycline binding during the remineralisation process. Representative fluorescence images of this sample groups are displayed in Figure 5-7 which compares the baseline images with the fluorescence images after-storage for each group in different dentinal tissues. Image analysis was performed and the percentage change before and after storage was calculated for each group (Figure 5-8). The results of the statistical analysis of the percentage change are presented in appendix 8.

- **Caries-infected dentine:**

Caries infected dentine showed insignificant changes regarding fluorescence lifetime and intensity within the GIC group compared to the controls ($p = 0.65, 0.71$). However, with Biodentine there was a highly significant increase in the intensity ($p = 0.002$), but no change in the lifetime ($p = 0.26$). Comparing the effect of the two cements on infected dentine, significant differences were found in the intensity results only ($p = 0.01$).

- **Caries affected dentine:**

Biodentine and GIC groups showed a significant decrease in the fluorescence lifetime within caries affected dentine with the presence of Tetracycline. The lifetime images of both cement groups tend towards the darker blue scale which represents a shorter lifetime than the baseline images as shown in Figure 5-7. Calculating the percentage change before and after storage resulted in a decreased lifetime of the Biodentine group ($-26.4\% \pm 3.2, p = 0.0001$), and GIC ($-17.4\% \pm 5.2, p = 0.0001$) when compared to the control samples ($-2.6\% \pm 0.9$). Biodentine samples showed a more significant decrease in the lifetime than GIC samples ($p = 0.001$).

Fluorescence intensity images also showed an increase in the Biodentine and GIC samples when compared to the baseline intensity images of the caries affected dentine (Figure 5-7). However this increase in the intensity was not significant when compared to the control group. The Biodentine group exhibited the highest percentage change regarding fluorescence intensity ($69.10\% \pm 21$). However, this change was insignificant when compared to the change in the control group

(22.66% \pm 17, $p= 0.09$). Likewise, the change in the GIC group was insignificant (44.1% \pm 30, $p= 0.51$) see appendix 8.

- **Sound dentine:**

The fluorescence changes in sound dentine after storage were minimal. Changes in all the cement groups were not significant when compared to the control group. For the changes in the fluorescence lifetime p values were $p= 0.53$ and 0.22 regarding Biodentine and GIC. Comparing the changes in fluorescence intensity, the p value for the Biodentine group was $p= 0.55$ and for the GIC $p= 0.41$. However, the percentage change in the fluorescence intensity of the control group was high (32.9% \pm 10) compared to the cement groups (5.7% \pm 10, 8% \pm 16).

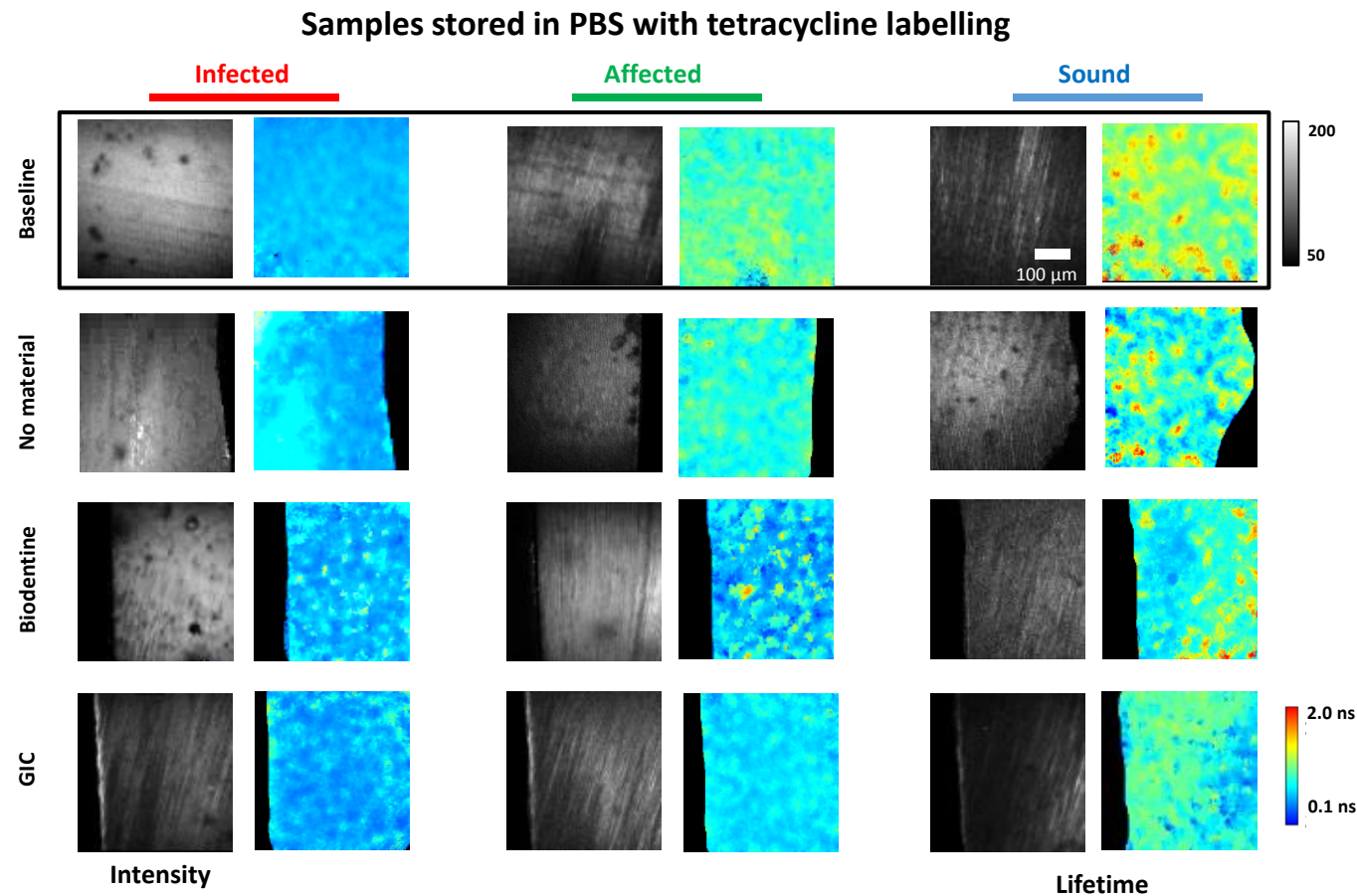


Figure 5-7 Representative fluorescence lifetime and intensity images for samples stored in Tetracycline as a mineral labelling fluorophore. Comparison between the fluorescent images of the baseline (before storage) and after storage regarding different dentinal tissues for the control, Biodentine and GIC groups.

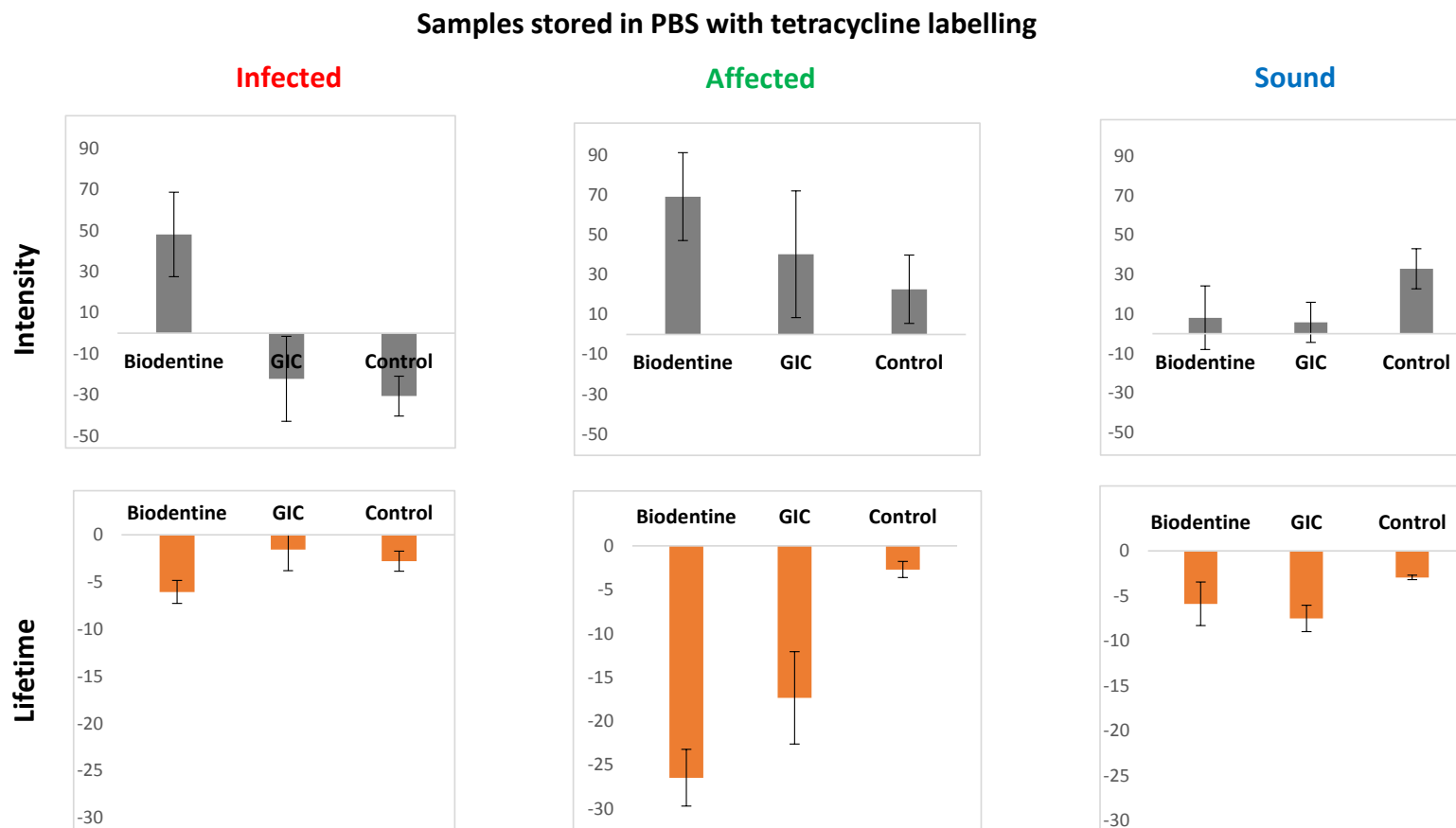


Figure 5-8 The percentage change in the fluorescence intensity and lifetime for samples stored in Tetracycline solution. Comparing Biodentine and GIC samples with control group for each dentine tissue type.

5.4 Discussion

In the current study, the interaction of Biodentine™ was compared to that of a GIC (Fuji IX™) when applied to unexcavated carious dentine. The teeth used in this study all had a large carious lesion that had been previously characterised to delineate the different caries zones (chapter.4). To our knowledge, this is the first in-vitro study that evaluate the Biodentine interaction with natural caries, using advanced optical techniques and quantitative chemical Raman analysis. This may be valuable in determining the bioactivity of the cement and its effect on carious tissues. Clinically, this investigation helps in the understanding of the material's properties and its behaviour when used as a restorative, indirect pulp capping therapeutic material. The indirect pulp protection technique preserves caries-affected dentine that is close to the pulp, reducing the risk of pulp exposure and minimising unnecessary tissue removal. After that, a suitable material (for example, GIC or Biodentine) is applied to offer a potential seal and rejuvenation of the dentine-pulp complex by providing a mineral supply and anti-bacterial properties in addition to chemical or mechanical bonding to the remaining dentine (Banerjee, 2013). As glass ionomer cements have been the material of choice in such techniques, the cement was chosen to compare its effectiveness to Biodentine. Both cements may be considered equivalent to some degree in their nature being water-based materials with similar clinical applications.

A novel sample model was introduced in the previous chapter where mapping the whole carious surface with registered point measurements was undertaken. This unique mapping facilitated precise point by point measurements and also enabled relocating these points for further testing. After tissue characterisation of all samples was successfully achieved, there was a recorded series of points within each sample assigned for caries infected, affected or sound dentine which allowed the study of the interaction between dental cements and different caries zones.

The optical data of the characterised carious lesion obtained in the last experiment (chapter 4), included fluorescence intensity and lifetime measurements that facilitated future comparison with the same parameters to detect any differences in the optical characteristics of the tissues. The same multiphoton fluorescent microscope with available fluorescence intensity and lifetime options was used. The imaging setup followed the protocol applied previously to allow comparable assessment before and after storage. This imaging technique provided evaluation

of the optical changes in each dentinal zone as a result of its interaction with either Biodentine or GIC. These findings were achieved with direct sample imaging without the need for sample preparation or staining.

Moreover, the study introduced tetracycline mineral labelling as an additional microscopic marker to assess mineralisation of natural carious dentine. Earlier studies showed that tetracycline chelates calcium ions at areas of development or calcifications and form a calcium orthophosphate complex in teeth and bones (Cheek and Heymann, 1999). There are no other in-vitro studies reporting the use of tetracycline to label active mineralisation within carious dentine (Tagger et al., 1975). A single in-vivo study reported the administration of tetracycline hydrochloride to label reparative dentine formation in teeth planned for extraction. It was confirmed that tetracycline incorporated only at sites of active mineralisation but it was not mentioned whether carious teeth were involved in this study. Human involvement with undesired side-effects of tetracycline were also not prevented in the study (Tagger et al., 1975). Similar to the current study, promising results in previous studies on demineralised dentine have been achieved (Atmeh et al., 2015). In addition, chapter 3 of this thesis established favourable results regarding mineral labelling with a basic understanding of tetracycline behaviour in the presence of carious dentine. In this study we presented various experimental groups to assess the use of tetracycline in evaluating mineralisation within samples with the full range of natural carious zones.

- **Caries-infected dentine**

For the assessment of the optical changes in the natural carious lesion after cement application, the results suggested that there was an active interaction between infected dentine and calcium silicate cement. This interaction was demonstrated optically as an increase in the fluorescence intensity but not the lifetime regarding the caries infected tissues. The mineral content within infected areas significantly increased with Biodentine which may be the only explanation of the significant changes observed in the intensity. This observation was also detected in the data of the Biodentine group with tetracycline labelling as significant increased fluorescence intensity compared to the control group. Such an outcome indicates the high potential of Biodentine to remineralise carious dental tissues. The control group showed decreased fluorescence intensity with tetracycline as well as GIC group, this could be explained by the antibacterial effect of tetracycline. With further investigation; this may have an influence on the clinical applications of Biodentine especially in regard to the management of deep carious lesions. There

were also significant differences in the intensity results (with and without tetracycline) between the two cements regarding their interaction with infected dentine. This variation is in agreement with other studies, although a different experimental substrate was used, that indicated the failure of GIC to induce mineralisation in totally demineralised dentine (Kim et al., 2010; Atmeh et al., 2015). Both studies suggested that GIC requires pre-existing nucleation sites in order to remineralise tissues through the mechanism of epitaxial growth of the remaining crystals. The analysis of the Raman mineral peak intensity also indicates similar mineral content within the GIC group as for the control group. However, Kim *et.al* reported the uptake of GIC-specific ions which resulted in the adaptation of the cement, yet, no ultrastructural evidence of mineral deposition or crystal formation was detected (Kim et al., 2010). Ionic uptake includes the diffusion of strontium, aluminum, and fluorine ions into the dentine matrix, where no source of Ca ions is available. Therefore, our finding within the GIC group when tetracycline was used also agrees with this hypothesis and validates the use of tetracycline as a mineral labelling fluorophore.

One could expect similar changes in the lifetime as concluded previously (in Chapter 2); however, the lifetime values of the infected dentine within the Biodentine group remain unchanged. A possible explanation is a quenching effect of the low pH caused by the large number of bacteria present within the infected dentine which may alter the mineralisation effect on the fluorescence lifetime. Decreased pH values cause a reduction in the fluorescence lifetime as observed in caries characterisation studies and when lifetime was assessed in prepared optical phantoms with different pH values (Gannot et al., 2004). Another explanation why the lifetime values remain unchanged may be that the fluorophore affecting dentine's lifetime is referred to collagen when only bound to minerals which reinforces its structure, providing the normal mechanical and optical properties of dentine. In caries-infected dentine the cross-striated banding pattern of collagen fibres no longer exists indicating denaturation and/or degradation of collagen molecules. Regardless of mineral deposition offered by Biodentine in this layer, the characteristics of collagen molecules was not restored, thus, no changes in the lifetime would be expected.

- **Caries- affected dentine**

The morphology and composition of caries-affected dentine provided a suitable scaffold for biomimetic dentine remineralisation and tissue healing. The collagen fibrils in this carious layer maintain their banding pattern as in sound dentine with

some apatite crystallites irregularly scattered promoting crystal growth and remineralisation of the organic matrix (Nakornchai et al., 2004; Ohgushi and Fusayama, 1975). In the present samples, natural caries had occurred resulting in dentine demineralisation. This process is believed to induce the expression of organic matrix non-collagenous proteins such as (DMP1). Therefore, the presence and the role of such proteins could not be excluded in our samples. In fact these non-collagenous proteins have been found to be increased in number within the caries infected layer due to caries attack (Nakornchai et al., 2004). Many studies have shown the regulatory role of these proteins in dentine remineralisation as they are critical for the stabilisation of the formed crystallites and ensure their transformation to HA crystals (Chen et al., 2015; George and Veis, 2008).

The results indicate a highly significant increase in the mineral peak intensity of samples stored with both GIC and Biodentine when compared to the control group. This mineral increase is reflected by the optical characteristics of the caries affected tissues and presented as an increase in both fluorescence intensity and lifetime. These findings are comparable to the optical changes observed due to the remineralisation of an artificially demineralised dentine model (Chapter.2).

Biodentine as a calcium silicate based cement is believed to induce remineralisation via a biomimetic bottom-up approach. Biodentine, provides a slowly releasing source of calcium and hydroxyl ions. With phosphate ions provided in the (PBS) storage solution, further de-novo nucleation is facilitated by the highly alkaline environment (Kawasaki et al., 1999). Thus forming initial ACP compounds on the surface of the collagen fibrils that consequently grow and transform into HA crystals as confirmed by the characteristic HA Raman peak at 959 cm^{-1} . Furthermore, the cement releases silica ions into the underlying dentine which act as a strong inducer for dentine mineralisation (Saito et al., 2003). However, the extent of this crystallisation and whether intra or extra-fibrillar mineralisation took place cannot be elucidated in this study. The interface evaluation was limited to the surface to facilitate a reliable comparison with the data obtained before restoration. In regards to the type of collagen mineralisation induced by Biodentine, previous studies suggested that inter-fibrillar as well as intra-fibrillar mineralisation was achieved with calcium silicate cements with the use of biomimetic analogues that substitute the regulatory role of non-collagenous matrix proteins (Tay and Pashley, 2008). However, despite no biomimetic substitutes being used in this study mineralisation was detectable in both infected, and more significantly, affected dentine. In addition, the contribution of remnant matrix phosphate and

phosphoproteins in regulating biomimetic remineralisation cannot be excluded within our samples (Saito et al., 1998; Saito et al., 2003).

Although the remineralisation process involved is different, GIC filled samples showed comparable optical and mineral intensity changes to the Biodentine group with no significant differences between the two groups found. When GIC is applied on partially demineralised dentine (as caries affected dentine), it undergoes an ion exchange process with the underlying dentine. This involves the transfer of strontium, aluminum, and fluorine ions, as a result of an ion concentration gradient between GIC and dentine, and is believed to be responsible for the excellent initial cement's adhesion properties through ionic bonding (Ngo et al., 2006). This process is accompanied by further dentine demineralisation and the release of Ca^{2+} ions caused by polyalkenoic acid. The result is an ion rich layer that would be involved in subsequent mineralisation of remaining apatite crystals present in the caries affected dentine (Sennou et al., 1999).

Samples stored with both cements in tetracycline containing solution exhibited optical characteristics similar to that of the tetracycline- Ca^{2+} complex with an increased fluorescence intensity and a decreased lifetime. This is in agreement with this study's earlier results (Chapter 3) as well as previous work done in our laboratory (Atmeh et al., 2015). This technique is found to be efficient in the assessment of remineralisation within the excavated carious substrate. The results of the tetracycline labelled group confirm that active mineralisation had occurred which enabled tetracycline binding as this was compatible with the changes in the mineral peak of a similar substrate. However, the changes observed in the fluorescence intensity although visible were statistically insignificant when compared to the control group. The lifetime values give a more reliable and significant evaluation when comparing the cement and control groups.

- **Sound dentine**

Previous studies had suggested a caustic effect of calcium silicate cements on dentine collagen matrix and advised caution when applying these materials on thin dentinal walls (Leiendecker et al., 2012). These effects were also suggested when evaluating Biodentine against completely demineralised dentine samples as complete degradation of the samples was noticed (Atmeh et al., 2015). The difference between the two is that when collagen was assessed in the former study, normal dentine was used where collagen is protected by inter-fibrillar apatites. Therefore, the amount of collagen degradation was considered minimal

but did actually exist. When dentine was completely demineralised in the second study, collagen fibres were exposed to the high alkaline environment provided by the cement and more visible degradation of the dentine disks was noticed in samples stored in PBS. In this study, similar storage media were used yet, no changes in the mineral content nor fluorescence characteristics were found. Our findings do not contradict the previous studies as the mineral content of the sound dentine was maintained and no collagen fibres were exposed for degradation. Moreover, since the degradation noticed by Leiendecker was minimal, no effect on the optical properties is expected. Mineral and optical changes in all other groups regarding sound dentine were insignificant when compared to the control group. This indicates that despite the observed interaction of these cements with sound dentine in previous studies it has minimal effect on the fluorescence characteristics of these tissues.

In conclusion, the present study evaluated for the first time the interaction between two water-based cements and natural dentine caries and sound tissues. Calcium silicate cements induced mineralisation in caries infected dentine while GIC failed to cause any significant changes. Both cements showed a significant increase in mineral peak intensity within caries affected dentine that resulted in comparable optical changes of the remineralised tissues. The association between mineralisation and fluorescence intensity and lifetime is most likely caused by collagen structural changes when attached to apatites. An increase in both fluorescence intensity and lifetime was observed as a result of dentine remineralisation. Tetracycline mineral labelling has shown equivalent observations regarding the mineralising ability of both cements. Therefore, using tetracycline as a mineral labelling fluorophore with carious/ sound dentine combined with multiphoton fluorescence intensity and lifetime imaging is a promising non-invasive, in-vitro, selective tool that can be utilised to assess a dental tissue's mineralisation.

6. Chapter Six: General summary and suggestions for future work

6.1 General summary

For the study of restorative materials and their interaction with dental tissues various optical imaging techniques have been widely used. These techniques depend on the interaction between an illuminating light and the matter within different substrates and therefore they provide valuable information about the matter with minimal if no alternation or damage caused to the samples. In the current work, an in-house built two photon microscope was used throughout different experiments providing fluorescence, SHG and lifetime data which was found useful to study and compare the interaction of dental cements with human dentine. The optical characteristics of the interfaces were complimented by Raman spectral analysis measuring changes in the mineral peak to indicate if demineralisation or remineralisation processes took place.

Biodentine is commercialised calcium silicate cement marketed as a dentine replacement material with extensive clinical applications in either coronal or radicular dentine. With the bioactive and physical properties that this material offers, more investigations on its effectiveness and tissue interactions were required. Aiming to interpret these investigations appropriately, GIC was selected as a control material for comparison throughout the studies presented in this thesis. Both cements share similar clinical applications and nature as water based materials (Nicholson, 1998). Other calcium-silicate based cements are available on the market and could offer more relevant comparison; however, none of them are indicated as a coronal dentine replacement (Torabinejad and Chivian, 1999). The dentine samples used were prepared from human teeth and included sound, demineralised, caries-infected, caries-affected and excavated caries-affected dentine. This wide range of substrates provides a profound understanding of these cements' interaction with dentine.

Optical characterisation of the dentine substrates:

Optical characterisation of these different substrates was achieved, specifying for the first time the relation between the change in mineral content and changes in the dentine fluorescence characteristics. The organic component within human dentine is believed to be responsible for its fluorescence behaviour (Van der Veen and Ten Bosch, 1996; Banerjee and Boyde, 1998; McConnell et al., 2007). When in-vitro demineralisation was performed, loss of mineral resulted in the decrease of both fluorescence intensity and lifetime. As those samples exhibited no changes in the collagen matrix according to SHG results, it was suggested that it is either the loss of minerals affected the collagen configuration with its optical properties consequently or the low pH of demineralisation protocol changed the lifetime values. These findings were in agreement with the results of a previous caries optical characterisation study. Caries infected dentine where complete collagen destruction has occurred exhibited a very fast lifetime, higher fluorescence intensity and decreased SHG signal (Lin et al., 2011). However, the effect of bacterial by-products present in this layer with the associated very low pH environment should not be excluded (Koenig and Schneckenburger, 1994).

The damage within the inner caries layer (affected dentine) is found to be reversible as collagen fibres appear to maintain their characteristic amino acid banding pattern in a manner similar to sound dentine. However, at an ultrastructural level, there has been evidence of a change in the intermolecular cross-linkage as they partly shifted to its precursor form, such as dihydroxynorleucine (DHNL) and hydroxynorleucine (HNL) that may change the dentine's fluorescence characteristics, but this change is reversible (Kuboki et al., 1977). In addition, the removal of minerals also leads to increased porosity and hence, changing the mechanical and possibly optical properties of the organic matrix in this layer (Wang et al., 2007).

The effect of dental cements on the optical properties of dentinal substrates

Biodentine is calcium silicate cement. On hydration it releases calcium hydroxide which is believed to be responsible for the cements' action and mediates its interaction with underlying dentine (Camilleri, 2007; 2008). The associated high alkalinity and caustic effect of the cement is a selective process affecting the organic components of dentine (Andreasen et al., 2002). In addition this alkaline environment favoured apatite formation, and thus biomineralisation, which was confirmed in our research by the increased HA Raman peak in dentine samples in contact with Biodentine (Tay et al., 2007). The Biodentine interaction with sound dentine has demonstrated insignificant changes regarding fluorescence lifetime or intensity. Likewise, there was no mineral deposition detected by Raman peak analysis. Although many previous studies indicated the caustic effect of Biodentine (Andreasen et al., 2002; Atmeh et al., 2012) this effect was detectable in our samples but appearing to be minimal, causing insignificant changes in the optical properties of sound dentine (Leiendecker et al., 2012). However, sound dentine localised under caries affected dentine (chapter 5) showed a higher increase in the intensity than the intensity from sound teeth (chapter 2). This could be explained by the difference in dentine structure. Under a large carious lesion, this layer may correspond to transparent or subtransparent zone; these tissues show a gradual infill of the tubular structure with very fine crystals, which give a hardness number similar to that of sound dentine but the collagen matrix may still be partially exposed and so affected by the cement caustic effect (Marshall et al., 2001).

When dentine samples were demineralised and in contact with Biodentine, a significant increase in the mineral peak was detected which led to an increase in both fluorescence lifetime and intensity. Within these samples the organic matrix was not affected so we can presume any optical changes are due to remineralisation of the underlying dentine. This also helped in regaining the dentine's mechanical properties, i.e. returning dentine hardness to its normal value. Comparable optical results were found when Biodentine was evaluated against caries-affected dentine. Both samples displayed partial loss of mineral content; this was recovered after tissue interaction with the cement.

In carious tissues, Biodentine's effect on caries infected dentine was evaluated for the first time. Comparable evaluation was performed on totally demineralised dentine (Atmeh et al., 2015). Both studies confirmed the ability of Biodentine to

induce mineralisation through de-novo nucleation of ions leaching from the cement and phosphate rich mineralising solution (PBS) (Tay and Pashley, 2008).

GIC (Fuji IX) performed differently with our experimental dentine substrates. The polyalkeonic acid is believed to penetrate deeper into the dentine. This acidic effect is associated with ion transfer from the cement accompanied by Ca^{+2} and PO_4^{-3} diffusion from the underlying dentine as a result of acidic demineralisation. This ion exchange is responsible for the initial bond formed between the cement and the dentine surface. The remineralisation potential of GIC cements has been shown to be dependent on the growth from pre-existing crystals. In our study, the increased mineral peak within partially demineralised dentine and caries affected dentine supported this theory. In addition, the absence of mineral changes within infected dentine also supported the failure of GIC to induce remineralisation by new crystal formation in this degraded substrate. Comparable to Biodentine, optical changes were also detected in demineralised dentine and caries affected dentine when restored with GIC, which might indicate an increase in the mineral content.

Tetracycline was used in part of this research as a mineral labelling fluorophore. Its effectiveness to detect sites of active mineral transfer was confirmed by the detected change in the fluorescence intensity and more significantly the lifetime of the tissues where remineralisation is expected to take place. The apatite formation was confirmed by Raman analysis in tissues under similar experimental conditions i.e. cement and substrate. Comparing the Biodentine effect on excavated carious dentine and caries affected dentine; the two studies revealed similar results and confirmed the cements' bioactivity that was detectable by tetracycline labelling. In addition, the control samples in these studies: sound dentine (Chapter 3) or caries free (Chapter 5) showed a similar increase in the intensity and decreased lifetime. Although these changes were insignificant when compared to the changes caused by the cement, they may indicate tetracycline interaction with sound dentine. This could have originated from tetracycline adsorption to the dentine matrix proteins (Bowles and Bokmeyer, 1997). However, tetracycline binding to fully formed HA crystal has also been reported and cannot be excluded in our samples (Perrin, 1965).

In conclusion, Biodentine™, the calcium silicate based restorative material, demonstrated a bioactive interaction with sound, demineralised and carious dentine. This activity is mediated by the high alkalinity provided by the cement, targeting the dentine organic components followed by mineral transfer. Both

factors offered a suitable environment for dentine remineralisation to take place providing the presence of phosphate in the media. Clinically, this bioactivity is vital in managing carious lesions when clinicians are pursuing a minimally invasive approach. The use of GIC or Biodentine as a coronal restoration could be beneficial to enhance tissue repair as both demonstrated evidence of bioactive remineralisation. The decision on which material to apply should be influenced by other clinical factors. Moreover, the introduced in-vitro model enabled the evaluation of changes occur across the carious lesion which could be used in different experimental settings. Using multiphoton fluorescence microscopy to obtain fluorescence intensity and lifetime data is a promising minimally invasive microscopic technique that introduces additional microscopic markers to study dental tissues and to detect remineralisation within these tissues.

6.2 Suggestions for future work

An in-vitro study investigating the depth of remineralisation after Biodentine placement on demineralised and carious dentine.

Determining the depth of the remineralisation effect under Biodentine could provide more information on the materials' biological properties. This can be achieved by using Raman spectroscopy to detect changes in mineral peak before and after storage. A larger scan area below the interface would be included to determine the depth where no further change in the mineral peak is detected.

Evaluating the effect of new adhesive and restorative materials on carious dentine

The carious dentine model used in this thesis can be utilised offering an examination of different carious zones before and after the application of therapeutic materials. Different types of dental material - tooth interactions could be tested using similar optical non-invasive techniques to delineate the effect of the dentine caries zones; the infected dentine could be either excavated or alternatively the entire carious lesion imaged, as in this thesis. This work is currently being carried out by another PhD student testing a modified glass ionomer cement.

Characterisation of the interface between calcium silicates based dental cements and dentine using the nano-indentation test and SHG imaging

Detailed study and characterisation of the mechanical properties of carious dentine under this type of cement would provide more information about the nature of the interface between the two substrates. The nano-indentation test would facilitate the detection of changes in dentine elastic modulus and surface hardness. Whilst SHG imaging would provide valuable information about the quality of collagen fibres within each layer.

7. Appendices

1. Publication

Appendix 1

DENTAL-2236; No. of Pages 12
ARTICLE IN PRESS
DENTAL MATERIALS xxx (2013) xxx-xxx


Available online at www.sciencedirect.com
SciVerse ScienceDirect
Journal homepage: www.intl.elsevierhealth.com/journals/dema


Present and future of glass-ionomers and calcium-silicate cements as bioactive materials in dentistry: Biophotonics-based interfacial analyses in health and disease

Timothy F. Watson*, Amre R. Atmeh, Shara Sajini, Richard J. Cook, Frederic Festy

King's College London Dental Institute, Biomaterials, Biometrics & Biophotonics (B³), Floor 17, Guy's Tower Wing, Guy's Hospital, London Bridge SE1 9RT, United Kingdom

ARTICLE INFO

Article history:
Received 1 July 2013
Received in revised form 5 August 2013
Accepted 5 August 2013
Available online xxx

Keywords:
Bioactivity
Calcium silicate
Glass ionomer
Cements
Caries
Remineralization
Biophotonic imaging

ABSTRACT

Objective. Since their introduction, calcium silicate cements have primarily found use as endodontic sealers, due to long setting times. While similar in chemistry, recent variations such as constituent proportions, purities and manufacturing processes mandate a critical understanding of service behavior differences of the new coronal restorative material variants. Of particular relevance to minimally invasive philosophies is the potential for ion supply, from initial hydration to mature set in dental cements. They may be capable of supporting repair and remineralization of dentin left after decay and cavity preparation, following the concepts of ion exchange from glass ionomers.

Methods. This paper reviews the underlying chemistry and interactions of glass ionomer and calcium silicate cements, with dental tissues, concentrating on dentin-restoration interface reactions. We additionally demonstrate a new optical technique, based around high resolution deep tissue, two-photon fluorescence and lifetime imaging, which allows monitoring of undisturbed cement-dentin interface complex behavior over time.

Results. The local bioactivity of the calcium-silicate based materials has been shown to produce mineralization within the subjacent dentin substrate, extending deep within the tissues. This suggests that the local ion-rich alkaline environment may be more favorable to mineral repair and re-construction, compared with the acidic environs of comparable glass ionomer based materials.

Significance. The advantages of this potential re-mineralization phenomenon for minimally invasive management of carious dentin are self-evident. There is a clear need to improve the bioactivity of restorative dental materials and these calcium silicate cement systems offer exciting possibilities in realizing this goal.

© 2013 Academy of Dental Materials. Published by Elsevier Ltd. All rights reserved.

* Corresponding author. Tel.: +44 (0)20 7188 1824; fax: +44 (0)20 7188 1823.
E-mail address: timothy.f.watson@kcl.ac.uk (T.F. Watson).
0109-5641/\$ - see front matter © 2013 Academy of Dental Materials. Published by Elsevier Ltd. All rights reserved.
<http://dx.doi.org/10.1016/j.dental.2013.08.202>

Please cite this article in press as: Watson TF, et al. Present and future of glass ionomers and calcium silicate cements as bioactive materials in dentistry: Biophotonics-based interfacial analyses in health and disease. *Dent Mater* (2013), <http://dx.doi.org/10.1016/j.dental.2013.08.202>

2. Tables

Appendix 2

Two-sample t-test with equal variances for the assessment of dentine demineralisation. Using independent samples t-test separately for different techniques (Fluorescence Intensity, FLIM, SHG, Raman-mineral peak and tissue Hardness,).

Fluorescence intensity			
Group	Mean (Std.Dev)	[95% Conf. Interval]	P value
Sound	23.64 (9.19)	20.21 to 27.07	< 0.0003
Demineralised	33.28 (12.24)	30.12 to 36.45	
Fluorescence lifetime			
Group	Mean (Std.Dev)	[95% Conf. Interval]	P value
Sound	0.994 (0.37)	0.856 to 1.13	< 0.0001
Demineralised	1.49 (0.10)	1.464 to 1.51	
Second Harmonic Generation signal			
Group	Mean (Std.Dev)	[95% Conf. Interval]	P value
Sound	1.17 (0.38)	1.03 to 1.32	<0.3386
Demineralised	1.31 (0.77)	1.12 to 1.52	
Raman-mineral peak			
Group	Mean (Std.Dev)	[95% Conf. Interval]	P value
Sound	23.64 (9.19)	20.21 to 27.07	< 0.0003
Demineralised	33.28 (12.24)	30.12 to 36.45	
Tissue Hardness KHN			
Group	Mean (Std.Dev)	[95% Conf. Interval]	P value
Sound	30.62 (3.84)	29.19 to 32.06	< 0.0001
Demineralised	50.57 (4.43)	49.42 to 51.72	

Appendix 3

Data analysis of samples stored with Biodentine. Fitted linear model for each technique and further Post-Hoc analysis with P values adjusted for multiple comparison.

Analysis for samples stored in Biodentine™		
• Fluorescence Intensity		
Biodentine Vs Control for Demineralised dentine		
Coef.	[95% Conf. Interval]	P value
37.94	32.81 to 43.06	<0.001
Biodentine Vs Control for Sound dentine		
Coef.	[95% Conf. Interval]	P value
-17.99	-19.83 to -12.58	<0.000
Sound Vs Demineralised dentine for Biodentine		
Coef.	[95% Conf. Interval]	P value
-54.42	-59.07 to -49.79	<0.0001
• Fluorescence lifetime		
Biodentine Vs Control for Demineralised dentine		
Coef.	[95% Conf. Interval]	P value
68.67	63.96 to 73.38	<0.001
Biodentine Vs Control for Sound dentine		
Coef.	[95% Conf. Interval]	P value
-0.74	-4.09 to 2.61	<0.663
Sound Vs Demineralised dentine for Biodentine		
Coef.	[95% Conf. Interval]	P value
-67.43	71.69 to -63.17	<0.001
• Raman- mineral peak		
Biodentine Vs Control for Demineralised dentine		
Coef.	[95% Conf. Interval]	P value
107.33	77.99 to 136.69	<0.001
Biodentine Vs Control for Sound dentine		
Coef.	[95% Conf. Interval]	P value
-6.69	-29.81 to 16.42	<0.569

Sound Vs Demineralised dentine for Biodentine		
Coef.	[95% Conf. Interval]	P value
-111.40	-138.6 to -48.14	<0.0001
<ul style="list-style-type: none"> Tissue Hardness KHN 		
Biodentine Vs Control for Demineralised dentine		
Coef.	[95% Conf. Interval]	P value
38.22	32.14 to 44.31	<0.0001
Biodentine Vs Control for Sound dentine		
Coef.	[95% Conf. Interval]	P value
-5.16	-9.61 to -0.71	<0.023
Sound Vs Demineralised dentine for Biodentine		
Coef.	[95% Conf. Interval]	P value
-47.16	-52.85 to -41.47	<0.0001

Appendix 4

Data analysis of samples stored with GIC. Fitted linear model for each technique and further Post-Hoc analysis with P values adjusted for multiple comparison

Analysis for samples stored in GIC		
• Fluorescence Intensity		
GIC Vs Control for Demineralised dentine		
Coef.	[95% Conf. Interval]	P value
18.12	12.99 to 23.25	< 0.001
GIC Vs Control for Sound dentine		
Coef.	[95% Conf. Interval]	P value
-17.99	-21.61 to -14.36	< 0.001
Sound Vs Demineralised dentine for GIC		
Coef.	[95% Conf. Interval]	P value
-36.39	-41.03 to -31.75	< 0.001
• Fluorescence lifetime		
GIC Vs Control for Demineralised dentine		
Coef.	[95% Conf. Interval]	P value
58.88	54.16 to 63.59	<0.001
GIC Vs Control for Sound dentine		
Coef.	[95% Conf. Interval]	P value
-2.23	-5.62 to 1.15	<0.195
Sound Vs Demineralised dentine for GIC		
Coef.	[95% Conf. Interval]	P value
-59.13	-63.42 to -54.85	<0.001
• Raman- mineral peak		
GIC Vs Control for Demineralised dentine		
Coef.	[95% Conf. Interval]	P value

81.38	55.19 to 107.56	< 0.0001
GIC Vs Control for Sound dentine		
Coef.	[95% Conf. Interval]	P value
-11.45	-33.52 to 10.61	< 0.308
Sound Vs Demineralised dentine for GIC		
Coef.	[95% Conf. Interval]	P value
-90.19	-112.9 to -67.39	< 0.0001
<ul style="list-style-type: none"> Tissue Hardness KHN 		
GIC Vs Control for Demineralised dentine		
Coef.	[95% Conf. Interval]	P value
41.72	35.64 to 47.81	< 0.0001
GIC Vs Control for Sound dentine		
Coef.	[95% Conf. Interval]	P value
-2.47	-6.92 to 1.97	< 0.274
Sound Vs Demineralised dentine for GIC		
Coef.	[95% Conf. Interval]	P value
-47.98	-53.67 to -42.29	< 0.0001

Appendix 5

Comparing data analysis of samples stored with Biodentine™ and GIC regarding both sound and demineralised dentine: Fitted linear model for each technique and further Post-Hoc analysis with P values adjusted for multiple comparison.

Comparing samples stored in Biodentine and GIC		
• Fluorescence intensity		
GIC Vs Biodentine for Demineralised dentine		
Coef.	[95% Conf. Interval]	P value
19.81	14.46 to 25.17	< 0.001
GIC Vs Biodentine for Sound dentine		
Coef.	[95% Conf. Interval]	P value
1.78	-2.01 to 5.57	< 0.36
• Fluorescence lifetime		
GIC Vs Biodentine for Demineralised dentine		
Coef.	[95% Conf. Interval]	P value
9.79	4.87 to 14.71	< 0.001
GIC Vs Biodentine for Sound dentine		
Coef.	[95% Conf. Interval]	P value
1.49	-2.02 to 5.0	< 0.403
• Raman- mineral peak		
GIC Vs Biodentine for Demineralised dentine		
Coef.	[95% Conf. Interval]	P value
25.96	-1.67 to 53.59	< 0.065
GIC Vs Biodentine for Sound dentine		
Coef.	[95% Conf. Interval]	P value
4.75	-17.59 to 27.09	< 0.676
• Tissue Hardness KHN		

GIC Vs Biodentine for Demineralised dentine		
Coef.	[95% Conf. Interval]	P value
-3.50	-10.07 to 3.07	<0.294
GIC Vs Biodentine for Sound dentine		
Coef.	[95% Conf. Interval]	P value
-2.68	-7.33 to 1.95	< 0.254

Appendix 6

Flourescnece lifetime and intensity statistical analysis results assessing the cement/caries interface for samples stored in PBS without tetracycline labelling

Fluorescence lifetime analysis results (samples stored in PBS only)			
Comparison	Effect	95% Confidence Interval	p value
For caries-infected dentine			
Control VS. Biodentine	3.43	-2.84 to 9.71	0.28
Control VS. GIC	2.70	-4.20 to 9.61	0.44
Biodentine VS. GIC	0.73	-6.91 to 8.37	0.85
For cries-affected dentine			
Control VS. Biodentine	-28.15	-36.25 to -20.06	< 0.0001
Control VS. GIC	-17.91	-25.77 to -10.05	< 0.0001
Biodentine VS. GIC	10.24	0.90 to 19.59	0.03
For sound dentine			
Control VS. Biodentine	3.68	-5.37 to 12.74	0.42
Control VS. GIC	-3.20	-11.94 to 5.54	0.47
Biodentine VS. GIC	-6.88	-17.16 to 3.39	0.19

Fluorescence intensity analysis results (samples stored in PBS only)

Comparison	Effect	95% Confidence Interval	p value
For caries-infected dentine			
Control VS. Biodentine	101.6	50.46 to 152.7	< 0.0001
Control VS. GIC	-1.08	-57.37 to 55.2	0.97
Biodentine VS. GIC	102.6	40.36 to 164.96	< 0.001

For caries-affected dentine

Comparison	Effect	95% Confidence Interval	p value
Control VS. Biodentine	-146.65	-217.55 to -75.74	< 0.0001
Control VS. GIC	-70.62	-134.7 to -6.56	0.03
Biodentine VS. GIC	76.03	-4.39 to 156.46	0.06

For sound dentine

Control VS. Biodentine	-30.72	-123.29 to 61.85	0.51
Control VS. GIC	-25.5	-110.22 to 59.28	0.55
Biodentine VS. GIC	5.26	-93.25 to 103.76	0.92

Appendix 7

Raman mineral peak intensity statistical analysis results for cement/ caries interface assessment.

Raman mineral peak intensity statistical analysis					
Comparison	Effect	95% Confidence Interval			p value
Infected Group					
Control Vs Biodentine	0.32	0.02	to	0.61	0.03
Control Vs GIC	0.25	-0.07	to	0.56	0.12
Biodentine Vs GIC	-0.07	-0.42	to	0.28	0.69
Comparison	Effect	95% Confidence Interval			p value
Affected Group					
Control Vs Biodentine	-1.15	-1.50	to	-0.80	<0.0001
Control Vs GIC	-1.02			-1.36	to -0.67
					<0.0001
Biodentine Vs GIC	0.12	-0.26	to	0.50	0.52
Sound Group					
Control Vs Biodentine	0.04	-0.36	to	0.44	0.84
Control Vs GIC	-.001	-0.43	to	0.41	0.96
Biodentine Vs GIC	-0.04	-0.51	to	0.41	0.83

Appendix 8

Statistical analysis results of the percentage change in the fluorescence lifetime and intensity comparing the cement experimental groups with the control for samples stored in tetracycline containing solution.

Fluorescence lifetime analysis results (samples with Tetracycline labelling)			
Comparison	Effect	95% Confidence Interval	p value
For caries-infected dentine			
Control VS. Biodentine	-3.28	-8.95 to 2.39	0.26
Control VS. GIC	1.21	-3.97 to 6.39	0.65
Biodentine VS. GIC	-4.49	-10.61 to 1.64	0.15
For caries-affected dentine			
Control VS. Biodentine	23.78	17.57 to 29.99	< 0.0001
Control VS. GIC	14.67	8.81 to 20.53	< 0.0001
Biodentine VS. GIC	-9.11	-15.98 to -2.24	< 0.001
For sound dentine			
Control VS. Biodentine	2.93	-6.33 to 12.19	0.53
Control VS. GIC	4.56	-2.76 to 11.88	0.22
Biodentine VS. GIC	1.63	-8.19 to 11.45	0.74

Fluorescence intensity analysis results (samples with Tetracycline labelling)			
Comparison	Effect	95% Confidence Interval	p value
For caries-infected dentine			
Control VS. Biodentine	78.74	29.02 to 128.4	< 0.002
Control VS. GIC	8.40	-36.93 to 53.73	0.71
Biodentine VS. GIC	70.3	16.27 to 124.40	0.01
For caries-affected dentine			
Control VS. Biodentine	-46.52	-101.83 to 8.79	0.09
Control VS. GIC	-17.56	-69.77 to 34.65	0.51
Biodentine VS. GIC	28.96	-31.66 to 89.58	0.35
For sound dentine			
Control VS. Biodentine	24.81	-56.94 to 106.54	0.55
Control VS. GIC	27.15	-37.47 to 91.77	0.41
Biodentine VS. GIC	2.34	-84.36 to 89.04	0.96

References

- Abraham T, Carthy J & McManus B. 2010. Collagen matrix remodeling in 3-dimensional cellular space resolved using second harmonic generation and multiphoton excitation fluorescence. *Journal of structural biology*, 169, 36-44.
- Alfano R R & Yao S S. 1981. Human teeth with and without dental caries studied by visible luminescent spectroscopy. *J Dent Res*, 60, 120-2.
- Almahdy A, Downey F C, Sauro S, Cook R J, Sherriff M, Richards D, Watson T F, Banerjee A & Festy F. 2012. Microbiochemical Analysis of Carious Dentine Using Raman and Fluorescence Spectroscopy. *Caries Research*, 46, 432-40.
- Altshuler G B, Belashenkov N R, Martsinovski G A & Solounin A A. Nonlinear transmission and second harmonic generation in dentin in the field of ultrashort Nd-laser pulses. *Advanced Laser Dentistry*, 1995. International Society for Optics and Photonics, 6-10.
- Andreasen J O, Farik B & Munksgaard E C. 2002. Long-term calcium hydroxide as a root canal dressing may increase risk of root fracture. *Dental Traumatology*, 18, 134-37.
- Atmeh A, Chong E, Richard G, Festy F & Watson T. 2012. Dentin-cement Interfacial Interaction Calcium Silicates and Polyalkenoates. *Journal of dental research*, 91, 454-59.
- Atmeh A R, Chong E Z, Richard G, Boyde A, Festy F & Watson T F. 2015. Calcium silicate cement-induced remineralisation of totally demineralised dentine in comparison with glass ionomer cement: tetracycline labelling and two-photon fluorescence microscopy. *Journal of Microscopy*, 257, 151-60.
- Bachoo I, Seymour D & Brunton P. 2013. A biocompatible and bioactive replacement for dentine: is this a reality? The properties and uses of a novel calcium-based cement. *British dental journal*, 214, E5-E5.
- Bagramian R A, Garcia-Godoy F & Volpe A R. 2009. The global increase in dental caries. A pending public health crisis. *Am J Dent*, 22, 3-8.
- Baldwin G C. 2012. *An introduction to nonlinear optics*, Springer Science & Business Media.
- Banerjee A & Boyde A. 1998. Autofluorescence and Mineral Content of Carious Dentine: Scanning Optical and Backscattered Electron Microscopic Studies. *Caries Research* 32:, 219–26.
- Banerjee A. 1999. *Applications of scanning microscopy in the assessment of dentine caries and methods for its removal*. University of London.
- Banerjee A, Sherriff M, Kidd E & Watson T. 1999. Cariology: A confocal microscopic study relating the autofluorescence of carious dentine to its microhardnes. *British dental journal*, 187, 206-10.

- Banerjee A, Watson T F & Kidd E. 2000. Conservative dentistry: Dentine caries excavation: a review of current clinical techniques. . *British Dental Journal*, 188, 476 - 82
- Banerjee A, Yasserli M & Munson M. 2002. A method for the detection and quantification of bacteria in human carious dentine using fluorescent in situ hybridisation. *Journal of dentistry*, 30, 359-63.
- Banerjee A, Cook R, Kellow S, Shah K, Festy F, Sherriff M & Watson T. 2010a. A confocal micro-endoscopic investigation of the relationship between the microhardness of carious dentine and its autofluorescence. *European journal of oral sciences*, 118, 75-79.
- Banerjee A, Kellow S, Mannocci F, Cook R J & Watson T F. 2010b. An in vitro evaluation of microtensile bond strengths of two adhesive bonding agents to residual dentine after caries removal using three excavation techniques. *Journal of Dentistry*, 38, 480-89.
- Banerjee A. 2013. Minimal intervention dentistry: part 7. Minimally invasive operative caries management: rationale and techniques. *British dental journal*, 214, 107-11.
- Banerjee A & Watson T F. 2015. *Pickards Guide to Minimally Invasive Operative Dentistry*, OUP Oxford.
- Becker W. 2008. *The bh TCSPC Handbook*, Becker & Hickl GmbH.
- Bensted J. 1976. Uses of Raman spectroscopy in cement chemistry. *Journal of the American Ceramic Society*, 59, 140-43.
- Berezin M Y & Achilefu S. 2010. Fluorescence lifetime measurements and biological imaging. *Chemical reviews*, 110, 2641-84.
- Bertassoni L E, Habelitz S, Marshall S J & Marshall G W. 2011. Mechanical recovery of dentin following remineralization in vitro--an indentation study. *J Biomech*, 44, 176-81.
- Billington R W, Williams J A & Pearson G J. 2006. Ion processes in glass ionomer cements. *Journal of Dentistry*, 34, 544-55.
- Billinton N & Knight A. 2001. Seeing the Wood through the Trees: A Review of Techniques for Distinguishing Green Fluorescent Protein from Endogenous Autofluorescence. *Analytical Biochemistry* (2001, 291, 175–97.
- Björkman U H, Sundström F & ten Bosch J J. 1991. Fluorescence in dissolved fractions of human enamel. *Acta Odontologica*, 49, 133-38.
- Black G V & Black A D. 1920. *A Work on Operative Dentistry in Two Volumes*, Medico-dental publishing Company.
- Booij M & Ten Bosch J. 1982. A fluorescent compound in bovine dental enamel matrix compared with synthetic dityrosine. *Archives of oral biology*, 27, 417-21.

- Bowles W H & Bokmeyer T J. 1997. Staining of adult teeth by minocycline: binding of minocycline by specific proteins. *Journal of Esthetic and Restorative Dentistry*, 9, 30-34.
- Boyd R W. 2003. The Non-linear Optical Susceptibility. *Non-linear optics*: Academic press, 1-65.
- Bresciani E, Wagner W, Navarro M, Dickens S & Peters M. 2010. In vivo dentin microhardness beneath a calcium-phosphate cement. *Journal of dental research*, 89, 836-41.
- Bulatov V, Feller L, Yasman Y & Schechter I. 2008. Dental enamel caries (early) diagnosis and mapping by laser Raman spectral imaging. *Instrumentation Science and Technology*, 36, 235-44.
- Butler W T. 1984. Dentin collagen: chemical structure and role in mineralization. In: LINDE, A. (ed.) *Dentin and dentinogenesis*, 2 Boca Raton: Florida 8, 37-53.
- Camilleri J. 2007. Hydration mechanisms of mineral trioxide aggregate. *International Endodontic Journal*, 40, 462-70.
- Camilleri J. 2008. Characterization of hydration products of mineral trioxide aggregate. *International Endodontic Journal*, 41, 408-17.
- Camilleri J. 2011. Characterization and hydration kinetics of tricalcium silicate cement for use as a dental biomaterial. *Dental Materials*, 27, 836-44.
- Camilleri J, Grech L, Galea K, Keir D, Fenech M, Formosa L, Damidot D & Mallia B. 2014. Porosity and root dentine to material interface assessment of calcium silicate-based root-end filling materials. *Clinical oral investigations*, 18, 1437-46.
- Cao Y, Mei M L, Xu J, Lo E C, Li Q & Chu C H. 2013. Biomimetic mineralisation of phosphorylated dentine by CPP-ACP. *Journal of dentistry*, 41, 818-25.
- Carvalho R V, Ogliari F A, De Souza A P, Silva A F, Petzhold C L, Line S R, Piva E & Etges A. 2009. 2-Hydroxyethyl methacrylate as an inhibitor of matrix metalloproteinase-2. *European journal of oral sciences*, 117, 64-67.
- Cawston T. 1998. Matrix metalloproteinases and TIMPs: properties and implications for the rheumatic diseases. *Molecular medicine today*, 4, 130-37.
- Chang C, Sud D & Mycek M. 2007. Fluorescence lifetime imaging microscopy. *Methods in cell biology*, 81, 495.
- Cheek C C & Heymann H O. 1999. Dental and oral discolorations associated with minocycline and other tetracycline analogs. *Journal of Esthetic and Restorative Dentistry*, 11, 43-48.
- Chen M-H, Chen W-L, Sun Y, Fwu P T & Dong C-Y. 2007. Multiphoton autofluorescence and second-harmonic generation imaging of the tooth. *Journal of biomedical optics*, 12, 064018-18-6.

- Chen Z et al. 2015. Biomimetic Remineralization of Demineralized Dentine Using Scaffold of CMC/ACP Nanocomplexes in an In Vitro Tooth Model of Deep Caries. *PloS one*, 10.
- Clarkson B, Wefel J & Miller I. 1984. A model for producing caries-like lesions in enamel and dentin using oral bacteria in vitro. *Journal of dental research*, 63, 1186-89.
- Damato F, Strang R & Stephen K. 1988. Comparison of solution-and gel-prepared enamel lesions-an in vitro pH-cycling study. *Journal of dental research*, 67, 1122-25.
- Dawes C. 2003. What is the critical pH and why does a tooth dissolve in acid? *Journal-Canadian Dental Association*, 69, 722-25.
- Deb S & Nicholson J W. 1999. The effect of strontium oxide in glass-ionomer cements. *Journal of Materials Science-Materials in Medicine*, 10, 471-74.
- Eichler J & Kim B-M. 2002. Nonlinear scattering in hard tissue studied with ultrashort laser pulses. *Zeitschrift für Medizinische Physik*, 12, 191-97.
- Ekstrand K, Ricketts D & Kidd E. 1998. Do occlusal carious lesions spread laterally at the enamel–dentin junction? *Clinical oral investigations*, 2, 15-20.
- Elbaum R, Tal E, Perets A, Oron D, Ziskind D, Silberberg Y & Wagner H. 2007. Dentin micro-architecture using harmonic generation microscopy. *Journal of dentistry*, 35, 150-55.
- Farge P, Alderete L & Ramos S. 2010. Dentin wetting by three adhesive systems: influence of etching time, temperature and relative humidity. *journal of dentistry*, 38, 698-706.
- Featherstone J. 2009. Remineralization, the natural caries repair process—the need for new approaches. *Advances in Dental Research*, 21, 4-7.
- Ferretti de Oliveira F, Ito A S & Bachmann L. 2010. Time-resolved fluorescence spectroscopy of white-spot caries in human enamel. *Appl Opt*, 49, 2244-9.
- Forsten L. 1998. Fluoride release and uptake by glass-ionomers and related materials and its clinical effect. *Biomaterials*, 19, 503-08.
- Francci C, Deaton T, Arnold R, Swift E, Perdigao J & Bawden J. 1999. Fluoride release from restorative materials and its effects on dentin demineralization. *Journal of dental research*, 78, 1647-54.
- Frantz B & Polson A. 1987. Tissue Interactions with Dentin Specimens after Demineralization Using Tetracycline. *Journal of Dental Research*, 66, 340-40.
- Funteas U R, Wallace J A & Fochtman E W. 2003. A comparative analysis of Mineral Trioxide Aggregate and Portland cement. *Aust Endod J*, 29, 43-4.
- Fusayama T, Okuse K & Hosoda H. 1966. Relationship between hardness, discoloration, and microbial invasion in carious dentin. *Journal of Dental Research*, 45, 1033-46.

- Fusayama T & Terashima S. 1972. Differentiation of two layers of carious dentin by staining. *The Bulletin of Tokyo Medical and Dental University*, 19, 83.
- Fusayama T, Nakamura M, Kurosaki N & Iwaku M. 1979. Non-pressure adhesion of a new adhesive restorative resin. *J Dent Res*, 58, 1364-70.
- Gannot I, Ron I, Hekmat F, Chernomordik V & Gandjbakhche A. 2004. Functional optical detection based on pH dependent fluorescence lifetime. *Lasers in surgery and medicine*, 35, 342-48.
- Garcia F C, Wang L, Pereira L C, e Silva S M d A, Júnior L M & de Oliveira Carrilho M R. 2010. Influences of surface and solvent on retention of HEMA/mixture components after evaporation. *Journal of dentistry*, 38, 44-49.
- George A & Veis A. 2008. Phosphorylated proteins and control over apatite nucleation, crystal growth, and inhibition. *Chemical reviews*, 108, 4670-93.
- Goldberg M, Kulkarni A B, Young M & Boskey A. 2011. Dentin: Structure, Composition and Mineralization: The role of dentin ECM in dentin formation and mineralization. *Frontiers in bioscience (Elite edition)*, 3, 711.
- Gopalakrishna A. 2009. Impact of different acid etching time on microtensile bond strength to vital dentin.
- Gruythuysen R, van Strijp G & Wu M-K. 2010. Long-term survival of indirect pulp treatment performed in primary and permanent teeth with clinically diagnosed deep carious lesions. *Journal of endodontics*, 36, 1490-93.
- Gu L et al. 2011. Biomimetic analogs for collagen biomineralization. *J Dent Res*, 90, 82-7.
- Han L & Okiji T. 2011. Uptake of calcium and silicon released from calcium silicate-based endodontic materials into root canal dentine. *International Endodontic Journal*, 44, 1081-87.
- Han L & Okiji T. 2013. Bioactivity evaluation of three calcium silicate-based endodontic materials. *International endodontic journal*, 46, 808-14.
- Hashem D, Mannocci F, Patel S, Manoharan A, Brown J, Watson T & Banerjee A. 2015. Clinical and Radiographic Assessment of the Efficacy of Calcium Silicate Indirect Pulp Capping A Randomized Controlled Clinical Trial. *Journal of dental research*, 94, 562-68.
- Hédoux A, Guinet Y & Descamps M. 2011. The contribution of Raman spectroscopy to the analysis of phase transformations in pharmaceutical compounds. *International journal of pharmaceutics*, 417, 17-31.
- Helmchen F & Denk W. 2005. Deep tissue two-photon microscopy. *Nat Methods*, 2, 932-40.
- Hench L L, Splinter R J, Allen W & Greenlee T. 1971. Bonding mechanisms at the interface of ceramic prosthetic materials. *Journal of Biomedical Materials Research*, 5, 117-41.

- Hibst R, Paulus R & Lussi A. 2001. Detection of occlusal caries by laser fluorescence: basic and clinical investigations. *Medical Laser Application*, 16, 205-13.
- Hilton T J. 2009. Keys to clinical success with pulp capping: a review of the literature. *Operative dentistry*, 34, 615.
- Hoshino E. 1985. Predominant obligate anaerobes in human carious dentin. *Journal of Dental Research*, 64, 1195-98.
- Hutchings J, Kendall C, Shepherd N, Barr H, Smith B & Stone N. Rapid Raman microscopic imaging for potential histological screening. Biomedical Optics (BiOS) 2008, 2008. International Society for Optics and Photonics, 685305-05-9.
- Inaba D, Ruben J, Takagi O & Arends J. 1996. Effect of sodium hypochlorite treatment on remineralization of human root dentine in vitro. *Caries Res*, 30, 218-24.
- Iwami Y, Hayashi N, Takeshige F & Ebisu S. 2008. Relationship between the color of carious dentin with varying lesion activity, and bacterial detection. *Journal of dentistry*, 36, 143-51.
- Jefferies S R. 2014. Bioactive and biomimetic restorative materials: a comprehensive review. Part I. *Journal of Esthetic and Restorative Dentistry*, 26, 14-26.
- Jones S J & Boyde A. 1984. Ultrastructure of dentin and dentinogenesis. *Dentin and dentinogenesis*, 1, 81-134.
- Kao F J. 2004. The use of optical parametric oscillator for harmonic generation and two-photon UV fluorescence microscopy. *Microscopy research and technique*, 63, 175-81.
- Karlsson L. 2010. Caries Detection Methods Based on Changes in Optical Properties between Healthy and Carious Tissue
International Journal of Dentistry, 2010, 9.
- Kawasaki K, Ruben J, Stokroos I, Takagi O & Arends J. 1999. The remineralization of EDTA-treated human dentine. *Caries Res*, 33, 275-80.
- Keiser K, Johnson C C & Tipton D A. 2000. Cytotoxicity of mineral trioxide aggregate using human periodontal ligament fibroblasts. *Journal of Endodontics*, 26, 288-91.
- Kidd E, Joyston-Bechal S & Beighton D. 1993. Microbiological validation of assessments of caries activity during cavity preparation. *Caries Research*, 27, 402-08.
- Kidd E. 2004. How 'clean' must a cavity be before restoration? *Caries research*, 38, 305-13.
- Kim B M, Eichler J, Reiser K M, Rubenchik A M & Da Silva L B. 2000. Collagen structure and nonlinear susceptibility: effects of heat, glycation, and

- enzymatic cleavage on second harmonic signal intensity. *Lasers in surgery and medicine*, 27, 329-35.
- Kim J R, Nosrat A & Fouad A F. 2015. Interfacial characteristics of Biodentine and MTA with dentine in simulated body fluid. *Journal of dentistry*, 43, 241-47.
- Kim Y, Yiu C, Kim J, Gu L, Kim S, Weller R, Pashley D & Tay F. 2010. Failure of a glass ionomer to remineralize apatite-depleted dentin. *Journal of dental research*, 89, 230-35.
- Kinoshita H, Miyoshi N, Fukunaga Y, Ogawa T, Ogasawara T & Sano K. 2008. Functional mapping of carious enamel in human teeth with Raman microspectroscopy. *Journal of Raman Spectroscopy*, 39, 655-60.
- Kirsten G A, Takahashi M K, Rached R N, Giannini M & Souza E M. 2010. Microhardness of dentin underneath fluoride-releasing adhesive systems subjected to cariogenic challenge and fluoride therapy. *Journal of dentistry*, 38, 460-68.
- Kjellsen K O & Justnes H. 2004. Revisiting the microstructure of hydrated tricalcium silicate - a comparison to Portland cement. *Cement & Concrete Composites*, 26, 947-56.
- Kleter G, Damen J, Buijs M & Ten Cate J. 1998. Modification of amino acid residues in carious dentin matrix. *Journal of dental research*, 77, 488-95.
- Ko A C-T, Hewko M, Leonardi L, Sowa M G, Dong C C, Williams P & Cleghorn B. 2005. Ex vivo detection and characterization of early dental caries by optical coherence tomography and Raman spectroscopy. *Journal of biomedical optics*, 10, 031118-03111816.
- Koenig K, Hibst R, Meyer H, Flemming G & Schneckenburger H. Laser-induced autofluorescence of carious regions of human teeth and caries-involved bacteria. Europto Biomedical Optics' 93, 1993. International Society for Optics and Photonics, 170-80.
- Koenig K & Schneckenburger H. 1994. Laser-induced autofluorescence for medical diagnosis. *Journal of fluorescence*, 4, 17-40.
- König K, Schneckenburger H & Hibst R. 1999. Time-gated in vivo autofluorescence imaging of dental caries. *Cellular and molecular biology (Noisy-le-Grand, France)*, 45, 233-39.
- Koubi G, Colon P, Franquin J-C, Hartmann A, Richard G, Faure M-O & Lambert G. 2013. Clinical evaluation of the performance and safety of a new dentine substitute, Biodentine, in the restoration of posterior teeth—a prospective study. *Clinical oral investigations*, 17, 243-49.
- Koutsopoulos S. 2002. Synthesis and characterization of hydroxyapatite crystals: a review study on the analytical methods. *Journal of biomedical materials research*, 62, 600-12.
- Kuboki Y, Ohgushi K & Fusayama T. 1977. Collagen biochemistry of the two layers of carious dentin. *Journal of Dental Research*, 56, 1233-37.

- Kwak E-S, Kang T J & Vanden Bout D A. 2001. Fluorescence lifetime imaging with near-field scanning optical microscopy. *Analytical chemistry*, 73, 3257-62.
- Lager A, Thornqvist E & Ericson D. 2002. Cultivable bacteria in dentine after caries excavation using rose-bur or carisolv. *Caries research*, 37, 206-11.
- Lakowicz J R. 2013. Principles of fluorescence spectroscopy. Springer Science & Business Media, pp 10-20.
- Laurent P, Camps J, De Meo M, Dejoui J & About I. 2008. Induction of specific cell responses to a Ca(3)SiO(5)-based posterior restorative material. *Dent Mater*, 24, 1486-94.
- Laurent P, Camps J & About I. 2012. Biodentine(TM) induces TGF-beta1 release from human pulp cells and early dental pulp mineralization. *International Endodontic Journal*, 45, 439-48.
- Learmonth R, Kable S & Ghiggino K. 2009. Basics of fluorescence. In: GLOYDS, E. (ed.) *Fluorescence applications in biotechnology and life science*.: New Jersey: Wiley-Blackwell, 1-26.
- Lee H-S, Berg J H, Garcia-Godoy F & Jang K-T. 2008. Long term evaluation of the remineralization of interproximal caries-like lesions adjacent to glass-ionomer restorations: A micro-CT study. *American journal of dentistry*, 21, 129.
- Lee S J, Monsef M & Torabinejad M. 1993. Sealing Ability of a Mineral Trioxide Aggregate for Repair of Lateral Root Perforations. *Journal of Endodontics*, 19, 541-44.
- LeGeros R & Tung M. 1983. Chemical stability of carbonate-and fluoride-containing apatites. *Caries Research*, 17, 419-29.
- Leiendecker A P, Qi Y-P, Sawyer A N, Niu L-N, Agee K A, Loushine R J, Weller R N, Pashley D H & Tay F R. 2012. Effects of Calcium Silicate-based Materials on Collagen Matrix Integrity of Mineralized Dentin. *Journal of Endodontics*, 38, 829-33.
- Lin P-Y, Lyu H-C, Hsu C-Y S, Chang C-S & Kao F-J. 2011. Imaging carious dental tissues with multiphoton fluorescence lifetime imaging microscopy. *Biomedical optics express*, 2, 149-58.
- Liu Y, Kim Y K, Dai L, Li N, Khan S O, Pashley D H & Tay F R. 2011a. Hierarchical and non-hierarchical mineralisation of collagen. *Biomaterials*, 32, 1291-300.
- Liu Y, Mai S, Li N, Yiu C K Y, Mao J, Pashley D H & Tay F R. 2011b. Differences between top-down and bottom-up approaches in mineralizing thick, partially demineralized collagen scaffolds. *Acta Biomaterialia*, 7, 1742-51.
- Liu Y, Tjäderhane L, Breschi L, Mazzoni A, Li N, Mao J, Pashley D & Tay F. 2011c. Limitations in bonding to dentin and experimental strategies to prevent bond degradation. *Journal of Dental Research*, 90, 953-68.
- Luciano Bachmanna D M Z, Adriana da Costa Ribeirob, Laércio Gomesb & Amando Siuiti Itoa. 2006. Fluorescence Spectroscopy of Biological Tissues. *Applied Spectroscopy Reviews*, Volume 41, 575-90.

- Lussi A, Hibst R & Paulus R. 2004. DIAGNOdent: An Optical Method for Caries Detection. *Journal of Dental Research*, 83, 80-83.
- Malkondur Ö, Kazandağ M K & Kazazoğlu E. 2014. A review on biodentine, a contemporary dentine replacement and repair material. *BioMed research international*, 2014.
- Marshall G, Habelitz S, Gallagher R, Balooch M, Balooch G & Marshall S. 2001. Nanomechanical properties of hydrated carious human dentin. *Journal of Dental Research*, 80, 1768-71.
- Marshall G W, Inai N, Magidi I-C W, Balooch M, Kinney J H, Tagami J & Marshall S J. 1997. Dentin demineralization: effects of dentin depth, pH and different acids. *Dental Materials*, 13, 338-43.
- Martinez-Ramirez S, Frías M & Domingo C. 2006. Micro-Raman spectroscopy in white portland cement hydration: long-term study at room temperature. *Journal of Raman Spectroscopy*, 37, 555-61.
- Matsumoto H, Kitamura S & Araki T. 1999. Autofluorescence in human dentine in relation to age, tooth type and temperature measured by nanosecond time-resolved fluorescence microscopy. *Arch Oral Biol*, 44, 309-18.
- McConnell G, Girkin J M, Ameer-Beg S M, Barber P R, Vojnovic B, Ng T, Banerjee A, Watson T F & Cook R J. 2007. Time-correlated single-photon counting fluorescence lifetime confocal imaging of decayed and sound dental structures with a white-light supercontinuum source. *Journal of Microscopy-Oxford*, 225, 126-36.
- Mertz-Fairhurst E J, CURTIS J W, Ergle J W, Rueggeberg F A & Adair S M. 1998. Ultraconservative and cariostatic sealed restorations: results at year 10. *The Journal of the American Dental Association*, 129, 55-66.
- Milan A M, Sugars R V, Embery G & Waddington R J. 2006. Adsorption and interactions of dentine phosphoprotein with hydroxyapatite and collagen. *European journal of oral sciences*, 114, 223-31.
- Milly H, Festy F, Watson T F, Thompson I & Banerjee A. 2014. Enamel white spot lesions can remineralise using bio-active glass and polyacrylic acid-modified bio-active glass powders. *Journal of dentistry*, 42, 158-66.
- Moseley R, Waddington R, Sloan A J, Smith A J, Hall R & Embery G. 2003. The influence of fluoride exposure on dentin mineralization using an in vitro organ culture model. *Calcified tissue international*, 73, 470-75.
- Nakajima M, Kunawarote S, Prasansuttiorn T & Tagami J. 2011. Bonding to caries-affected dentin. *Japanese Dental Science Review*, 47, 102-14.
- Nakornchai S, Atsawasuan P, Kitamura E, Surarit R & Yamauchi M. 2004. Partial biochemical characterisation of collagen in carious dentin of human primary teeth. *Archives of oral biology*, 49, 267-73.
- Neves A A, Coutinho E, De Munck J, Lambrechts P & Van Meerbeek B. 2011a. Does DIAGNOdent provide a reliable caries-removal endpoint? *Journal of Dentistry*, 39, 351-60.

References

- Neves A d A, Coutinho E, Vivan Cardoso M, Jaecques S V & Van Meerbeek B. 2010. Micro-CT based quantitative evaluation of caries excavation. *Dental Materials*, 26, 579-88.
- Neves A d A, Coutinho E, ardoso M, Lambrechts P & Van Meerbeek B. 2011b. Current concepts and techniques for caries excavation and adhesion to residual dentin. *Journal of Adhesive Dentistry*, 13(1), 7-22.
- Neves A d A, Coutinho E, De Munck J & Van Meerbeek B. 2011c. Caries-removal effectiveness and minimal-invasiveness potential of caries-excitation techniques: a micro-CT investigation. *journal of dentistry*, 39, 154-62.
- Ng T, Parsons M, Hughes W, Monypenny J, Zicha D, Gautreau A & Arpin M. 2001. S. 658 Gschmeissner, PJ Verveer, PI Bastiaens, and PJ Parker. 2001. Ezrin is a 659 downstream effector of trafficking PKC-integrin complexes involved in the control of 660 cell motility. *Embo J*, 20, 2723-41.
- Ngo H C, Mount G, Mc Intyre J, Tuisuva J & Von Doussa R. 2006. Chemical exchange between glass-ionomer restorations and residual carious dentine in permanent molars: an in vivo study. *Journal of dentistry*, 34, 608-13.
- Ngo H C, Mount G, McIntyre J & Do L. 2011. An in vitro model for the study of chemical exchange between glass ionomer restorations and partially demineralized dentin using a minimally invasive restorative technique. *Journal of dentistry*, 39, S20-S26.
- Nicholson J W. 1998. Chemistry of glass-ionomer cements: a review. *Biomaterials*, 19, 485-94.
- Niu L-n, Zhang W, Pashley D H, Breschi L, Mao J, Chen J-h & Tay F R. 2014. Biomimetic remineralization of dentin. *Dental Materials*, 30, 77-96.
- Nowicka A, Lipski M, Parafiniuk M, Sporniak-Tutak K, Lichota D, Kosierkiewicz A, Kaczmarek W & Buczkowska-Radlińska J. 2013. Response of human dental pulp capped with biodentine and mineral trioxide aggregate. *Journal of endodontics*, 39, 743-47.
- Ogawa K, Yamashita Y, Ichijo T & Fusayama T. 1983. The Ultrastructure and Hardness of the Transparent of Human Carious Dentin. *Journal of Dental Research*, 62, 7-10.
- Ohgushi K & Fusayama T. 1975. Electron microscopic structure of the two layers of carious dentin. *Journal of dental research*, 54, 1019-26.
- Osorio R, Yamauti M, Osorio E, Ruiz-Requena M, Pashley D, Tay F & Toledano M. 2011. Zinc reduces collagen degradation in demineralized human dentin explants. *Journal of dentistry*, 39, 148-53.
- Paranjpe A, Zhang H & Johnson J D. 2010. Effects of mineral trioxide aggregate on human dental pulp cells after pulp-capping procedures. *Journal of endodontics*, 36, 1042-47.
- Parker A S et al. 2014. Measurement of the efficacy of calcium silicate for the protection and repair of dental enamel. *journal of dentistry*, 42, S21-S29.

- Pashley D. 1991. Clinical correlations of dentin structure and function. *The Journal of prosthetic dentistry*, 66, 777-81.
- Pearce E. 1983. A microradiographic and chemical comparison of in vitro systems for the simulation of incipient caries in abraded bovine enamel. *Journal of dental research*, 62, 969-74.
- Penel G, Leroy G, Rey C & Bres E. 1998. MicroRaman spectral study of the PO₄ and CO₃ vibrational modes in synthetic and biological apatites. *Calcified Tissue International*, 63, 475-81.
- Perdigão J & Lopes M. 2001. The effect of etching time on dentin demineralization. *Quintessence Int*, 32, 19-26.
- Perrin D. 1965. Binding of tetracyclines to bone.
- Petruska J A & Hodge A J. 1964. A subunit model for the tropocollagen macromolecule. *Proceedings of the National Academy of Sciences of the United States of America*, 51, 871.
- Pitt F T R, Torabinejad M, Abedi H R, Bakland L K & Kariyawasam S P. 1996. Using mineral trioxide aggregate as a pulp-capping material. *The Journal of the American Dental Association*, 127, 1491-94.
- Popović-Bajić M, Prokić B, Prokić B, Jokanović V, Danilović V & Živković S. 2013. Histological evaluation of direct pulp capping with novel nanostructural materials based on active silicate cements and Biodentine® on pulp tissue. *Acta veterinaria*, 63, 347-60.
- Pretty I A. 2006. Caries detection and diagnosis: Novel technologies. *Journal of Dentistry* 3 4, 72 7 – 73 9.
- Qi Y P, Li N, Niu L N, Primus C M, Ling J Q, Pashley D H & Tay F R. 2012. Remineralization of artificial dentinal caries lesions by biomimetically modified mineral trioxide aggregate. *Acta Biomaterialia*, 8, 836-42.
- Qin C, Baba O & Butler W. 2004. Post-translational modifications of sibling proteins and their roles in osteogenesis and dentinogenesis. *Critical Reviews in Oral Biology & Medicine*, 15, 126-36.
- Ramamurthy N, Schroeder K, McNamara T, Gwinnett A, Evans R, Bosko C & Golub L. 1998. Root-surface caries in rats and humans: inhibition by a non-antimicrobial property of tetracyclines. *Advances in dental research*, 12, 43-50.
- Ramasetty P, Bhat K & Prasanna M. 2014. Comparative evaluation of remineralization, fluoride release and physical properties of conventional GIC following incorporation of 1% and 2% zinc acetate: An in vitro study. *International Journal of Oral Health Sciences*, 4, 4.
- Ribeiro A, Rousseau C, Girkin J, Hall A, Strang R, John Whitters C, Creanor S & Gomes A S. 2005a. A preliminary investigation of a spectroscopic technique for the diagnosis of natural caries lesions. *J Dent*, 33, 73-8.

- Ribeiro F A C, Kurachi C & Bagnato V.S. 2005b. Comparison of Fluorescence Detection of Carious Dentin for Different Excitation Wavelengths. *Caries Research* 39, 393-96
- Rivera E & Yamauchi M. 1993. Site comparisons of dentine collagen cross-links from extracted human teeth. *Archives of oral biology*, 38, 541-46.
- Saito T, Yamauchi M & Crenshaw M A. 1998. Apatite induction by insoluble dentin collagen. *Journal of Bone and Mineral Research*, 13, 265-70.
- Saito T, Toyooka H, Ito S & Crenshaw M A. 2003. In vitro study of remineralization of dentin: effects of ions on mineral induction by decalcified dentin matrix. *Caries Res*, 37, 445-9.
- Sakoolnamarka R, Burrow M, Swain M & Tyas M. 2005a. Microhardness and Ca: P ratio of carious and Carisolv™ treated caries-affected dentine using an ultra-micro-indentation system and energy dispersive analysis of x-rays—A pilot study. *Australian dental journal*, 50, 246-50.
- Sakoolnamarka R, Burrow M F, Praver S & Tyas M J. 2005b. Raman spectroscopic study of noncarious cervical lesions. *Odontology*, 93, 35-40.
- Salehi H, Terrer E, Panayotov I, Levallois B, Jacquot B, Tassery H & Cuisinier F. 2013. Functional mapping of human sound and carious enamel and dentin with Raman spectroscopy. *Journal of biophotonics*, 6, 765-74.
- Santos A, Moraes J, Araújo E, Yukimitu K & Valério Filho W. 2005. Physico-chemical properties of MTA and a novel experimental cement. *International endodontic journal*, 38, 443-47.
- Sarkar N, Caicedo R, Ritwik P, Moiseyeva R & Kawashima I. 2005. Physicochemical basis of the biologic properties of mineral trioxide aggregate. *Journal of Endodontics*, 31, 97-100.
- Sauer G, Zunic W, Durig J & Wuthier R. 1994. Fourier transform Raman spectroscopy of synthetic and biological calcium phosphates. *Calcified tissue international*, 54, 414-20.
- Schneider S, Schmitt M O, Brehm G, Reiher M, Matousek P & Towrie M. 2003. Fluorescence kinetics of aqueous solutions of tetracycline and its complexes with Mg 2+ and Ca 2+. *Photochemical & Photobiological Sciences*, 2, 1107-17.
- Selwitz R H, Ismail A I & Pitts N B. 2007. Dental caries. *The Lancet*, 369, 51-59.
- Sennou H, Lebugle A & Gregoire G. 1999. X-ray photoelectron spectroscopy study of the dentin–glass ionomer cement interface. *Dental Materials*, 15, 229-37.
- Shayegan A, Jurysta C, Atash R, Petein M & Abbee A V. 2012. Biodentine used as a pulp-capping agent in primary pig teeth. *Pediatric dentistry*, 34, 202E-08E.
- Shi X, Tranaeus S & Angmar-Månsson B. 2001. Comparison of QLF and DIAGNOdent for quantification of smooth surface caries. *Caries Research* 35, 21-26.

- Shia U-Q, B. W & Angmar-Månssona. 2000. Occlusal Caries Detection with KaVo DIAGNOdent and Radiography: An in vitro Comparison. *Caries Research*, 34, 151-58.
- Shigetani Y, Okamoto A, Abu-Bakr N, Tanabe K, Kondo S & Iwaku M. 2003. Caries diagnosis using a laser fluorescence system--observation of autofluorescence of dental caries. *Dent Mater J*, 22, 56-65.
- Shigetani Y, Takenaka S, Okamoto A, Abu-Bakr N, Iwaku M & Okiji T. 2008. Impact of *Streptococcus mutans* on the generation of fluorescence from artificially induced enamel and dentin carious lesions in vitro. *Odontology*, 96, 21-25.
- Silverio K G, Martinez A E & Rossa C, Jr. 2007. Effects of basic fibroblast growth factor on density and morphology of fibroblasts grown on root surfaces with or without conditioning with tetracycline or EDTA. *J Oral Sci*, 49, 213-20.
- Silverstone L. 1968. The surface zone in caries and in caries-like lesions produced in vitro. *British dental journal*, 125, 145-57.
- So M B a. 2008. *Handbook of biomedical non-linear optical microscopy*, Oxford university Press New York.
- So P T, Dong C Y, Masters B R & Berland K M. 2000. Two-photon excitation fluorescence microscopy. *Annual review of biomedical engineering*, 2, 399-429.
- Sofia Tranæus X-Q S a B A-M n. 2005. Caries risk assessment: methods available to clinicians for caries detection. *Community Dentistry and Oral Epidemiology* 33, 265–73.
- Song J S, Mante F K, Romanow W J & Kim S. 2006. Chemical analysis of powder and set forms of Portland cement, gray ProRoot MTA, white ProRoot MTA, and gray MTA-Angelus. *Oral Surg Oral Med Oral Pathol Oral Radiol Endod*, 102, 809-15.
- Spencer P, Wang Y, Walker M, Wieliczka D & Swafford J. 2000. Interfacial chemistry of the dentin/adhesive bond. *Journal of Dental Research*, 79, 1458-63.
- Spitzer D & Ten J B. 1976. The total luminescence of bovine and human dental enamel. *Calcified tissue research*, 20, 201-08.
- Stookey G K. 2005. Quantitative light fluorescence: a technology for early monitoring of the caries process. *Dental Clinics of North America*, 49, 753-70, vi.
- Subhash N, Thomas S S, Mallia R J & Jose M. 2005. Tooth caries detection by curve fitting of laser-induced fluorescence emission: A comparative evaluation with reflectance spectroscopy. *Lasers in Surgery and Medicine*, 37, 320-28.
- Tagger M, Perlmutter S, Galon H & Helft M. 1975. In vivo tetracycline labeling of experimentally induced reparative dentin in human teeth. *Journal of dental research*, 54, 444-48.

- Tanumiharja M, Burrow M F, Cimmino A & Tyas M J. 2001. The evaluation of four conditioners for glass ionomer cements using field-emission scanning electron microscopy. *Journal of Dentistry*, 29, 131-38.
- Tay F R, Pashley D H, Rueggeberg F A, Loushine R J & Weller R N. 2007. Calcium Phosphate Phase Transformation Produced by the Interaction of the Portland Cement Component of White Mineral Trioxide Aggregate with a Phosphate-containing Fluid. *Journal of Endodontics*, 33, 1347-51.
- Tay F R & Pashley D H. 2008. Guided tissue remineralisation of partially demineralised human dentine. *Biomaterials*, 29, 1127-37.
- Taylor H F W. 1997. *Cement Chemistry, Second Edition*, Thomas Telford.
- Ten Cate J M, Buus M J & Damen J J M. 1995. The Effects of Gic Restorations on Enamel and Dentin Demineralization and Remineralization. *Advances in Dental Research*, 9, 384-88.
- Terrer E et al. 2016. Laboratory Studies of Nonlinear Optical Signals for Caries Detection. *Journal of Dental Research*, 0022034516629400.
- Toledano M, Aguilera F S, Cabello I & Osorio R. 2014. Remineralization of mechanical loaded resin–dentin interface: a transitional and synchronized multistep process. *Biomechanics and modeling in mechanobiology*, 13, 1289-302.
- Tonami K-i, Araki K, Mataka S & Kurosaki N. 2003. Effects of chloramines and sodium hypochlorite on carious dentin. *Journal of medical and dental sciences*, 50, 139-46.
- Torabinejad M & Chivian N. 1999. Clinical applications of mineral trioxide aggregate. *Journal of Endodontics*, 25, 197-205.
- Trairatvorakul C, Techalertpaisarn P, Siwawut S & Ingprapankorn A. 2009. Effect of glass ionomer cement and fluoride varnish on the remineralization of artificial proximal caries in situ. *Journal of Clinical Pediatric Dentistry*, 34, 131-34.
- Tramini P, Pélissier B, Valcarcel J, Bonnet B & Maury L. 2000. A Raman spectroscopic investigation of dentin and enamel structures modified by lactic acid. *Caries research*, 34, 233-40.
- Tran X, Gorin C, Willig C, Baroukh B, Pellat B, Decup F, Vital S O, Chaussain C & Boukpessi T. 2012. Effect of a calcium-silicate-based restorative cement on pulp repair. *Journal of dental research*, 0022034512460833.
- Tsanidis V & Koulourides T. 1992. An in vitro model for assessment of fluoride uptake from glass-ionomer cements by dentin and its effect on acid resistance. *Journal of dental research*, 71, 7-12.
- Tsuda H & Arends J. 1997. Raman spectroscopy in dental research: a short review of recent studies. *Advances in Dental Research*, 11, 539-47.
- Van der Veen M & Ten Bosch J. 1996. The influence of mineral loss on the auto-fluorescent behaviour of in vitro demineralised dentine. *Caries research*, 30, 93-99.

- Vernazza C, Steele J, Whitworth J, Wildman J & Donaldson C. 2014. Factors affecting direction and strength of patient preferences for treatment of molar teeth with nonvital pulps. *International endodontic journal*.
- Vollenweider M, Brunner T J, Knecht S, Grass R N, Zehnder M, Imfeld T & Stark W J. 2007. Remineralization of human dentin using ultrafine bioactive glass particles. *Acta Biomaterialia*, 3, 936-43.
- Walls A W G. 1986. Glass Polyalkenoate (Glass-Ionomer) Cements - a Review. *Journal of Dentistry*, 14, 231-46.
- Wang Y, Spencer P & Walker M P. 2007. Chemical profile of adhesive/caries-affected dentin interfaces using Raman microspectroscopy. *Journal of Biomedical Materials Research Part A*, 81, 279-86.
- Watson A B E A M K T F. 2000. In vitro Evaluation of Five Alternative Methods of Carious Dentine Excavation. *Caries Research*, 34, 144-50.
- Watson T, Cook R, Festy F, Pilecki P, Sauro S, Curtis R & Watson T. 2008. Optical imaging techniques for dental biomaterials interfaces. *Dental Biomaterials: Imaging, Testing and Modelling*.
- Watson T F. 1999. Bonding glass-ionomer cements to tooth structure. In: DAVIDSON, C. L. & MJÖR, I. A. (eds.) *Advances in glass-ionomer cements*: Quintessence Pub. Co.
- Watson T F, Atmeh A R, Sajini S, Cook R J & Festy F. 2014. Present and future of glass-ionomers and calcium-silicate cements as bioactive materials in dentistry: biophotonics-based interfacial analyses in health and disease. *Dental Materials*, 30, 50-61.
- Webb S E D et al. 2002. Wavelength-Resolved 3-Dimensional Fluorescence Lifetime Imaging. *Journal of Fluorescence*, 12, 279-83.
- Wesseling-Perry K, Pereira R C, Wang H, Elashoff R M, Sahney S, Gales B, Juppner H & Salusky I B. 2009. Relationship between plasma fibroblast growth factor-23 concentration and bone mineralization in children with renal failure on peritoneal dialysis. *The Journal of Clinical Endocrinology & Metabolism*, 94, 511-17.
- Williams Q & Knittle E. 1996. Infrared and Raman spectra of Ca₅(PO₄)₃F 2-fluorapatite at high pressures: compression-induced changes in phosphate site and Davydov splittings. *Journal of Physics and Chemistry of Solids*, 57, 417-22.
- Wilson A, Prosser H & Powis D. 1983. Mechanism of adhesion of polyelectrolyte cements to hydroxyapatite. *Journal of dental research*, 62, 590-92.
- Wilson N H F. 2007. *Minimally invasive dentistry: the management of caries*, Germany, Quintessence.
- Xu R. 2001. Light scattering in: *Particle characterization: light scattering methods*, 13: Springer Science & Business Media, P. 56.

- Yiu C K Y, Tay F R, King N M, Pashley D H, Sidhu S K, Neo J C L, Toledano M & Wong S L. 2004. Interaction of glass-ionomer cements with moist dentin. *Journal of Dental Research*, 83, 283-89.
- Yoshida Y et al. 2012. HEMA inhibits interfacial nano-layering of the functional monomer MDP. *J Dent Res*, 91, 1060-65.
- Zezell D M, Ribeiro A C, Bachmann L, Gomes A S L, Rousseau C & Girkin J. 2007. Characterization of natural carious lesions by fluorescence spectroscopy at 405-nm excitation wavelength. *Journal of biomedical optics*, 12, 064013-13-5.
- Zhang X, Neoh K G, Lin C C & Kishen A. 2012. Remineralization of partially demineralized dentine substrate based on a biomimetic strategy. *J Mater Sci Mater Med*, 23, 733-42.